Members of the jury

Prof. dr. M. Ameloot, Hasselt University, Diepenbeek, Belgium, chairman

Prof. dr. V. Somers, Hasselt University, Diepenbeek, Belgium, promoter

Prof. dr. S. Hendrix, Hasselt University, Diepenbeek, Belgium, co-promoter

Prof. dr. P. Stinissen, Hasselt University, Diepenbeek, Belgium

Prof. dr. A. Timmermans, Hasselt University, Diepenbeek, Belgium

dr. E. Ydens, Hasselt University, Diepenbeek, Belgium

Prof. dr. G.W. Hergenroeder, University of Texas Health Science Center at Houston-McGovern Medical School, Houston, Texas, USA

Prof. dr. P. Popovich, Center for Brain and Spinal Cord Repair, The Ohio State University Wexner Medical Center, Columbus, Ohio, USA

Dr. M. Pouw, Acute Spinal Cord Unit, Radboud University Hospital, Nijmegen, The Netherlands

Table of Contents

Table of contents I

List of Figures V

List of Tables VI

List of Abbreviations VII

CHAPTER 1. General introduction and aims 1

1.1 Spinal cord injury 2

1.1.1 Epidemiology 2

1.1.2 Pathophysiology 2

1.1.3 Humoral immunity in SCI pathology 4

1.1.4 Clinical management of SCI patients 11

1.1.5 Treatment 13

1.1.6 Animal models 14

1.2 Biomarkers in SCI 17

1.2.1 Structural and functional biomarkers 18

1.2.2 Inflammatory biomarkers 23

1.2.3 Biochemical modelling of biomarkers 28

1.2.4 Towards an unbiased approach 28

1.3 Aims of the study 32

CHAPTER 2. The construction and detailed characterization of a human spinal cord cDNA phage display library 35

2.1 Abstract 36

2.2 Introduction 37

2.3 Materials and methods 39

2.3.1 Construction of a hSC cDNA display library 39

2.3.2 Insert PCR and sequencing analysis of the hSC-pSPVI library 40

2.4 Results 42

2.5 Discussion 48

CHAPTER 3. Antibody profiling identifies novel antigenic targets in spinal cord injury patients **51**

3.1 Abstract **52**
3.2 Introduction **53**
3.3 Materials and methods **55**
3.3.1 Patient samples 55
3.3.2 Construction of a human spinal cord (hSC) cDNA phage display library 55
3.3.3 Serological antigen selection procedure 56
3.3.4 Phage Enzyme Linked Immunosorbent Assay (ELISA) 57
3.3.5 Statistical analysis 57
3.4 Results **58**
3.4.1 Antibody profiling of SCI plasma samples using SAS 58
3.4.2 Antibody reactivity is increased in plasma of traumatic SCI patients 59
3.4.3 Identity of antigens targeted by SCI-related antibodies 60
3.4.4 Validation of the identified antibody responses in SCI patients 63
3.5 Discussion **68**

CHAPTER 4. Development and optimization of peptide and protein ELISA for autoantibody testing in spinal cord injury patients **73**

4.1 Abstract **74**
4.2 Introduction **75**
4.3 Materials and methods **77**
4.3.1 Competition assay 77
4.3.2 Recombinant protein expression and purification 77
4.3.3 Peptide and recombinant protein ELISA 78
4.3.4 Data analysis 78
4.4 Results **80**
4.4.1 Confirmation of the antigenic specificity of SCI-associated antibodies to synthetic peptides 80
4.4.2 Peptide ELISA development and validation 81

4.4.3 Confirmation of UH.SCI.2 and UH.SCI.7 *in vivo* target identity 84

4.5 Discussion 86

CHAPTER 5. PSMD4 and S100B autoantibodies in spinal cord injury patients 89

5.1 Abstract 90

5.2 Introduction 91

5.3 Materials and methods 92

5.3.1 Patient samples 92

5.3.2 Peptide ELISA 93

5.3.3 Data analysis 94

5.4 Results 95

5.4.1 PSMD4 and S100B autoantibody prevalence in SCI patients 95

5.4.2 Exploration of the clinical relevance of PSMD4 and S100B autoantibodies in SCI patients 97

5.4.3 PSMD4 and S100B autoantibody specificity 98

5.5 Discussion 100

CHAPTER 6. Biological characterization of PSMD4 autoantibody responses in spinal cord injury 103

6.1 Abstract 104

6.2 Introduction 105

6.3 Materials and methods 108

6.3.1 Animal experiments 108

6.3.2 RNA isolation and RT-qPCR 110

6.3.3 Western blot 111

6.3.4 Peptide and recombinant protein ELISA 112

6.3.5 Immunohistochemistry 112

6.3.6 Data analysis 114

6.4 Results 115

6.4.1 PSMD4 is expressed by endothelial, neuronal and glial cells in the spinal cord 115
6.4.2 PSMD4 protein expression and PSMD4 antibody production were not induced after SCI in mice 118
6.4.3 The pathologica role of antibodies against the C-terminus of mouse PSMD4 in SCI therapy 120
6.5 Discussion 122

CHAPTER 7. Summary, general discussion and future perspectives 125
7.1 Summary and general discussion 126

CHAPTER 8. Nederlandse samenvatting 139

Reference list 146
Curriculum Vitae 158
Dankwoord 161

List of Figures

Figure 1.1 Pathological processes induced after SCI
Figure 1.2 Putative mechanism for humoral immune response activation after SCI
Figure 1.3 Level of the injury: influence on functional loss
Figure 1.4 Overview of biomarker discovery approaches for SCI
Figure 2.1 M13 Gene VI phage display
Figure 2.2 Construction of a hSC cDNA phage display library
Figure 2.3 Diversity of the hSC cDNA libraries
Figure 2.4 Characterization of the hSC cDNA library
Figure 2.5 Gene ontology of the identified gene sequences
Figure 3.1 Increased antibody reactivity in plasma of traumatic SCI patients
Figure 3.2 Antibody reactivity in SCI samples collected at hospitalization and 3 weeks after injury or surgery
Figure 4.1 Schematic representation of the phage versus peptide ELISA
Figure 4.2 Competition assays for confirmation of target specificity
Figure 4.3 Coating optimization of the peptides of the SCI-associated panel
Figure 4.4 UH.SCI.2 and UH.SCI.7 phage versus peptide ELISA
Figure 4.5 Confirmation of the *in vivo* target identity of UH.SCI.2 and UH.SCI.7
Figure 5.1 PSMD4 and S100B autoantibody responses in SCI patients
Figure 5.2 PSMD4 and S100B autoantibody responses in SCI patients: influence of gender and age
Figure 5.3 PSMD4 and S100B autoantibodies in neuroinflammatory and autoimmune disorders
Figure 6.1 Amino acid sequence of PSMD4/AF, angiocidin and UH.SCI.2
Figure 6.2 Schematic representation of a T-cut hemisection SCI in rodents (coronal view)
Figure 6.3 PSMD4 expression in human spinal cord tissue
Figure 6.4 PSMD4 expression in mouse spinal cord tissue
Figure 6.5 PSMD4 and PSMD4 antibodies in SCI mice
Figure 6.6 Effect of C-terminal mouse PSMD4 antibodies in a SCI mouse model

List of Tables

Table 1.1 Humoral immunity in SCI pathology

Table 1.2 The American Spinal Injury Association Impairment Scale (AIS)

Table 1.3 Structural and functional biomarkers in human SCI

Table 1.4 Inflammation-related biomarkers in human SCI

Table 2.1 cDNA sequences identified in the new hSC cDNA library

Table 3.1 Characteristics of traumatic SCI patients used for the SAS procedure (identification cohort)

Table 3.2 Target identity of the SCI-related antibody responses

Table 3.3 Characteristics of the study populations

Table 3.4 Antibody reactivity in the SCI cohort and age- and gender-matched healthy controls

Table 4.1 Peptide identities

Table 5.1 Characteristics of the study populations

Table 6.1 Primer sequences

List of Abbreviations

AA	Amino acids
AEBP1	adipocyte enhancer-binding protein 1
AF	Antisecretory factor
AIS	American Spinal Injury Association impairment scale
AKAP13	A-kinase anchoring protein 13
ALDOC	Aldolase, fructose-bisphosphate C
AP3S2	Adaptor related protein complex 3 sigma 2 subunit
APRIL	A proliferation-inducing ligand
ARHGEF2	Rho/Rac guanine nucleotide exchange factor 2
AU	Arbitrary units
BAFF	B-cell activating factor
BBB	Blood-brain barrier
BCA	Bicinchoninic acid
BCMA	B-cell maturation antigen
BDNF	Brain-derived neurotrophic factor
BLAST	Basic local alignment search tool
BMS	Basso Mouse Scale
bp	Base pairs
BSA	Bovine serum albumin
BSCB	Blood-spinal cord barrier
C	Cervical level
CDCA7	Cell division cycle associated 7
Cfu	Colony forming units
CNS	Central nervous system
CSF	Cerebrospinal fluid
CSF	Colony-stimulation factor
CXCL	C-X-C motif chemokine
CYCA	Cyclophilin A
DAB	3, 3’-diaminobenzidine
DAPI	4',6-Diamidino-2-Phenylindole
DBNDD	Dysbindin (dystrobevin Binding protein 1) domain containing 2
dpi	Days post-injury

Ds	Double-stranded
DTT	Dithiothreitol
E.coli	Escherichia coli
EAE	Experimental autoimmune encephalomyelitis
ELISA	Enzyme-linked Immuno Sorbent Assay
GAPDH	Glyceraldehyde-3-phosphate dehydrogenase
GFAP	glial fibrillary acidic protein
GM-CSF	Granulocyte-macrophage colony-stimulation factor
GS	Glycine/serine linker
h	Hour
HBA1	Hemoglobin subunit alpha 1
HGF	Hepatocyte growth factor
His	Histidine
HO	heme oxygenase
HRP	Horseradish peroxidase
hSC	human spinal cord
HSP90AA1	Heat shock protein 90 alpha family class A member 1
ICAM-1	Intercellular adhesion molecule-1
IFN	Interferon
IgG	Immunoglobulin G
IL	Interleukin
IL-1RA	IL-1 receptor antagonist
KLHL	Kelch-like family member
L	Lumbar
MBP	Myelin basic protein
MCP	Monocyte chemoattractant protein
MCS	Multiple cloning site
M-CSF	Macrophage colony-stimulating factor
METRN	Meteorin, glial cell differentiation regulator
MIF	Macrophage migration inhibitory factor
Min	Minutes
MIP	Macrophage inflammatory protein
MMP	Matrix metalloproteinase
MP	Methylprednisolone

MPBS	Skimmed milk powder in PBS
MRI	Magnetic resonance imaging
mRNA	Messenger RNA
MS	Multiple sclerosis
MYEOV2	Myeloma-overexpressed gene 2
NAP	Neutrophil attractant protein
NADP	Nicotinamide adenine dinucleotide phosphate
NCBI	National Center for Biotechnology Information
NEG	Antibody-negative
NeuN	Neuronal nuclei
NF	Neurofilament
NF-L	Neurofilament light
NGF	Nerve growth factor
NMDAR	Anti-N-methyl-D-aspartate receptor
NS	Not significant
NSE	Neuron specific enolase
NT	Neurotrophin
OD	Optical density
PBS	Phosphate buffered saline
PBS-T	Phosphate buffered saline-Tween20
PEA	Phosphoprotein enriched in astrocytes 15
PFA	Paraformaldehyde
PIP4K2A	Phosphatidylinositol-5-phosphate 4-kinase type 2 alpha
PLA2G2A	Phospholipase A2 group IIA
pNF-H	Phospho-neurofilament heavy
POS	Antibody-positive
pSCI	Pathologic spinal cord injury
PSMD4	26S proteasome non-ATPase regulatory subunit 4
PTPRJ	Receptor tyrosine-protein phosphatase eta
RA	Rheumatoid arthritis
RBMS1	RNA binding motif single stranded interacting protein 1
RPL37A	Homo sapiens ribosomal protein L37a
rRNA	Ribosomal RNA
RT	Room temperature

S	Sacral
s	Seconds
S100B	Protein S100-B
SAS	Serological antigen selection
SC	Spinal cord
SCGFβ	Stem cell growth factor beta
SCI	Spinal cord injury
SCRG1	Stimulator of chondrogenesis 1
SDS-PAGE	Sodium dodecyl sulfate polyacrylamide gel electrophoresis
SPAG16	Sperm Associated Antigen 16
SYNGAP1	Ras/Rap GTPase-activating protein
T	Thoracic
T0	At hospitalization or preoperatively
T1	3 weeks after injury/surgery
T2	6 weeks after injury/surgery
T3	12 weeks after injury/surgery
T4	18 weeks after injury/surgery
TBI	Traumatic brain injury
TFE	Transcription factor binding to IGHM enhancer
THIO	Thioredoxin
TIMP	Tissue inhibitors of metalloproteinase
TMB	3,3’,5,5’ tetramethyl-benzidine dihydrochloride
TMEM236	Transmembrane protein 236
TNF	Tumor necrosis factor
tSCI	Traumatic spinal cord injury
TTC19	Tetratricopeptide repeat domain 19
U	Units
UBiLim	University Biobank Limburg
UIM	Ubiquitin-interacting motif
UTR	Untranslated region
WT	Wild type
YWHAZ	Tyrosine 3-monooxygenase/tryptophan 5-monooxygenase activation protein, zeta polypeptide
ZEB1	Zinc finger E-box binding homeobox 1

ZN148	Zinc finger protein 148
β	Beta

1

General introduction and aims

Based on:
The Next Generation of Biomarker Research in Spinal Cord Injury.
Ydens E*, Palmers I*, Hendrix S, Somers V.
*Authors contribute equally
Published in Molecular Neurobiology (2017 Mar;54(2):1482-1499)

1.1 SPINAL CORD INJURY

1.1.1 Epidemiology

Spinal cord injury (SCI) can be defined as any lesion in the spinal cord with either temporary or permanent dysfunction of the motor, sensory and/or autonomic systems [1, 2]. The most common causes of traumatic SCI (tSCI) are falls (53%), road traffic accidents (21.6%), sports/recreational injuries (14.1%) and violence (1.6%). In non-traumatic SCI, an underlying pathology such as infectious disease, tumour, musculoskeletal disease (osteoarthritis) or vascular disorders are involved [2-4]. Globally, the incidence of SCI varies from 3.6 to 195 patients per million and, currently, no reliable global or regional estimate of the SCI prevalence is available [5]. This life-altering condition mainly affects young male adults (80%; between 15 and 29 years) and males and females over 65 years [1, 4]. SCI comprises a very heterogeneous patient population, which is caused by differences in injury pattern, severity, location, genetic background, pre-injury health situation, and variability in medical, surgical and rehabilitative care. Currently, no treatments are available that result in complete neurological or functional recovery and significant health care resources are needed to manage an SCI, which results in a substantial financial burden on patients, their families and the community [5, 6].

1.1.2 Pathophysiology

The initial mechanical insult to the spinal cord caused by compression, contusion, stretching or kinking of the spinal cord results in severed axons, neural and glial death and ruptured blood vessels, and is referred to as the primary injury (figure 1.1) [7]. Vascular disruption immediately culminates into an environment of hemorrhages, edema and ischemia [8]. Subsequently, a secondary phase of tissue degeneration is initiated that occurs over weeks or even months (figure 1.1). In this phase, events like electrolyte shifts and necrotic or apoptotic cell death are continued, while processes such as oxidative stress, neuroinflammation, excitotoxicity and demyelination are triggered. These secondary injury processes eventually lead to further destruction of tissue surrounding the initial lesion and hinders repair mechanisms (e.g. glial scar formation and maturation, angiogenesis and axonal regeneration) [7, 9, 10]. During the chronic phase (> 6 months after SCI), a glial scar is formed via reactive gliosis and severed or injured axons underwent degeneration (Wallerian degeneration). Furthermore, a cyst develops at the lesion

site which can fill with cerebrospinal fluid (syrinxes) [11]. Once stabilized, the lesion contains a cyst cavity and tissue in the final stage of necrotic death [8].

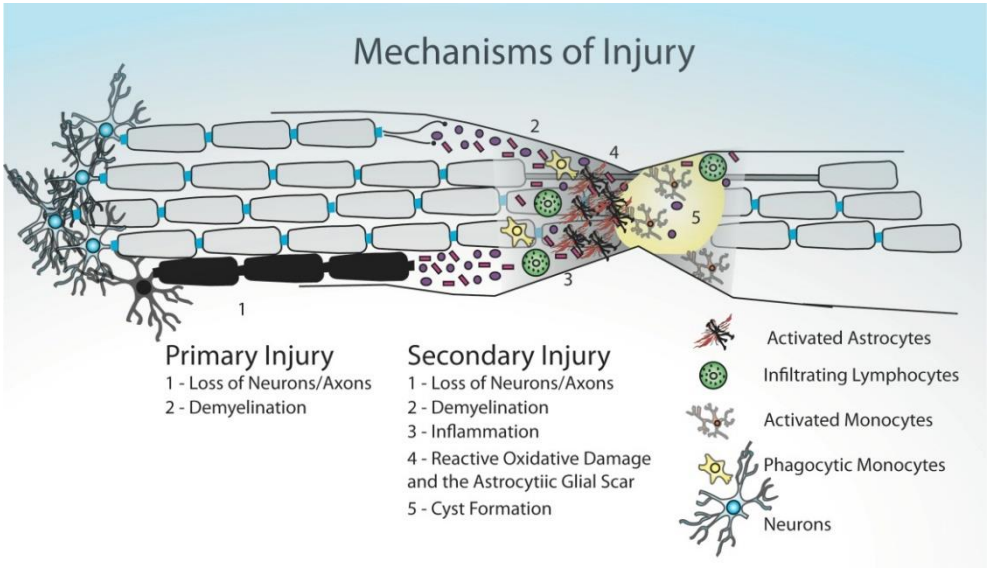

Figure 1.1: Pathological processes induced after SCI

The initial mechanical insult to the spinal cord results in primary injury consisting of loss of neurons/axons and demyelination (1-2). Subsequently, a cascade of pathological changes is induced (secondary injury) (1-5), including further loss of neurons/axons, demyelination, inflammation, reactive oxidative damage, formation of an astrocytic glial scar and cyst formation. Reprinted by permission from Dr. Michael Fehlings. (2010). Panminerva Med 52:125-147 [12].

A key process within the secondary injury phase is neuroinflammation. Immediately after injury, resident microglia and astrocytes are activated and start to proliferate [13]. In an excitotoxic and inflammatory environment, local microglial cells can adopt a "classically-activated" pro-inflammatory (M1) or "alternatively-activated" anti-inflammatory (M2) phenotype. SCI mainly elicits a long-lasting M1 response (and a transient M2 response) with secretion of pro-inflammatory cytokines such as interleukin (IL)-1β, IL-6, tumor necrosis factor-alpha (TNF-α), macrophage colony-stimulating factor (M-CSF) and oxidative metabolites [14]. The presence of these pro-inflammatory factors together with the disruption of the blood-spinal cord barrier (BSCB), contributes to the accumulation of circulating peripheral immune cells (e.g. neutrophils, macrophages and lymphocytes) in the

central nervous system (CNS). Neutrophils are the first circulating inflammatory cells that infiltrate in the spinal cord lesion and start clearing cellular debris in order to restore homeostasis. Additionally, these cells also secrete proteolytic (e.g. matrix metalloproteinase-9) and oxidative enzymes (e.g. nicotinamide adenine dinucleotide phosphate (NADP) oxidase and myeloperoxidase) which triggers the recruitment and activation of other inflammatory cells (e.g. monocytes/macrophages/microglia) [10, 13]. Macrophages derived from resident microglia or from peripheral monocyte differentiation have a phagocytic role and are involved in the induction of angiogenesis and the activation of the adaptive immune system. CNS-derived antigens presented by microglia/macrophages, astrocytes or dendritic cells activate both T and B lymphocytes, which start to proliferate and infiltrate the lesion site. Three days post-injury, T cells are present in the lesion and, in line with the M1-like microglia/macrophage response, secrete a Th1 cytokine profile (e.g. interferon gamma (IFN-γ)), which induces free radical production and increasing levels of pro-inflammatory cytokines (IL-6, IL-12, IL-1β, and TNF-α) as well as apoptotic signaling pathways. Besides the production of pro-inflammatory factors, a protective and regenerative environment is promoted by synthesis of several growth factors (e.g. brain-derived neurotrophic factor (BDNF), neurotrophin-3 (NT-3) and nerve growth factor (NGF)) [13]. Within hours after activation, B cells accumulate in the injured spinal cord, are able to form follicle-like structures, contribute to aggravation of tissue damage and produce pathologic antibodies [15, 16]. Both B cells and antibodies exert complex pathophysiological effects from which the role in recovery after SCI is still unknown (table 1.1).

1.1.3 Humoral immunity in SCI pathology

In experimental SCI, it is hypothesized that damage to the BSCB leads to exposure of CNS antigens to secondary lymphoid tissues, eliciting a chronic systemic and intraspinal B cell activation (figure 1.2). Subsequently, ectopic follicles have been demonstrated in the spinal cord and antibodies targeting nuclear antigens (e.g. DNA and RNA) and CNS proteins are synthesized [15, 17]. At present, the functional implications of this humoral immune response remain unclear. Transgenic mice lacking mature T and B lymphocytes (RAG2-/-) with a severe compression lesion at thoracic (T) level 10-11 demonstrated improved behavioural recovery 6 weeks after injury in comparison with wild type mice of the same inbred background [16].

This detrimental role of mature lymphocytes in functional recovery after SCI was suggested to be mediated by microglia/macrophage activation and damage to the myelin sheath [16]. In RAG2-/- mice, both cell-mediated and humoral mechanisms are affected, making it difficult to unravel the exact mechanism responsible for the restricted locomotor recovery. Ankeny et al. studied B cell-mediated effects in SCI and demonstrated improved neurological recovery and markedly reduced lesion pathology in B cell knockout mice with a contusion injury at T9-10 [17]. These results are in line with the study of Casili et al. (2016) which showed that B cell depletion immediately after a spinal cord clip compression reduced the developing inflammatory response and tissue pathology after SCI induction [18]. To unravel whether this pathologic effect is caused by SCI-induced B cell activation or the production of antibodies, Ankeny et al. performed a passive transfer experiment with intraspinal injection of serum antibodies from SCI mice into naive/uninjured mice. Here, it was shown that these SCI-induced antibodies participated in neuroinflammatory responses and exerted a degenerative effect in the spinal cord by causing cell death and sustained neurological dysfunction [15, 17]. Effector mechanisms that operate to cause antibody-mediated pathology are partly due to immune complex formation with intraspinal activation of complement and cells with Fc receptors (e.g. microglia, macrophages, etc.) [17]. Despite evidence that B cells are activated and produce pathologic antibodies after mid-thoracic SCI, Lucin et al. demonstrated that after high thoracic (T3) SCI antibody synthesis is suppressed. This injury level-dependent regulation of the humoral immune response might be explained by an impaired sympathetic-immune system axis, but whether this level-dependent immunosuppression is also present in SCI patients is still unclear [19].

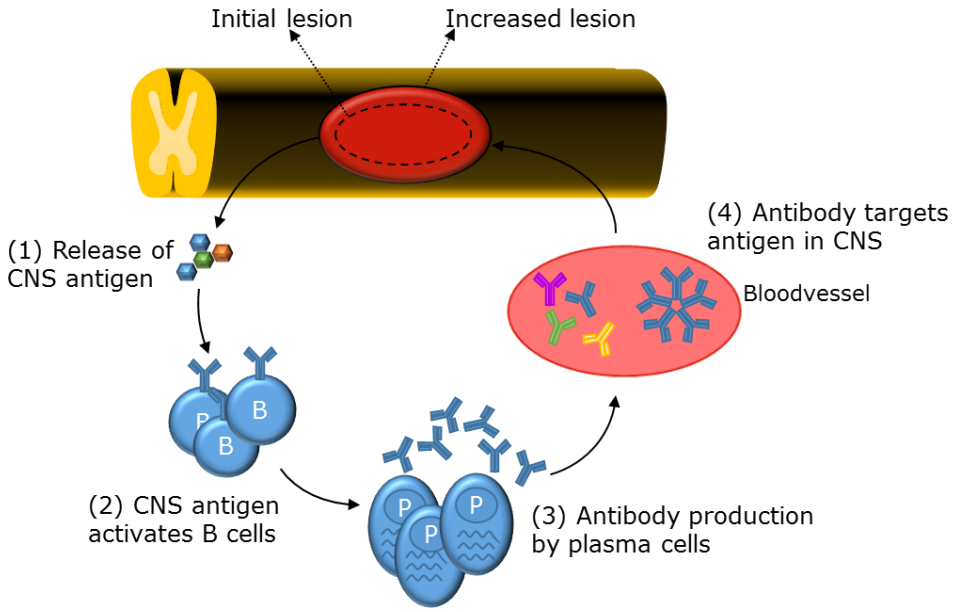

Figure 1.2: Putative mechanism for humoral immune response activation after SCI
After SCI, cell death occurs and the blood-spinal cord barrier is damaged. Circulating humoral immune components migrate into the lesion and central nervous system (CNS) antigens are released into the bloodstream, activating peripheral immune cells (e.g. B cells) (1/2). Activated B cells differentiate into plasma cells and synthesize antibodies, which are released into the circulation (3/4). Both activated B cells and the produced antibodies infiltrate into the lesion, where they contribute to degenerative processes, increasing the initial lesion size (4).

In comparison with the data available on the humoral immune response in SCI models, less is known about the human situation. Riegger et al. demonstrated a rapid decrease in monocytes (CD14+), T (CD3+) and B lymphocytes (CD19+) and MHC class II+ (HLA-DR) cells within 24 hours after SCI and minimum cell numbers were reached within the first week, suggesting an early onset immune suppression in SCI patients [20]. B-cell maturation antigen (BCMA), B-cell activating factor (BAFF) and a proliferation-inducing ligand (APRIL) are involved in B cell development, proliferation, activation and survival and are associated with autoantibody-mediated pathologies (e.g. systemic lupus erythematosus) [21]. In SCI patients, these endogenous factors were found to be over-expressed in peripheral blood mononuclear cells, indicating that B cells are also affected after SCI in humans [22]. Furthermore, until years after the initial trauma, SCI patients

demonstrate increased levels of antibody responses towards myelin and gangliosides in sera [23-29]. In chronic SCI, the presence of autoantibodies may contribute to SCI complications [23, 24], but up to now, the exact role of antibody responses in SCI recovery is still unknown.

Table 1.1: Humoral immunity in SCI pathology

Adaptive immune response component	Species	Animal model	SCI model	Detection, functionality/role	Reference
B cells	Mouse	Wild type mice	Moderate severe contusion injury at thoracic level (T) 9	*Chronic systemic and intraspinal B cell activation *B cell-dependent organ-specific and systemic autoimmune response *Antibody synthesis with reactivity against central nervous system (CNS) proteins and nuclear antigens (e.g. DNA and RNA) *Antibodies demonstrated a neurotoxic potential ➔ Mammalian SCI impaired B cell function with pathological potential	15
Deficient functional T and B lymphocytes with no initiation of V(D)J recombination	Mouse	Recombination activating gene 2 deletion RAG2-/- mice	Compression lesion at T10-11	*Improved recovery at 6 weeks after injury in RAG2-/- mice *Decreased number of microglia/macrophages in the lumbar spinal cord of RAG2-/- mice *Increased number of astrocytes in RAG2-/- mice ➔ T and B lymphocytes hampered functional recovery after SCI by increasing numbers of microglia/macrophages as well as decreasing axonal sprouting and myelination	16
Deficient functional B cells and antibody production	Mouse	IgH-6 B cell knockout (BCKO) mice	Moderate severe contusion injury at T9	*Improved locomotor recovery and reduced lesion pathology in BCKO mice *Plasma cells and immunoglobulins accumulated in the CSF and/or injured spinal cord of wild type mice with a SCI, but not in BCKO mice ➔ Humoral immunity components impaired functional recovery and lesion pathology after SCI	17
SCI serum antibodies	Mouse	Wild type mice	Microinjection into the right ventral horn at T12	*SCI-induced antibodies caused pathology (behavioral deficits and neurotoxicity) via activation of complement and cells bearing Fc-receptors in the spinal cord ➔ B cells affected SCI pathology via the production of antibodies	
B cell depletion	Mouse	Glycoengineered anti-muCD20 antibody (18B12, intraperitoneal injected)	Spinal cord vascular clip compression (T5-8)	*18B12 slowed severe hindlimb motor dysfunction and neuronal death *18B12 decreased nuclear factor-kB, inducible nitrix oxide synthase, cytokines and glial fibrillary acidic protein (GFAP) expression *18B12 reduced microglia and B and T lymphocyte expression ➔ 18B12 treatment restricted the developing inflammatory response and tissue damage by immune modulation	18
Antibodies	Mouse	Wild type mice	Contusion/ complete	*Contusion or complete transection SCI at T9 resulted in similar levels of antibody synthesis *High-level SCI (T3) resulted in impaired antibody synthesis	19

			transection injury at T3 or T9	➔ Immune suppression after SCI is level-dependent	
Antibodies	Rat	Wild type rats	Clip compression injury at cervical level (C) 7 until T1	*Increased antibody levels (immunoglobulin G (IgG) and M (IgM)) in the spinal cord 2 weeks post-injury, but not in chronic phases (10 and 20 weeks) *Antibodies at the injury epicenter during the subacute phase, targeting the astroglial scar and neurons of the ventral horn ➔ Cervical SCI in rats potentially triggered the development of autoantibody responses	30
B cells	Human (n=16)		C4 – lumbar level 1	*After SCI in humans, CD19+ B-lymphocytes decreased rapid and drastic within 24 hours and reached minimum numbers within the first week *CD19+ B lymphocytes recovered significantly 1 week after SCI to enhanced numbers in comparison with the control group *CD19+ B lymphocytes returned to control numbers in the chronic phase ➔ SCI was associated with an early onset of immune suppression and secondary immune deficiency syndrome Remark: all patients received a high dose methylprednisolone	20
B cells	Human (n=13)		C5 – T12	*Increased expression of B-cell activating factor (BAFF) and a proliferation-inducing ligand (APRIL) in peripheral blood mononuclear cells of chronic SCI patients ➔ Systemic regulation of SCI-autoimmunity via APRIL and BAFF mediated activation of B cells through B cell maturation antigen (BMCA)	22
Antibodies	Human (n=44)			*Ganglioside and/or myelin basic protein (MBP) antibodies were detected in 86% of traumatic SCI patients (serum samples collected at various stages following the injury)	26
	Human (n=24)			*GM1 ganglioside (IgG/IgM) and myelin-associated glycoprotein (MAG) antibodies in serum of infection-free, chronic (>12 months) traumatic SCI patients * GM1 ganglioside IgM levels differed significant between SCI patients and controls	24
	Human (n=56)			*Autoantibodies against MAG and GM1 ganglioside (IgG/IgM) in post-acute (2-52 weeks after injury) or chronic (>52 week after injury) SCI subjects * GM1 ganglioside IgG levels were increased in SCI patients compared to control group values *Correlations were found between the presence of GM1 ganglioside IgG autoantibodies and clinical parameters (e.g. neuropathic pain and urinary tract infection)	31

Human (n=117)	*Autoantibodies toward galactocerebroside (GalC) in chronic traumatic SCI patients (18 months to 46 years post-injury) *The level of GalC autoantibody production, the degree of nervous system destruction and the type of the course of post-traumatic myelopathy were found interrelated	[27]
Human (n=12)	*Serum autoantibodies toward MBP differed significantly in titer between SCI patients (12-29 years post-injury) and controls *SCI patients with American Spinal Injury Association Impairment Scale (AIS) B presented a higher immune reaction	[29]
Human (n=1)	*Autoantibodies toward GFAP and its breakdown products in a SCI patient	[28]
Human (n=18)	*GFAP autoantibodies in 22% of the plasma samples of SCI patients *GFAP autoantibodies were detected in the subacute (2-4 weeks after injury), but not in the acute (<48 hours after injury) phase, indicating post-injury production	[25]

1.1.4 Clinical management of SCI patients

SCI is diagnosed based on neurological symptoms and imaging of the spinal cord. Clinical characteristics of a tSCI are paralysis, numbness, tingling or loss of sensation, pain, loss of bowel and bladder control, difficulties in temperature regulation, susceptibility to infections and cardiovascular and sexual dysfunction. The extent of functional loss mostly depends on the level of the injury along the spinal cord (figure 1.3) and the neurological (motor/sensory) completeness of the injury. Higher lesion levels, with an injury in the upper part of the spinal cord, generally affect a larger area of the body, while complete lesions show more severe and predictable patterns of functional impairment [32, 33]. Besides the long-term physical disabilities, SCI patients also experience difficulties in social functioning, psychological (e.g. depression) and/or medical complications (e.g. urinary tract infections, pressure ulcers and spasticity) and sleep issues [34]. Magnetic resonance imaging (MRI) is currently considered the best imaging technique for evaluating tSCI during the acute phase [35]. Standard clinical MRI images effectively identify spinal cord compression, transection, edema, and hemorrhage.

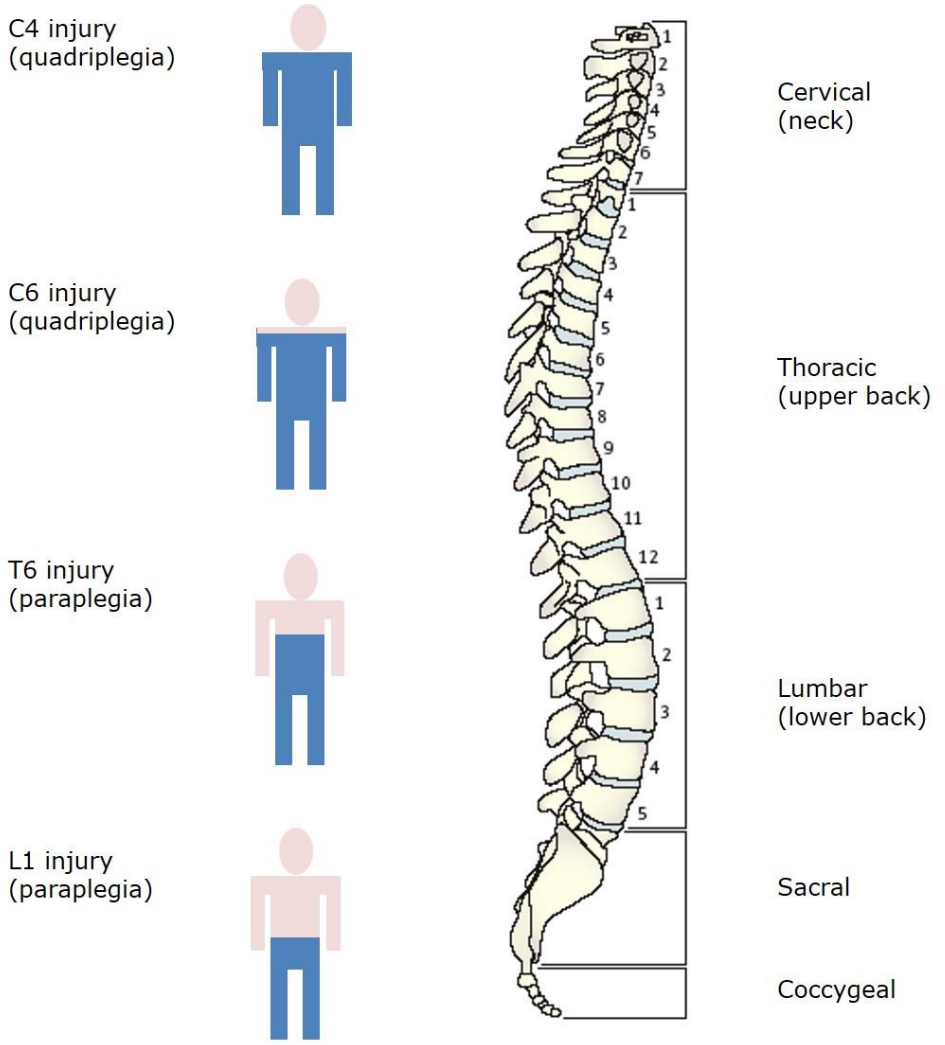

Figure 1.3: Level of the injury: influence on functional loss

The level of the injury in the spinal cord determines in which parts of the body functionality is affected. C, cervical; T, thoracic; L, lumbar. Adapted from Nature Reviews Neuroscience (2006) 7:628-643 [36].

While the diagnosis of acute tSCI is usually quite straightforward, the identification of the precise degree of severity and the prognosis of neurologic outcome has proven to be more challenging. Currently, neurological examination according to the American Spinal Injury Association impairment scale (AIS, table 1.2) is the most used predictive tool to assess functional outcome, especially when combined

with MRI findings [37-39]. The AIS scores are considered to be reliable and prognostic in SCI patients when assessed 72 hours after the initial trauma [40, 41]. However, within the first 72 hours, several factors such as spinal shock, concomitant brain injury, coma or sedation may affect the reliability of this neurological examination [40]. Moreover, clinical examination is not always feasible and reliable in patients with unstable early clinical status and other systemic injuries.

Table 1.2: The American Spinal Injury Association Impairment Scale (AIS)

AIS impairment scale	Definition	Explanation
A	Complete injury	No sensory or motor function is preserved in sacral segment (S) 4-5
B	Incomplete motor injury	Sensory, but not motor function is preserved below the neurologic level and extends through S4-5
C	Incomplete injury	Motor function is preserved below the neurologic level, and most key muscles below the neurologic level have a muscle grade of less than 3
D	Incomplete injury	Motor function is preserved below the neurologic level, and most key muscles below the neurological level have a muscle grade that is greater than or equal to 3
E	Normal	Sensory and motor functions are normal

MRI is a second tool for assessing a patient's recovery potential as MRI findings such as parenchymal hemorrhage, transection, and longer lesion length were shown to correlate with less favorable neurological outcomes [39]. The conventional MRI sequences, however, do not provide in depth information about the integrity of critical long white matter tracts which are responsible for the observed functional deficits after SCI [42, 43]. In addition, MRI is often unavailable in many locations and even when available, patients with multiple injuries may be too unstable and inaccessible for early MRI.

Altogether, neurological examination and MRI are not always accessible, feasible and reliable in unstable SCI patients. Moreover, the outcome measures that are traditionally used are insufficiently sensitive to predict recovery over time. These pitfalls for predicting functional outcome in SCI patients highlight the need for more accurate means to define injury severity and better predict neurological outcome and for more sensitive outcome measures that can identify small changes in neurological function to assess recovery.

1.1.5 Treatment

Primary injury to the spinal cord is largely irreversible due to a limited regenerative capacity of the CNS [44]. Moreover, the initial lesion size is often

expanded by activation of secondary injury processes. Therefore, early intervention to modulate the developing pathological processes is essential to improve long-term functional outcome and reduce mortality rates. SCI treatment mainly focusses on the prevention of primary injury, the minimization of secondary injury and the preservation of neurological function. Primary measures aim to prevent an SCI by for example improving vehicle safety and home security [45]. In the acute phase after an SCI, stabilization, decompression and perfusion of the injured spinal cord is essential to avoid additional neurologic injury [10, 32, 46, 47]. Next to a surgical intervention, corticosteroids (e.g. methylprednisolone (MP)) and gangliosides are administered early in the treatment of SCI patients. MP stimulates the secretion of anti-inflammatory cytokines and reduces oxidative stress, resulting in an enhanced neuronal cell survival. Besides the beneficial effects, the use of high concentrations of MP is still controversial because of deleterious side-effects (e.g. gastrointestinal bleeding and infection) [10]. Gangliosides demonstrate enhanced motor and sensory function in SCI patients and in combination with physical therapy, an improvement is seen in motor scores, walking velocity and walking distance [48]. Physical therapy is also an important element in the treatment of SCI patients and prevents joint contractures and the loss of muscle strength, helps to conserve bone density and insures normal functioning of the respiratory and digestive system [49, 50]. When medical stability of the patient is obtained, an interdisciplinary team (e.g. physiotherapist, psychologist and other consultant specialists) is involved in the rehabilitation process to allow the patient to go back to a productive and satisfying life [49].

Current treatment strategies demonstrate some improvements in neurological function, but, at present there is no treatment that results in complete neurological or functional recovery [9, 45]. In order to explore new therapeutic strategies, research has shifted to nanotechnology (e.g. nanofiber scaffolds), cellular therapy, and tissue engineering to promote neuroregeneration and block multiple degenerative mechanisms in the secondary injury phase [51, 52] .

1.1.6 Animal models

In order to understand the mechanisms of SCI pathology and to study reliable treatment strategies, various SCI models have been developed in different animal species (e.g. rats, mice, sheep, rabbits, dogs, opossums and baboons). In SCI

experimental studies, rodents are preferred because of their availability, ease of handling, high reproductive rates and relatively low cost of use [53]. To reflect the different lesion types and severities of the heterogeneous patient population, a wide variety of animal models has been developed such as compressive, contusive, and laceration/transection models [9, 54].

One of the most commonly used methods for modelling of SCI in animals, is the transection model. This type of injury provides an idealized setting for the investigation of neuronal regeneration following injury, the assessment of axonal regeneration and subsequent functional recovery [53, 55, 56]. Complete transection of the spinal cord creates a hostile tissue environment and is rarely encountered in human SCI. Therefore, selectively lesioning of the spinal cord (e.g. partial transection) was developed to better represent the human condition. A partial transection model allows not only the investigation of injured and healthy fibers in the same animal, it can furthermore be used to examine locomotor function and recovery in different spinal tracts [55, 57]. To induce a partial transection or hemisection lesion, the spinal cord is exposed by performing a partial laminectomy at T8. Using the "T-cut" procedure, the right and left dorsal funiculus, the dorsal horns and the ventral funiculus are transected, resulting in a complete transection of the dorsomedial and ventral corticospinal tract and impairment of several other descending and ascending motor and sensory tracts [58]. After the "T-cut" hemisection, the spinothalamic tract in the lateral column, the reticulospinal and vestibulospinal pathway in the ventral white matter and the ventral horn are spared, allowing the observation of pain and temperature [59]. Besides these macroscopic changes, a hemisection model causes focal tissue pathology including white matter apoptosis, demyelination, incomplete remyelination, macrophage infiltration and microglia activation at the epicentre with limited pathologic features further away from the epicentre of the lesion [9]. Clinical symptoms of hindlimb paralysis and loss of bladder control are present immediately after surgery. The bladder function restores gradually, while recovery in the hindlimb locomotor function is limited to the point that the animal is able to perform plantar stepping with weight support. To evaluate the hindlimb locomotor function, the Basso Mouse Scale (BMS) locomotor rating scale is used. The BMS is a 10-point scale (9=normal locomotion; 0 =complete hind limb paralysis) in which mice are scored based on forelimb and hindlimb coordination during sustained locomotion,

trunk stability, paw orientation and tail position in an open field during a 4-minute interval [60, 61]. The extent of the neuropathology in the injured spinal cord is reflected in the BMS scores which enables us to grade the outcome of SCI [61].

1.2 BIOMARKERS IN SCI

According to the Biomarkers Definitions Working Group, a biomarker is defined as 'a characteristic that is objectively measured and evaluated as an indicator of normal biological processes, pathogenic processes or pharmacological responses to a therapeutic intervention' [62]. In the case of SCI, an objective and quantifiable method such as the assessment of biomarkers in biofluids, might significantly aid in the evaluation of the extent of traumatic injury, particularly in the early phase of the injury, to more accurately predict how the patient will progress. The increased extent of injury may be reflected in the presence or altered concentration of biomarkers. Additionally, biomarkers are an efficient way to measure the progression of the injury over time. A better characterization of SCI patients using biomarkers will ultimately result in a more personalized disease management. For SCI, several biomarkers have already been suggested that are involved in both primary and secondary responses to SCI. An overview of the discussed strategies for biomarker discovery and their strengths and weaknesses is given in figure 1.4 (lower panel).

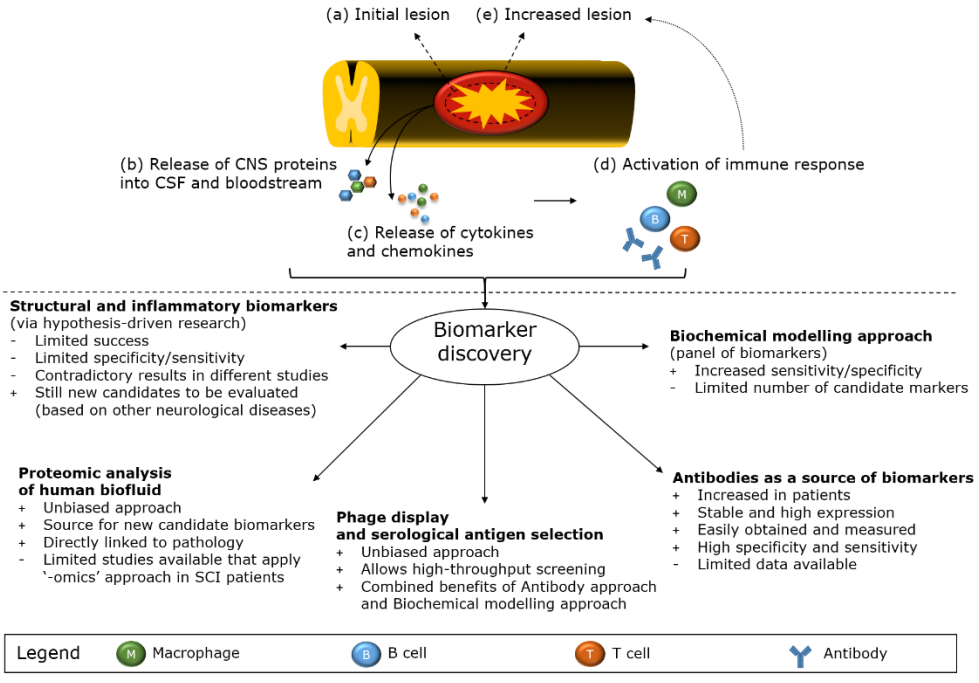

Figure 1.4: Overview of biomarker discovery approaches for SCI

Upon injury to the spinal cord (a), central nervous system (CNS) specific proteins are released into the cerebrospinal fluid (CSF) and bloodstream (b). The injury triggers the activation of the immune response with the release of cytokines and chemokines (c). These inflammatory mediators activate and recruit inflammatory cells to the lesion site thereby further amplifying the inflammatory response (d) which may contribute to an increased lesion in the spinal cord (e). Released CNS proteins and inflammatory mediators in the CSF and bloodstream are ideal targets for biomarker discovery (lower panel). Starting from these processes, biomarker research in SCI has focused on analyzing structural and inflammatory proteins. More recently, proteomics and biochemical modelling of candidate biomarkers have been applied to advance biomarker discovery and applicability. As antibodies generally represent good biomarkers, phage display and serological antigen selection can complement the more traditional approaches in the discovery of novel SCI biomarkers. The strengths and weaknesses of the different approaches for SCI biomarker discovery are listed as well.

Trauma to the spinal cord results in an acute physical injury, and leads to axonal damage and neuronal necrosis (figure 1.4a). This primary neuronal destruction may cause leakage of cellular proteins and breakdown products into the cerebrospinal fluid (CSF) and subsequently into the bloodstream (figure 1.4b). Also glial cells are damaged, triggering glial-specific protein release into biofluids. As described above, in the secondary phase, an injury-triggered inflammatory response results in elevated levels of inflammatory mediators such as cytokines and chemokines (figure 1.4c). The amplified inflammatory response can persist months to years after the initial injury (figure 1.4d) and may contribute to the expansion of the initial lesion (figure 1.4e). Starting from these key processes, the search for SCI-specific biomarkers has been approached in two ways; 1) by analysing structural proteins that are abundant in the spinal cord and that might be released from damaged nervous tissue during the primary phase, and 2) by measuring components of the inflammatory response in the secondary phase [63]. The biomarkers identified via these hypothesis-driven approaches have been extensively reviewed and are discussed below, where we focus mainly on the data from recent human studies [64-66].

1.2.1 Structural and functional biomarkers

In CNS diseases (e.g. acute CNS trauma, ischemia, and neurodegenerative diseases), mainly structural proteins that maintain cell shape and compose structural elements of neurons and glia have been studied for their biomarker

potential as they may reflect the degree of injury. Likewise, functional proteins with CNS-specific biological activity have also been addressed in SCI biomarker research. Neuron-derived proteins such as neuron specific enolase (NSE), tau and neurofilaments (NFs) have been of considerable interest to be evaluated in serum and CSF as SCI biomarkers (table 1.3). Glial proteins may also be used as biomarkers of SCI, reflecting the injury of the glial population residing in the spinal cord. Therefore, glial cell-associated proteins such as protein S100-B (S100B) and glial fibrillary acidic protein (GFAP) have been investigated as potential SCI biomarkers (table 1.3).

Neuron-derived biomarkers

NSE is a subunit of the glycolytic enzyme enolase and is localized predominantly in the cytoplasm of neurons. Upregulated NSE is released from damaged neurons to maintain homeostasis [67]. While animal models highlighted promising features for NSE as an SCI biomarker [68-70], studies in humans have only recently addressed the NSE biomarker potential. The levels of NSE within CSF in a cohort of 16 SCI patients were increased and correlated with the baseline neurologic impairment being either motor complete (AIS A and B) or motor incomplete (AIS C and D) [71]. Ahadi et al. (2015) recently found that also serum NSE levels were significantly higher during the first 48 hours after injury in the 26 tSCI patients included in the study compared to the control group [72]. In a population of 34 patients with vertebral spine fractures, however, the analysis of NSE levels revealed no significant difference [73].

Tau is a microtubule-binding phosphoprotein that is highly enriched in axons. Data on the use of tau as a biomarker for traumatic brain injury (TBI) is inconsistent (reviewed by [74]). Measurement of tau in CSF of 27 patients with complete (AIS A; n=14) and incomplete (AIS B and C; n=13) SCI showed that tau levels were elevated in a severity-dependent manner [75]. On the other hand, tau levels were not increased in the 3 patients with postoperative spinal cord ischemia and paraparesis compared to the group of 20 patients without neurological complications [76].

Another class of neuronal proteins that has been addressed as biomarkers in SCI are NFs. These major cytoskeletal components are expressed in axons and the NF-polymer consists of light, medium and heavy chains. After injury, the phosphorylation state of NFs is altered, which leads to the local loss of

cytoskeleton integrity [77]. In SCI patients, phospho-neurofilament heavy (pNF-H) levels in blood became detectable already 12 h after injury and remained elevated at day 21 post-injury [72, 78]. The increase in pNF-H plasma levels of 14 SCI patients was more pronounced in the patients with complete SCI compared to the patients with incomplete SCI and might reflect a greater magnitude of axonal damage [78]. Another study that included 16 SCI patients reported that also CSF levels of unphosphorylated NF-H were significantly increased in motor complete patients versus motor incomplete patients [71]. Furthermore, neurofilament light (NF-L) levels were shown to be elevated in CSF of SCI patients [79, 80]. Recently, Kuhle et al. (2015) found that serum NF-L levels increased over time and that the levels correlated with the AIS scores at baseline and after 24 h and with motor outcome several months after the injury based on NF-L screening in 13 motor complete, 10 motor incomplete and 67 healthy controls [79]. Altogether, these results indicate a potential prognostic value of NFs in SCI patients.

Glial-derived biomarkers

S100B is a dimeric calcium-binding protein localized predominantly in astroglial and Schwann cells and is the most intensively studied marker in SCI. Both serum and CSF levels of S100B are elevated in SCI patients [71, 73, 75, 81]. The concentration of S100B was significantly higher in patients with a motor complete injury compared to patients with motor incomplete injury [71, 75]. Furthermore, in 12 patients with vertebral fractures which showed neurologic deficits, S100B levels were higher compared to the 22 patients without neurological deficits [73]. In patients with spinal cord compression resulting from epidural accumulation of purulent material (empyema; n=34) or metastases (n=11), normal or transiently increased S100B levels were associated with a beneficial outcome, whereas persistently elevated S100B levels were related to a lower extremity muscle power outcome [82, 83]. The same trend was seen in complicated courses of postoperative deterioration in a cohort of 51 patients with spondylotic cervical myelopathy, in which a single subject that showed major functional decline had persistently elevated S100B levels while the 2 patients that recovered after neurological decline showed no or a transient increase in S100B levels [84]. S100B levels might thus have prognostic relevance in several SCI pathologies.

A second glial protein that has been addressed in SCI biomarker research is GFAP, which is exclusively found in the CNS and is a part of the astroglial skeleton. While

CSF levels of GFAP have been found to be increased in a severity-dependent fashion in SCI patients by several studies [75, 80], elevated serum levels of GFAP were only recently reported [72]. The serum level of GFAP was useful for estimating SCI severity within the first 24 hours after injury in a cohort of 26 SCI patients [72]. Altogether, the functional proteins NSE and S100B have been found to be more increased in patients with complete injury compared to patients with incomplete injury, yet as both proteins can also be found in red blood cells and platelets [85], their diagnostic utility as an SCI-specific marker can be questioned, especially in polytraumatized patients. On the other hand, structural biomarkers such as tau, NFs and GFAP are increased in serum and CSF in a severity-dependent fashion. Although extensive validation of these markers is still needed, they emerge as promising candidate biomarkers for the estimation of injury severity. These data encourage the evaluation of known and new structural biomarkers for injury severity in SCI pathology.

Table 1.3: Structural and functional biomarkers in human SCI

Marker	Function	Cellular source	Biofluid	Evidence	Reference
Neuron specific enolase (NSE)	Glycolytic neuronal enzyme	Neurons	CSF Serum	*CSF levels of NSE were increased in SCI patients *CSF levels correlated with baseline neurological impairment *Serum levels were increased during the first 48 h after injury *Serum NSE levels in patients with vertebral spine fractures were not different from controls	71-73
Tau	Microtubule associated protein	Neurons (axons)	CSF	*CSF Tau levels were increased in a severity-dependent manner *CSF Tau levels correlated with severity of injury (measured at 24h) *CSF Tau levels were not increased in patients with post-operative spinal cord ischemia and paraperesis	75, 76
Neuro-filaments (NFs)	Components of cytoskeleton (light, medium and heavy NFs)	Neurons	Plasma Serum CSF	*Plasma phospho-NF-H levels were elevated *Phospho-NF-H was elevated to a greater extend in motor complete compared to motor incomplete SCI patients *NF-H concentration in the CSF was also increased in motor complete versus motor incomplete patients *Serum and CSF NF-L levels were increased in SCI patients *Serum NF-L increased over time and correlated with AIS scores at baseline and months after injury	71, 78-80
S100B	Calcium-binding protein with neurotrophic activity	Astrocytes and Schwann cells	Serum CSF	*Serum and CSF levels were elevated in SCI patients *CSF S100B levels were higher in motor complete versus motor incomplete SCI patients *Serum levels were higher in patients with vertebral fractures with neurological deficits compared to those without deficits *In patients with epidural empyema or spinal metastasis increased serum levels of S100B had unfavorable motor outcome *Elevated serum levels of S100B were seen in patients with spondylotic cervical myelopathy with complicated course of post-operative deterioration	71, 73, 75, 81-84, 86
Glial fibrillary acidic protein (GFAP)	Intermediate filament of cytoskeleton	Astrocytes	CSF Serum	*Elevated levels in CSF and serum of SCI patients *CSF levels measured at 24 h correlated with injury severity *In ischemic SCI, elevated levels of CSF GFAP correlated with injury severity and prognosis *GFAP breakdown products were found in serum of SCI patients	66, 72, 75, 80

1.2.2 Inflammatory biomarkers

Inflammation is considered to play a central role in the pathophysiology of secondary injury after SCI. Moreover, it is almost certain that therapeutic strategies for acute SCI will influence or be influenced by the inflammatory response, which makes the investigation of inflammatory mediators highly essential. Animal models, in which the lesion severity to the spinal cord was precisely controlled, have demonstrated that concentrations of inflammatory mediators such as IL-1β, IL-6 and tumor necrosis factor (TNF) after injury are 'titrated' according to the severity of the neurologic deficit [87]. This aspect further justifies the evaluation of inflammatory mediators as potential biomarkers of injury severity.

Blood-derived versus CSF-derived inflammatory biomarkers

Ideally, peripheral biomarkers are measured in an easy accessible biofluid such as blood (serum and plasma). Blood is easily processed, provides relatively homogenous samples, and there is a large amount of normative data available [88]. Analysis of blood samples can also present difficulties such as deciphering the origin of proteins as blood comes in contact with all tissues and organs. Moreover, issues regarding the sensitivity and dynamic range have been reported for protein biomarkers in blood [89]. CSF samples might be more relevant for SCI biomarker discovery, however, collecting CSF samples is much more invasive and not always feasible from patients that suffered multiple trauma or that are unstable. Especially when addressing cytokine levels as potential SCI biomarkers, one has to carefully consider which biofluid to use. It was shown that the increased IL-1β levels within the spinal cord of rats with a contusion injury were comparable to the levels within the CSF. However, the systemic (serum) levels of this cytokine were much lower and did not correlate with those in the injured spinal cord [90]. A similar phenomenon was observed for TNF levels, with levels measured in the CSF correlating closely with those in the spinal cord, but not with those in serum [91]. Similarly, in SCI patients, serum concentrations of the inflammatory mediators were often found to be substantially lower than CSF concentrations taken at the same time [75].

Inflammatory biomarkers in CSF

In CSF samples of SCI patients, a plethora of inflammatory mediators have been investigated. Pro-inflammatory cytokines (e.g. IL-1β, IL-6, IL-8, IL-16, TNF), chemokines (e.g. C-X-C motif chemokine (CXCL)-10, monocyte chemoattractant protein (MCP)-1 and neutrophil attractant protein (NAP)-2), as well as growth factors (e.g. NGF) have been found to be increased in CSF of SCI patients compared to controls (table 1.4) [75, 92, 93]. Despite the detection of a broad range of inflammatory mediators in CSF of SCI patients, the majority of cytokines (including TNF and IL-1β) and growth factors were not measurable when using a multiplex kit [75]. In addition, levels of enzymatic proteins (e.g. heme oxygenase (HO)-1 and matrix metalloproteinase (MMP)-2 and MMP-9) and their inhibitors (e.g. tissue inhibitors of metalloproteinase (TIMP) 1) that control the ongoing inflammatory response are elevated in SCI patients [92, 93]. The CSF levels of several of these inflammatory proteins (IL-6, IL-8 and MCP-1) were even elevated in a severity-dependent fashion in a cohort of 27 acute SCI patients [75] and cumulative concentrations of IL-1β, MMP-9 and CXCL-10 showed a statistically significant correlation with injury severity [93].

Inflammatory biomarkers in blood-derivatives

SCI subjects exhibited serum concentrations of a considerable amount of pro-inflammatory cytokines (colony-stimulation factor (CSF)-1, IL-2, IL-2R, IL-3, IL-6, IL-9, IL-16, IL-18 and TNF) that were greater than in controls (table 1.4) [24, 31, 94-98]. In contrast to several other studies, Frost et al. (2005) did not observe elevated levels of IL-6 and TNF in 37 subjects with chronic SCI [31, 96-98]. In addition to a pro-inflammatory cytokine profile, the levels of the anti-inflammatory cytokine IL-10 and the IL-1 receptor antagonist (IL-1RA) are increased in SCI patients [31, 99]. When comparing 21 SCI patients to 21 trauma patients without neurological damage, especially circulating levels of IL-10 were significantly increased in SCI compared to non-SCI patients, whereas the levels of several pro-inflammatory cytokines (IL-1β, sIL-2Rα, IL-4, IL-5, IL-7, IL-13, IL-17, and IFN-γ) and chemokines (macrophage inflammatory protein (MIP)-1α and -1β and granulocyte-macrophage colony-stimulation factor (GM-CSF)) were significantly reduced [99]. The elevated levels of IL-10, however, were not found in an earlier study in which 24 SCI patients were compared to healthy controls [24]. Recently, IL-10 levels were found to be significantly lower in a later phase after SCI (>12

hours - 12 weeks after SCI) in comparison with the level at admission, unfortunately, control subjects were not included [94]. Additionally, increased serum levels of chemokines (CCL4, MCP-1, macrophage migration inhibitory factor (MIF), CXCL-1, CXCL-9, CXCL-10 and CXCL-12) were evident in SCI patients [95, 96, 100, 101]. The levels of CXCL-1, CXCL-9 and CXCL-10 reached a peak on day 7 after SCI and then declined to control level. In contrast, the increased expression of CXCL-12 was persistent up to 28 days after SCI [101]. Furthermore, increased levels of growth factors (stem cell growth factor beta (SCGFβ) and hepatocyte growth factor (HGF)), acute phase protein (C-reactive protein) and an adhesion molecule (intercellular adhesion molecule (ICAM-1)) have been reported in serum of SCI patients [95-98].

In most studies that assessed correlations between serum levels of inflammatory mediators and clinical parameters (level of injury or AIS classification), no association could be found [31, 95]. Still, levels of IL-6 and IL-1RA did show a further increase in subjects with pain, urinary tract infection and pressure ulcers compared to SCI subjects who were asymptomatic for medical complications [31]. SCI patients with high plasma levels of CXCL-10 had a significant prolonged stay in the hospital and a worse respiratory function [99]. Moreover, by evaluating the levels of TNF in SCI patients with and without neuropathic pain, the authors showed that TNF could be a potential sensitive diagnostic biomarker for chronic neuropathic pain in SCI patients [102]. Recently, Moghaddam et al. (2015) analyzed the complete temporal profile (from 4 hours to 12 weeks after SCI) of 7 different cytokines and growth factors and compared serum levels between patients with neurological improvement to those without improvement [94]. TNF, IL-1β, IL-6, IL-8 and IL-10 levels were all higher in patients without neurological remission and in patients with an initial AIS A. While still many discrepancies exist, several inflammatory mediators do show potential as an SCI biomarker (table 1.4).

Table 1.4: Inflammation-related biomarkers in human SCI

Marker	Function	Biofluid	Evidence	Reference
Interleukin 6 (IL-6)	Pleiotropic pro-inflammatory cytokine	CSF Serum	*Early post-injury elevation in CSF *At 24 h post-injury CSF IL-6 levels correlated with injury severity *Serum IL-6 was found elevated in serum, although this could not be confirmed by others *Serum IL-6 was increased in SCI patients with AIS A compared to other AIS subgroups	75, 97, 99
Interleukin 8 (IL-8)	Pleiotropic pro-inflammatory cytokine	CSF Serum	*Early post-injury elevation in CSF *At 24 h post-injury IL-8 CSF levels correlated with injury severity *Serum IL-8 was increased in SCI patients with AIS A compared to the other AIS subgroups	75, 99
Monocyte chemoattractant protein-1 (MCP-1)	Chemokine; also known as CCL2	CSF Serum	*MCP-1 levels were increased in CSF in patients with complete and incomplete SCI (peak at 24 to 36 h post-injury) *Early post-injury elevation in CSF *At 24 h post-injury, MCP-1 CSF levels correlated with injury severity	75, 92
Interleukin 1 beta (IL-1β)	Pleiotropic pro-inflammatory cytokine	CSF Serum	*In an animal model, IL-1β was elevated in spinal cord and CSF and a correlation was found between spinal cord and CSF (but not with serum) *Elevated in CSF of SCI patients *In SCI patients, cumulative CSF concentrations correlated with injury severity and negatively correlated with neurological recovery months after injury *Not detectable in CSF by another study *Serum IL-1β was increased in SCI patients with AIS A compared to other AIS subgroups	75, 90, 92, 93, 99
Matrix metallo-proteinase-9 (MMP-9)	Enzyme, protease	Serum	*In SCI patients, cumulative CSF concentrations correlated with injury severity	93
C-X-C motif chemokine (CXCL)-10	Chemokine	CSF Serum	*Early post-injury elevation in CSF *Cumulative CSF concentrations correlated negatively with neurological recovery at 12 months	65, 92, 99
Interleukin 10 (IL-10)	Anti-inflammatory cytokine	Serum	*Serum IL-10 was increased in SCI patients with AIS A compared to other AIS subgroups	93, 99
Tumor necrosis factor (TNF)	Pleiotropic pro-inflammatory cytokine	CSF Serum	*In an animal model, TNF was elevated in spinal cord and CSF and a correlation was found between spinal cord and CSF (but not with serum) *Not detectable in CSF by another study *Serum TNF was found elevated in serum, although this could not be confirmed by others *Elevated in serum of SCI patients with neuropathic pain compared to patients without pain *Serum TNF was increased in SCI patients with AIS A compared to other AIS subgroups	75, 91, 99, 102

Antibodies as a novel source of potential SCI biomarkers

Within the circulation, also antibodies are present. Besides the production of antibodies against foreign molecules, the immune system generates antibodies to self-proteins in response to many pathological processes. It is believed that these antibodies are generated against overexpressed, mutated or misfolded proteins, against aberrantly degraded or glycosylated proteins or against proteins released from damaged tissues. Since after tSCI, the BSCB is compromised, spinal cord specific proteins can be released into the periphery and trigger an immune response, including the development of antibodies. In an animal model, SCI induced a strong increase of circulating pathogenic antibodies and antibodies against brain proteins have already been implicated in a variety of neurological disorders such as stroke, multiple sclerosis, epilepsy and Alzheimer's disease. In SCI, Yokobori et al. (2013) found GFAP and its breakdown products in CSF of an SCI patient. Interestingly, this patient had also developed an antibody response against GFAP and the breakdown products starting from day 6 after injury [66]. This finding is confirmed by the study of Hergenroeder et al. (2015), which demonstrated autoantibodies towards GFAP in subacute (2-4 weeks after injury), but not in acute (<48 hours after injury) plasma samples [25]. Together, these results highlight that antibody reactivity against self-proteins can develop upon SCI in humans, once these proteins are 'secreted' from the CNS. Furthermore, antibodies against gangliosides, myelin basic protein, myelin associated glycoprotein and against nuclear antigens have been found after SCI [24, 26, 31, 103-105]. Elevated titers of antibodies against several myelin proteins were found in sera of SCI patients until years after the initial injury, showing that antibodies are prolonged present in the blood of SCI patients. Interestingly, correlations between the presence of these antibodies and clinical parameters (e.g. SCI complications) were found by several independent studies [24, 31, 103, 105]. Next to the pathologic and clinical involvement, antibodies also contain several general properties which make them interesting candidates for the next generation biomarkers in SCI. Antibodies are secreted and are therefore highly accessible and easily measured in serum and plasma (figure 1.4, lower panel). Unlike most other proteins found in serum, antibodies are stable as they are not degraded by proteolysis and have a long half-live in blood. Due to their inherent amplification within the immune system, antibodies are relatively abundant and easily measured. Upon admittance

to the emergency room, patients often receive fluids and blood products that might introduce a sensitivity issue as the blood of the patient and thus the concentration of the protein biomarker, is being diluted. This problem can again be circumvented when considering antibodies as biomarkers. The concentration of the stable and continuously produced antibodies will be elevated again when a sample is taken at a later time point. Moreover, since reagents bind to the constant regions of immunoglobulins, antibodies of the same class which recognize different antigens can be detected simultaneously, enabling high-throughput biomarker isolation and simplifying assay development. Based on these properties, antibodies are of particular interest to be studied as biomarkers and could rapidly advance the diagnosis and treatment of disease.

1.2.3 Biochemical modelling of biomarkers

Even though elevated concentrations of potential biomarkers have been identified in patients with SCI, the current candidate biomarkers do not yet provide a sensitive diagnostic or prognostic tool. Main issues that none of the biomarkers can be efficiently used as an individual marker for SCI involve the sensitivity of the candidate biomarkers, the lack of correlation with certain outcome measures and the heterogeneity of the SCI population. It is likely that for a complex condition such as SCI, a single biomarker will not reflect the full spectrum of the response of the injury. A strategy to attain an improved sensitivity and specificity for the characterization of the injury severity involves the biochemical modelling of biomarkers, thereby combining different markers into a biomarker panel that is more specific for certain outcome measures (figure 1.4, lower panel) [66, 106]. Kwon et al. (2010) used the CSF concentrations of a combination of both putative structural and inflammatory biomarkers, namely S100B, GFAP and IL-8, to classify the injury severity of SCI patients. This study was able to predict the AIS grade with an accuracy of 89% using these CSF biomarkers [75]. The panel of biomarkers could even predict motor outcome at 6 months better than the standard clinical AIS classification. More studies that model biomarkers into panels are highly required to fully characterize a specific SCI fingerprint that can be of great use from a clinical point of view.

1.2.4 Towards an unbiased approach

While combining biomarkers into a panel is a reliable and powerful strategy, up till now, there is only a limited number of candidate biomarkers available for SCI.

Most studies described above use a hypothesis-driven approach, in which biofluids are screened for biomarkers that are known to be associated with SCI pathology, that have a high expression in the spinal cord or that have been linked to a similar pathology such as TBI. As a consequence, SCI biomarker research has largely been biased towards the investigation of structural and inflammatory biomarkers. This approach yielded only limited success in identifying markers that can be used clinically and there is a strong need for the identification of additional candidate biomarkers. The heterogeneous nature of the SCI population further underscores the importance of a unbiased, high-throughput approach to identify the full spectrum of potential SCI biomarkers. With the innovation of high-throughput detection methods, such as multiplex analysis, metabolomics, proteomics and genomics, the field of biomarker research has progressed rapidly in many disease entities. Unfortunately, in SCI research, studies using the 'omics' approach are limited.

Proteomics approach to identify putative biomarkers for SCI

Proteomics is used to comprehend the relationship between different proteins and their expression profile in healthy and disease conditions to better understand the human pathophysiology, and ultimately to provide new therapeutic options and clinical tools. There are several limitations to the use of proteomic techniques such as the low sensitivity of 2D gel electrophoresis towards integral membrane proteins and the possible display of artifacts and protein degeneration due to sample collection and storage [89, 107, 108]. Still, high-throughput proteomics has emerged as an invaluable tool in the quest to unravel the biochemical changes (e.g. protein expression levels or structure), and is a powerful approach to identify novel biomarkers for SCI.

To our knowledge, only a few studies investigated protein biomarkers in SCI patients using proteomics [25, 109-112]. Sengupta et al. (2014) compared CSF of SCI patients with either complete injury (AIS A) or incomplete injury (AIS B or C) at an early time point (1-8 days post-injury), while Streijger et al. (2017) analyzed CSF samples of SCI patients acquired at 24, 48 and 72 hours post-injury. Both studies resulted in a description of protein changes in the CSF after acute human SCI and identified several protein candidates for further validation as potential biomarkers [111, 112]. At present, only Hergenroeder et al. (2015) studied the formation of autoantibodies in SCI patients via western blotting of human brain

homogenates followed by antibody target identification using mass spectrometry and demonstrated GFAP antibodies in subacute plasma samples [25]. Data from proteomic studies are valuable for SCI biomarker discovery, provided that these findings are further checked and validated in biofluids of SCI patients. Next to high-throughput immunoblotting and antigen microarrays, also other techniques such as phage display technology can be used to study the antibody profile for candidate biomarkers.

Phage display and serological antigen selection

Phage display is based on the potential of a filamentous phage particle to display exogenous proteins or peptides on the surface and is widely used to investigate protein-protein interactions, receptor- and antibody-binding sites, and for selecting antibodies against a range of antigens [113]. A disease-relevant system is created by the fusion of the entire cDNA of the target tissue to a gene encoding a phage coat protein, so that the phage display library is fully representative for the heterogeneity of genes present within the *in vivo* target tissue. Furthermore, the physical link between genotype and phenotype enables an easy identification of the expressed target. A limitation of the phage display technology is the lack of post-translational modifications on the displayed proteins as the bacterial protein machinery is used to generate proteins. Phage display methods have been based on the insertion of high diversity random peptide libraries (10^{10} independent clones). This approach only allows the detection of linear epitopes, identify many target-unrelated peptides and mimotypes, e.a. peptides forming epitopes that mimick the actual *in vivo* antigens. A labour-intensive characterization is required for the identification of the actual *in vivo* target antigen of the detected antibody. By using a cDNA library (10^6-10^7 clones) instead of a peptide library, key problems of previous methods are circumvented, rapid isolation of novel antibody targets is possible and generic antibody targets are identified by selection on patient samples. Moreover, cDNA libraries allow the identification of cell surface and secreted molecules as well as intracellular targets.

Pathology-specific autoantibodies can be identified from biofluids (e.g. blood or CSF) in an unbiased way via a procedure called serological antigen selection (SAS), a molecular approach based on cDNA phage display. Using SAS on human target tissue-based cDNA display libraries, we have successfully identified novel antibody targets in many diseases such as colorectal cancer [114], atherosclerotic

plaques [115], clinically isolated syndrome [116], multiple sclerosis (MS) [117, 118] and rheumatoid arthritis (RA) [119, 120]. The identification of novel antigenic targets in MS resulted in the discovery of Sperm Associated Antigen 16 (SPAG16) isoform 2. Initial characterization of SPAG16 as a candidate biomarker for MS revealed that anti-SPAG16 antibodies cannot only be found in CSF, but also in serum of MS patients. The serum levels of the anti-SPAG16 antibodies correlated with clinical characteristics of MS patients [121]. These results further emphasize the relevance of directly investigating candidate antibody biomarkers in serum of SCI patients. Moreover, we have not only demonstrated the diagnostic and prognostic value of these serum antibody biomarkers [117-119] but also the pathogenic *in vivo* relevance of these novel antibodies [122].

Altogether, by selecting antibodies in SCI patient samples for reactivity against a cDNA library from specific target tissue, SAS is a powerful and unbiased screening method to identify novel (auto)antibodies and corresponding antigenic targets with pathologic relevance for SCI. These novel antibodies might not only serve as potential SCI biomarkers, but additionally hint to new antibody-based therapeutic options for SCI pathology.

1.3 AIMS OF THE STUDY

As the current diagnostic and prognostic tools have various limitations and candidate biomarkers lack sensitivity and correlation to clinical data, there is a clear need for novel clinically relevant disease markers for SCI patients. Antibodies generally represent good biomarkers and it has been shown that they contribute to SCI-induced degenerative processes, therefore, the goal of this study was to determine the antibody reactivity profile after SCI using SAS to identify novel disease markers for SCI patients and to discover biological relevant antibody responses.

AIM 1: Discovery of novel disease markers for SCI patients by application of the SAS procedure

A prerequisite for the application of the SAS procedure is the construction of a high diversity cDNA phage display library which is representative for the antigenic repertoire of the human spinal cord. **Chapter 2** provides an overview of the construction and detailed characterization of our newly generated cDNA phage display library. As described in **Chapter 3**, this human spinal cord cDNA phage display library was screened for antibody reactivity using SAS with pooled plasma from traumatic SCI patients. Enriched phage clones represent novel antibody targets and were evaluated for their prevalence in SCI patients and controls using phage ELISA.

AIM 2: Clinical validation of the novel identified antibody responses

An SCI-associated panel of 6 antigenic targets was identified using the SAS procedure and phage ELISA screening. In order to validate the clinical relevance of these newly identified antibody responses in SCI patients, the phage-mediated research test was translated into high-throughput and sensitive peptide ELISA (**Chapter 4**). Assay validation screening revealed UH.SCI.2 and UH.SCI.7 as the most interesting antigenic targets and BLAST analysis showed correspondence to parts of the proteins 26S proteasome non-ATPase regulatory subunit 4 (PSMD4) and S100B, respectively. Using recombinant peptides and proteins in competition ELISA, we confirmed the *in vivo* target identity of both antibody responses. In **Chapter 5**, we validated the prevalence of PSMD4 and S100B autoantibody responses in our early SCI cohort (samples collected within 1 year after

injury/surgery), containing follow-up samples of both traumatic and pathologic SCI patients. The course of these autoantibodies was investigated by comparing antibody reactivity in healthy controls, our early traumatic SCI cohort and chronic traumatic SCI patients (samples collected >1 year after injury). Next, the presence and levels of both autoantibodies were analyzed for correlations with general patient characteristics and prognostic parameters. Finally, the disease specificity of PSMD4 and S100B autoantibodies was determined by screening plasma samples of healthy controls and patients with distinct pathologies (e.g. stroke, MS and RA).

AIM 3: Characterization of the biological relevance of PSMD4 autoantibodies in SCI

PSMD4 autoantibodies have not been previously reported in SCI pathology and therefore, further characterization of these autoantibody responses may provide more insight into the underlying pathology. In **Chapter 6**, the biological relevance of the PSMD4 autoantibody response and its associated *in vivo* target was addressed in the context of SCI. Therefore, the expression profile of PSMD4 was investigated in normal human spinal cord tissue and SCI and healthy spinal cord tissue of mice. Furthermore, by performing a passive transfer experiment of C-terminal mouse PSMD4 antibodies in a T-cut hemisection SCI animal model, the *in vivo* effect of these antibodies on the functional recovery after SCI was observed. By investigating the biological relevance of PSMD4 autoantibody responses and the *in vivo* target, more insight into the role of antibodies in SCI pathology will be obtained.

2

The construction and detailed characterization of a human spinal cord cDNA phage display library

Based on:
The Next Generation of Biomarker Research in Spinal Cord Injury.
Ydens E*, Palmers I*, Hendrix S, Somers V.
*Authors contribute equally
Published in Molecular Neurobiology (2017 Mar;54(2):1482-1499)

2.1 ABSTRACT

Phage display has proven to be a powerful technology to study protein interactions for novel targets or drug discovery. In this chapter, the construction of a high-quality cDNA phage display library derived from normal human spinal cord tissue is described. Characterization of the novel cDNA library demonstrated a total library size of 6.32 $x10^6$ independent clones with a high variety of insert lengths. Sequencing analysis identified cDNA inserts encoding intracellular, membrane and extracellular proteins involved in a variety of general biological processes as well as neuroinflammatory-related responses (e.g. immune response, response to stress and apoptosis). In conclusion, our newly generated, high diversity cDNA library represents the *in vivo* antigenic repertoire of the spinal cord, resulting in a platform suitable for the identification of the autoantibody profile in spinal cord injury (SCI) patients.

2.2 INTRODUCTION

Since 1985, phage display technology has been successfully applied to express exogenous proteins or peptides on the phage surface, allowing the investigation of for example therapeutic antibodies, peptides and vaccines [123-125]. The strength of this technology lies within the physical link between genotype and phenotype, which enables sequential rounds of specific target enrichment followed by easy target identification via DNA sequencing. Additionally, the use of large diversity peptide (10^{10} independent clones) or cDNA (10^6-10^7 clones) libraries enhances the chance for identifying relevant, high-affinity protein interactions, which is important for phage display applications such as epitope mapping of antibodies. Phage display, furthermore, circumvents issues related to the gel-based high-throughput techniques such as the denaturation of target peptides or proteins.

Phage display can be performed using different types of bacteriophage such as filamentous M13 phage, the temperate lambda phage or the lytic T7 phage. Filamentous bacteriophages belong to the *Inoviridae* family and infect host cells (e.g. *Escherichia coli* (*E.coli*)) via attachment with the F pili. Upon entry, the bacteriophage genome is replicated by the host cell machinery and in phage display conditions genes encoding coat proteins are provided by helper phage superinfection. Subsequently, functional phage particles are formed and extruded at the bacterial plasma membrane without lysis of the host cell. Filamentous bacteriophage have a rod-like shape (approximately 900 nm in length and 6 nm in width) and their single-stranded circular DNA genome is enclosed in a protein capsid, composed of minor (pIII, pVI, pVII and pIX) and major coat proteins (pVIII) [126, 127]. In phage display, the size limit of the fused peptide or protein as well as the number of copies on the surface of the phage is determined by the coat protein. Major coat protein pVIII and minor coat protein pIII are most commonly used for display purposes and their fusions are formed at the N-terminal side. Fusion of cDNA at the N-terminus hinders the formation of a fusion protein due to the presence of an endogenous stop codon [123]. Fusions to minor coat protein pVI, however, can occur at the outwardly directed C-terminal end, enabling the expression of full-length cDNA libraries. This display mode is monovalent (one cDNA product per phage particle), which allows the formation of high-affinity interactions and was successfully applied by Jespers et al. (1995) to isolate serine protease inhibitors as well as by our research group to construct

cDNA libraries expressing antigens of a colorectal cancer or autoantigens of rheumatoid arthritis, multiple sclerosis and clinically isolated syndrome [120, 128-133]. In this chapter, the construction and detailed characterization of a novel human spinal cord (hSC) cDNA phage display library via fusion to minor coat protein pVI is described to study the antibody repertoire in spinal cord injury (SCI) patients.

2.3 MATERIALS AND METHODS

2.3.1 Construction of a hSC cDNA display library

Commercially derived poly (A+) RNA (5-10 µg, size range of 0.2-10 kb, Clontech, Saint-Germain-en-Laye, France) from normal spinal cord tissue of 18 Caucasians (ages 25-63 years) was converted to double-stranded cDNA flanked with EcoRI and XhoI restriction sites by using the Superscript Choice System for cDNA synthesis kit (Life Technologies, Gent, Belgium) as described by the manufacturer with minor modifications. Five µg human spinal cord poly (A+) RNA was incubated with an oligo(dT) primer with a XhoI restriction site (5'-GAGAGAGAGAGAGAGAGAGAACTAGTCTCGAGTTTTTTTTTTTTTTTTT-3', Eurogentec, Serain, Belgium) at 70°C for 10 minutes (min) and quickly chilled on ice to remove possible secondary structures in the RNA template. Next, first-strand buffer, nucleotide mix (100 mM dATP/dGTP/dTTP (Roche Diagnostics, Vilvoorde, Belgium), 10 mM methylated dCTP (Gentaur, Aachen, Germany)) and 10 mM dithiothreitol (DTT) were added and preheated at 37°C for 2 min. Methylated dCTPs were incorporated during the first-strand synthesis reaction to protect the cDNA from restriction digestion in subsequent reactions. The first-strand synthesis reaction was started by addition of 1000 units (U) of SuperScript II reverse transcriptase and incubated for 1 hour (h) at 37°C. For the second-strand synthesis, second-strand buffer, dNTP mix (10 mM dATP/dGTP/dTTP and 26 mM dCTP (Roche Diagnostics, Vilvoorde, Belgium)), 10 U *E.coli* DNA ligase, 40 U *E. coli* DNA Polymerase I and 2 U *E. coli* RNase H were added to the first-strand reaction. After 2 h of incubation at 16°C, the resulting double-stranded cDNA was blunted by addition of 10 U T4 DNA Polymerase for 15 min at 16°C and cDNA fragments were purified from the reaction mixture by phenol/chloroform/isoamyl alcohol (25:24:1) extraction and ethanol precipitation. EcoRI adapters were ligated to the cDNA inserts at 16°C for a minimum of 16 h. Next, cDNA inserts were phosphorylated by T4 Polynucleotide kinase (30 U) at 37°C for 30 min followed by a XhoI restriction (Promega, Leiden, the Netherlands) which resulted in double-stranded cDNA fragments with an overhanging EcoRI at the 5' side and XhoI at the 3' side. cDNA fragments were purified using the illustra GFX PCR DNA and Gel Band Purification Kit (GE Healthcare Life Sciences, Diegem, Belgium) and directionally ligated into pVI phage display vector, pSPVIC, cut with EcoRI and XhoI. After amplification of the primary pSPVIC library, cDNA inserts were

restricted out of the vector by using EcoRI and XhoI and subcloned into pSPVIA and pSPVIB. In this way, cDNA inserts are present in the three different reading frames (by addition of 1 or 2 nucleotides), ensuring that in-frame expression of the inserts occurs in one of the vectors [134]. By cloning the cDNA products into the phagemid as a 3' fusion of gene VI, corresponding peptide/protein products are displayed at the surface of the filamentous phage, fused to the C-terminus of minor coat protein pVI (figure 2.1). Ligation mixtures were used to transform *E. coli* TG1 cells ([F' *traD36 proAB lacIqZ ΔM15] supE thi-1 Δ(lac-proAB) Δ(mcrB-hsdSM)5(rK - mK -)*; Lucigen, Middleton, United States) by electroporation. All resulting colonies were scraped and pooled to obtain separate pSPVIA, pSPVIB and pSPVIC libraries. Dilutions of electroporated bacteria were plated onto Difco lysogeny broth agar (Invitrogen, Merelbeke, Belgium) plates with 100 µg/ml ampicilline (Sigma-Aldrich, Overijse, Belgium) to determine the titer of the libraries (number of colony forming units, cfu).

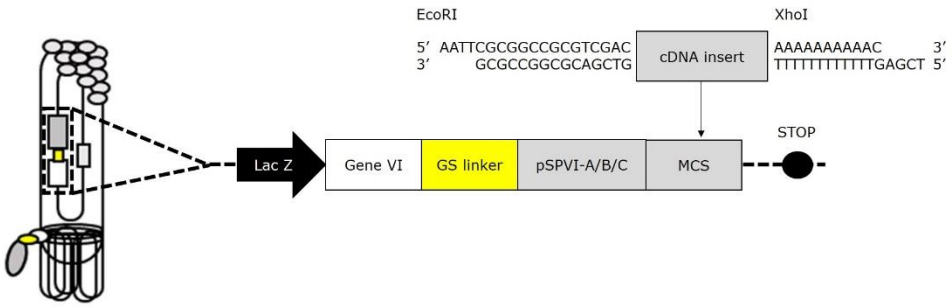

Figure 2.1: M13 Gene VI phage display

Double-stranded cDNA fragments with EcoRI/XhoI adapters were directionally cloned with the M13 phage gene VI, resulting in the expression of the corresponding protein as a C-terminal fusion of M13 minor coat protein pVI at the surface of the filamentous phage. GS, glycine/serine linker; MCS, multiple cloning site.

2.3.2 Insert PCR and sequencing analysis of the hSC-pSPVI library

For each analyzed bacterial clone, the cDNA insert and a part of gene VI flanking it, were amplified via a colony PCR reaction with vector primers (forward primer 5'-ttaccctctgactttgttca-3' and reverse primer 5'-cgccagggttttcccagtcacgac-3' (Eurogentec, Seraing, Belgium)). A small amount of cells from a bacterial colony was added to a PCR mix consisting of 10 pmol forward and reverse primer, PCR

buffer (Roche Diagnositics, Vilvoorde, Belgium), 12.5 pmol dNTP's (Roche Diagnostics, Vilvoorde, Belgium) and 2 U TAQ DNA polymerase (Roche Diagnostics, Vilvoorde, Belgium). After an initial denaturation step (10 min at 95°C), cDNA inserts were amplified for 35 cycles (30 seconds (s) at 95°C, 30 s at 55 °C and 1 min at 72°C) and analyzed on a 2% agarose gel. cDNA inserts of the hSC cDNA library were identified by sequencing. Insert PCR products were purified using ExoSAP-IT (Fisher Scientific, Erembodegem, Belgium) to remove remaining primers and dNTPs. Cycle sequencing reactions (30 s at 96°C followed by 35 cycles (10 s at 96 °C, 5 s at 50°C, 3 min at 60°C) and 10 min at 60°C) were performed on purified insert PCR product with gene VI primer (2 pmol/µl, 5'-ctcccgtctaatgcgcttc-3') and Big Dye TMT Terminator Cycle Sequence Ready Reaction Kit II (Applied Biosystems, Warrington, United Kingdom). The sequencing reaction was ethanol precipitated and analyzed on ABI Prism 310 Genetic Analyzer (Applied Biosystems). The basic local alignment search tool (BLAST) of the National Center for Biotechnology (NCBI) was used to compare nucleotide and amino acid sequences of cDNA inserts with public nucleotide and protein databases (http://blast.ncbi.nlm.nih.gov).

2.4 RESULTS

In order to investigate the antibody repertoire present in SCI patients, a novel cDNA phage display library from normal human spinal cord tissue was constructed. An outline of the construction of the library is shown in figure 2.2. Commercially derived poly (A+) RNA of human spinal cord was converted to double-stranded cDNA using oligo(dT) primers. The resulting cDNA inserts were directionally ligated into the pVI phage display vectors, namely pSPVIA/B/C. These display vectors allow fusion of the cDNA insert to the filamentous phage gene VI in three different reading frames, ensuring that in-frame expression of the inserts occurs in one out of the three vectors. The generated hSC-pSPVIA, hSC-pSPVIB and hSC-pSPVIC phage display libraries had a primary diversity of 7.42×10^6, 1.44×10^6 and 2.44×10^6 clones, respectively, showing a high diversity in the 3 libraries. When combined, this results in a phage display library with a primary diversity of 6.32×10^6 different clones.

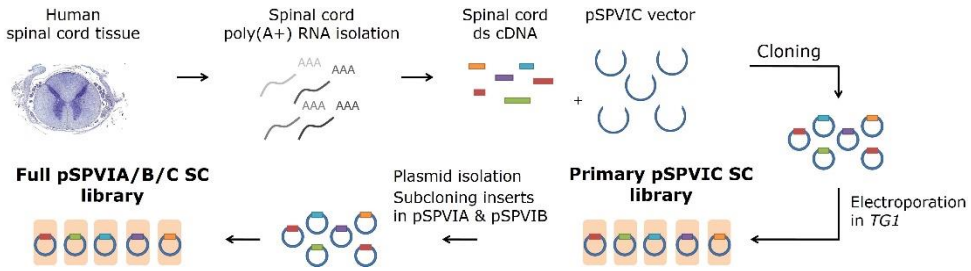

Figure 2.2: Construction of a hSC cDNA phage display library

Poly (A+) RNA obtained from healthy human spinal cord tissue was converted to double-stranded cDNA fragments which were cloned into phagemid vector pSPVIC (primary pSPVIC spinal cord (SC) library). After quality evaluation of the primary SC library, cDNA inserts were isolated and subcloned into pSPVIA and pSPVIB. Cloning of the cDNA library occurred by fusion of cDNA fragments to the 3' end of gene VI (encoding minor coat protein pVI), which resulted in 3 cDNA display libraries (full pSPVIA/B/C SC library) allowing expression of the cDNA inserts in three readings frames. ds, double-stranded; TG1, *Escherichia coli* TG1 cells.

By cloning the cDNA as a 3' fusion of gene VI, corresponding peptide/protein products are displayed at the surface of the filamentous phage, fused to the C-terminus of minor coat protein pVI. In order to investigate the length of the cDNA inserts, PCR amplification of more than 250 randomly selected clones from each

of the three hSC cDNA libraries was performed. These results show that all three libraries had a high variety of lengths ranging from 350 to >1600 base pairs and that the frequency of PCR products with a similar length was comparable in the 3 hSC cDNA libraries (figure 2.3).

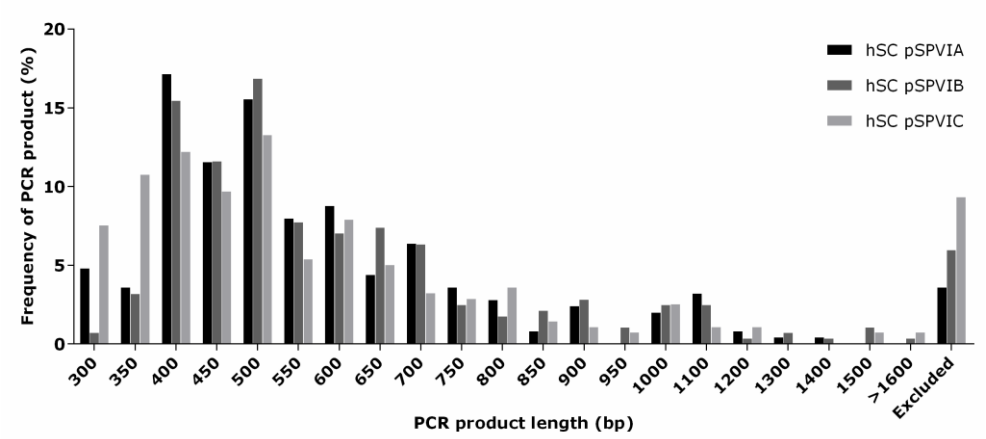

Figure 2.3: Diversity of the hSC cDNA libraries

PCR analysis was performed on random clones of each human spinal cord (hSC) cDNA library (hSC pSPVIA n= 253; hSC pSPVIB n= 285; hSC pSPVIC n= 281). PCR products with a length of 300 base pairs (bp) correspond to the empty vector and products with an unclear or double band were excluded from the analysis.

To further asses the quality and diversity of the hSC cDNA libraries, equal amounts of the hSC-pSPVIA, hSC-pSPVIB and hSC-pSPVIC were mixed and a small fraction of randomly selected clones were sequenced (table 2.1). The nucleotide sequences were compared to GenBank databases with the BLAST software of NCBI (http://blast.ncbi.nlm.nih.gov/Blast.cgi). This allowed us to analyze the distribution of pSPVIA, -B and -C vectors in the full library, and provides insight in the different genes that are cloned in the library, the exact position of their fusion to gene VI and the percentage of clones that express cDNA in frame with gene VI, resulting in the display of a human protein on the phage surface. The sequenced clones demonstrated a slightly increased presence of the pSPVIA (44 %) phagemid vector in comparison with pSPVIB (21 %) and pSPVIC (34 %) (figure 2.4a). Of the clones with an insert arising from messenger RNA (mRNA), 2 contained a sequence starting in the 5' untranslated region (UTR) of the cDNA

(2%), 17 in the coding region (15%) and 45 in the 3'UTR (39%). Sixty-one % of the cDNA inserts with a fusion in the coding region were cloned in frame with M13 gene VI with 1 clone encoding the full-length cDNA sequence of Homo sapiens ribosomal protein L37a (RPL37A). From the remaining clones, cDNA inserts originated from ribosomal RNA (rRNA) (13 clones, 11%), genomic DNA (22 clones, 19%) or represented other sequences (16 clones, 14%) (figure 2.4b).

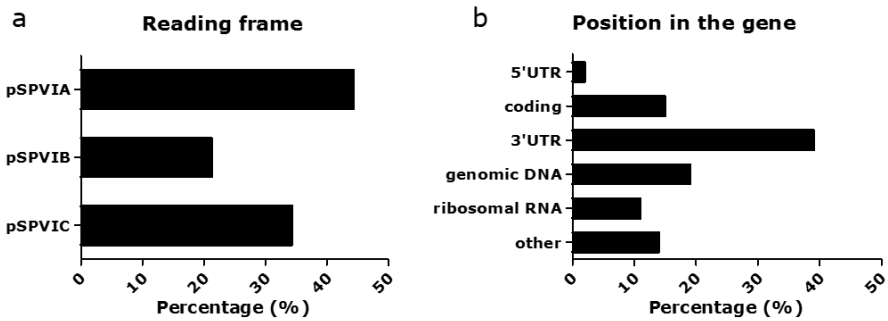

Figure 2.4: Characterization of the hSC cDNA library

The reading frame distribution was analyzed for all 160 sequenced clones (a). The origin of the cDNA insert (b) could be determined for 116 clones. UTR, untranslated region.

Most of the cDNA sequences identified genes encoding known and characterized proteins. While the majority of the genes encoded for intracellular proteins (73%), also a large proportion of genes whose product is membrane-bound (17%) or secreted (10%) were found (figure 2.5a). Several of the identified gene products were located both intracellularly and at the membrane, such as A-kinase anchoring protein 13 (AKAP13) and phosphatidylinositol-5-phosphate 4-kinase type 2 alpha (PIP4K2A). Of the intracellular proteins, 57% were specifically located to the cytoplasm, such as phosphoprotein enriched in astrocytes (PEA) 15, dysbindin domain containing (DBNDD) 2 and kelch-like family member (KLHL) 42, and 26% were nuclear proteins, such as transcription factor binding to IGHM enhancer (TFE) 3 and zinc finger E-box binding homeobox 1 (ZEB1). Moreover, genes encoding proteins specific to the endoplasmic reticulum (10%), mitochondria (10%), golgi complex (3%) and endosomes (2%) were identified, which shows that gene products of a wide variety of cellular components were represented in the hSC cDNA library. Approximately 10% of the sequenced genes

encoded extracellular proteins that were secreted including meteorin, glial cell differentiation regulator (METRN) and stimulator of chondrogenesis 1 (SCRG1). Furthermore, the identified genes were also involved in a variety of general biological processes (figure 2.5b) such as signal transduction (2%) (e.g. phospholipase A2 group IIA (PLA2G2A)), cell cycle (14%) (e.g. tetratricopeptide repeat domain 19 (TTC19)), transport and cellular processes (16%) (e.g. hemoglobin subunit alpha 1 (HBA1) and adaptor related protein complex 3 sigma 2 subunit (AP3S2)), metabolic and biosynthetic processes (17%) (e.g. aldolase, fructose-bisphosphate C (ALDOC)) and transcription and translation (22%) (e.g. RNA binding motif single stranded interacting protein 1 (RBMS1)). Sequences encoding genes with a nervous system specific expression pattern were also present (10%), such as myelin basic protein (MBP) and glial fibrillary acidic protein (GFAP), indicating that the constructed hSC cDNA library is a valuable source for the identification of nervous system specific antibody responses. Despite the use of normal spinal cord tissue for the construction of the cDNA library, genes encoding proteins involved in the immune response and response to stress (21%) (e.g. Rho/Rac guanine nucleotide exchange factor 2 (ARHGEF2) and heat shock protein 90 alpha family class A member 1 (HSP90AA1)) and apoptosis (5%) (e.g. cell division cycle associated 7 (CDCA7)) were also present. It is therefore quite likely that the constructed hSC cDNA library also allows identification of antigenic targets of the SCI-induced secondary processes. Besides the identification of genes encoding known proteins, also sequences encoding proteins with an as yet unidentified function were found, which underscores the benefits of using phage display technology as an unbiased approach.

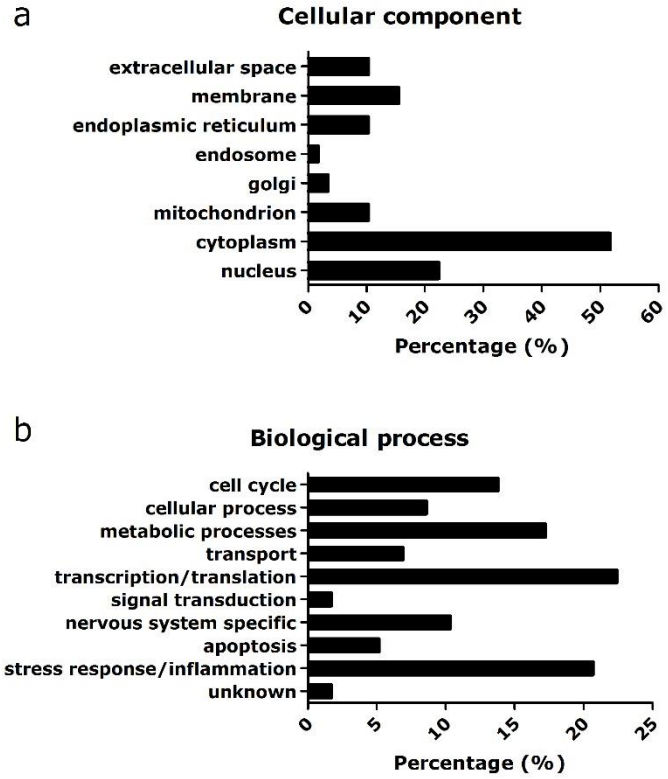

Figure 2.5: Gene ontology of the identified gene sequences

Bar charts depict the distribution of the identified genes (58 clones) within the library in terms of cellular localization (a) and biological process (b). Due to the multiple overlapping cellular localizations and biological processes of some of the genes, the total percentage in each chart is greater than 100.

Table 2.1: cDNA sequences identified in the new hSC cDNA library

Clone	NCBI code	cDNA identity
SCI-1	NM_001161727.1	Homo sapiens phospholipase A2 group IIA (PLA2G2A)
SCI-2	NM_002792.3	Homo sapiens proteasome subunit alpha 7 (PSMA7)
SCI-3	NM_001305626.1	Homo sapiens calmodulin 2 (CALM2)
SCI-4	NM_021109.3	Homo sapiens thymosin beta 4, X-linked (TMSB4X)
SCI-5	NM_201384.2	Homo sapiens plectin (PLEC)
SCI-6	NM_001318906.1	Homo sapiens glutamate dehydrogenase 1 (GLUD1)
SCI-7	NM.014167.4	Homo sapiens coiled-coil domain containing 59 (CCDC59/TAP26)
SCI-8	NM_000558.4	Homo sapiens hemoglobin subunit alpha 1 (HBA1)
SCI-9	NM_002897.4	Homo sapiens RNA binding motif single stranded interacting protein 1 (RBMS1)
SCI-10	NM_005165.2	Homo sapiens aldolase, fructose-bisphosphate C (ALDOC)
SCI-11	NM_001004.3	Homo sapiens ribosomal protein lateral stalk subunit P2 (RPLP2)
SCI-12	NM_004928.2	Homo sapiens chromosome 21 open reading frame 2 (C21orf2)
SCI-13	NM_000998.4	Homo sapiens ribosomal protein L37a (RPL37A)
SCI-14	NM_005905.5	Homo sapiens SMAD family member 9 (SMAD9)

SCI-15	NM_001404.4	Homo sapiens eukaryotic translation elongation factor 1 gamma (EEF1G)
SCI-16	NM_005252.3	Homo sapiens Fos proto-oncogene, AP-1 transcription factor subunit (FOS)
SCI-17	NM_007281.3	Homo sapiens stimulator of chondrogenesis 1 (SCRG1)
SCI-18	NM_153234.4	Homo sapiens limb and CNS expressed 1 (LIX1)
SCI-19	NM_001164732.1	Homo sapiens receptor accessory protein 1 (REEP1)
SCI-20	NM_001271420.1	Homo sapiens tetratricopeptide repeat domain 19 (TTC19)
SCI-21	NM_004107.4	Homo sapiens Fc fragment of IgG receptor and transporter (FCGRT)
SCI-22	BC013086.1	Homo sapiens TIMP metallopeptidase inhibitor 3 (TIMP3)
SCI-23	NM_001162384.1	Homo sapiens Rho/Rac guanine nucleotide exchange factor 2 (ARHGEF2)
SCI-24	NM_001329749.1	Homo sapiens N-terminal EF-hand calcium binding protein 2 (NECAB2)
SCI-25	NM_018710.2	Homo sapiens transmembrane protein 55A (TMEM55A)
SCI-26	NM_001253383.1	Homo sapiens ribosomal protein L15 (RPL15)
SCI-27	NM_006738.5	Homo sapiens A-kinase anchoring protein 13 (AKAP13)
SCI-28	JX171109.1	Homo sapiens isolate diabetic patient 33 mitochondrion (ATP6)
SCI-29	NM_004545.3	Homo sapiens NADH:ubiquinone oxidoreductase subunit B1 (NDUFB1)
SCI-30	NM_003350.2	Homo sapiens ubiquitin conjugating enzyme E2 V2 (UBE2V2)
SCI-31	NM_001301856.1	Homo sapiens ELOVL fatty acid elongase 5 (ELOVL5)
SCI-32	NM_005348.3	Homo sapiens heat shock protein 90 alpha family class A member 1 (HSP90AA1)
SCI-33	NM_001306213.1	Homo sapiens thrombospondin 4 (THBS4)
SCI-34	NM_031942.4	Homo sapiens cell division cycle associated 7 (CDCA7)
SCI-35	NM_001309443.1	Homo sapiens secreted protein acidic and cysteine rich (SPARC)
SCI-36	NM_001113349.1	Homo sapiens endothelin converting enzyme 1 (ECE1)
SCI-37	NM_002055.4	Homo sapiens glial fibrillary acidic protein (GFAP)
SCI-38	NM_001010.2	Homo sapiens ribosomal protein S6 (RPS6)
SCI-39	NM_001048224.2	Homo sapiens dysbindin domain containing 2 (DBNDD2)
SCI-40	NM_001281720.1	Homo sapiens ubiquitin B (UBB)
SCI-41	NM_020782.1	Homo sapiens kelch like family member 42 (KLHL42)
SCI-42	NM_001303043.1	Homo sapiens TSC22 domain family member 4 (TSC22D4)
SCI-43	NM_024042.3	Homo sapiens meteorin, glial cell differentiation regulator (METRN)
SCI-44	NM_001292016.1	Homo sapiens TNFAIP3 interacting protein 2 (TNIP2)
SCI-45	NM_002385.2	Homo sapiens myelin basic protein (MBP)
SCI-46	NM_001286272.1	Homo sapiens tumor protein, translationally-controlled 1 (TPT1)
SCI-47	NM_001297578.1	Homo sapiens phosphoprotein enriched in astrocytes 15 (PEA15)
SCI-48	NM_005557.3	Homo sapiens keratin 16 (KRT16)
SCI-49	NM_001265591.1	Homo sapiens reticulon 3 (RTN3)
SCI-50	NM_001318219.1	Homo sapiens centrosomal protein 250 (CEP250)
SCI-51	NM_001282142.1	Homo sapiens transcription factor binding to IGHM enhancer 3 (TFE3)
SCI-52	NM_001323654.1	Homo sapiens zinc finger E-box binding homeobox 1 (ZEB1)
SCI-53	NM_001330631.1	Homo sapiens calpastatin (CAST)
SCI-54	NM_001330062.1	Homo sapiens phosphatidylinositol-5-phosphate 4-kinase type 2 alpha (PIP4K2A)
SCI-55	NM_005829.4	Homo sapiens adaptor related protein complex 3 sigma 2 subunit (AP3S2)
SCI-56	NM_003133.5	Homo sapiens signal recognition particle 9kDa (SRP9)
SCI-57	NM_001319035.1	Homo sapiens telomerase associated protein 1 (TEP1)
SCI-58	NM_030791.3	Homo sapiens sphingosine-1-phosphate phosphatase 1 (SGPP1)

2.5 DISCUSSION

In this chapter, the construction and characterization of our novel highly diverse hSC cDNA phage display library is described. An important component that determines the generation of a high-quality cDNA library is the origin of the starting material. Since antigen expression profiles may differ between individuals and the SCI patient population is very heterogeneous, mRNA from spinal cord tissue of 18 Caucasians was used to increase the chance for identifying antigenic sequences relevant within SCI pathology. While the antigenic complexity of damaged human spinal cord tissue might be higher, this type of material is very hard to obtain, and therefore, we used healthy spinal cord tissue for the construction of the cDNA library. Nevertheless, sequencing of our newly generated normal hSC cDNA library demonstrated cDNA inserts encoding intracellular, membrane-bound and extracellular proteins involved in a variety of biological processes, including SCI-induced secondary processes (e.g. immune response, response to stress and apoptosis). Additionally, Ankeny et al. demonstrated that SCI-induced antibodies can elicit neurotoxic effects in healthy spinal cord tissue, which suggests that the antigens that SCI-induced antibodies react against are present in an undamaged, healthy spinal cord [15, 17].

A high-quality cDNA library is characterized by a large diversity of cDNA inserts. Our hSC cDNA library resulted in a total library size of 6.32 $x10^6$ independent clones with a high variety of insert lengths ranging from 50 to >1300 base pairs. Both partial and full-length protein encoding cDNA sequences were present in our cDNA library, with 61% of the coding cDNA inserts cloned in frame with phage gene VI. This high percentage of clones fused in frame is probably due to the limited amount of phage clones that was sequenced, because in general only 1/3 of the coding inserts are expected to be in frame with phage gene VI. In the human genome project an estimate of 19,000-20,500 protein coding genes were identified [135, 136]. Our hSC cDNA library has a diversity of 6.32 $x10^6$ independent clones and assuming that approximately 5% of the cDNA inserts is coding and in frame with phage gene VI, each gene approximately has a 16-fold coverage on average, which highlights that also genes with low expression will be represented in our hSC cDNA library. Furthermore, cDNA inserts derived from the 3'UTR region of mRNA or genomic and ribosomal RNA resulted in the expression of random,

linear or conformational peptide sequences. Altogether, our hSC cDNA library consists of a highly diverse mix of cDNA sequences encoding partial and full-length proteins as well as random peptides.

In our newly generated hSC cDNA library, the majority of the cDNA inserts are located in the 3'UTR region and result in the expression of random epitopes. This limitation can be due to the reverse transcriptase enzyme used in the first-strand cDNA synthesis reaction or a suboptimal insert-vector ratio leading to preferential ligation of cDNA inserts with a certain length. By further optimization of the first-strand cDNA synthesis reaction and the vector-insert ratio for ligation, the frequency of full-length coding cDNA sequences can be increased in future cDNA library constructions. At present, peptide and protein arrays include random peptides and known full-length proteins, respectively, while phage display technology can offer the additional advantage of the expression of a mix of known and unknown proteins as well as peptides. Altogether, our newly generated highly diverse hSC cDNA library represents the *in vivo* antigenic repertoire of the spinal cord and forms an unbiased and high-throughput research platform for epitope mapping of SCI-induced antibodies.

3

Antibody profiling identifies novel antigenic targets in spinal cord injury patients

Based on:
Antibody profiling identifies novel antigenic targets in spinal cord injury patients
Palmers I, Ydens E, Put E, Depreitere B, Bongers-Janssen H, Pickkers P, Hendrix S, Somers V
Published in Journal of Neuroinflammation (2016;13(1):243)

3.1 ABSTRACT

Recent evidence implicates antibody responses as pivotal damaging factors in spinal cord injury (SCI)-induced neuroinflammation. To date, only a limited number of the antibody targets has been uncovered, and the discovery of novel targets with pathologic and clinical relevance still represents a major challenge. In this study we, therefore, applied an unbiased, innovative and powerful strategy, called serological antigen selection (SAS), to fully identify the complex information present within the antibody repertoire of SCI patients.

We constructed a high quality cDNA phage display library derived from human spinal cord tissue to screen for antibody reactivity in pooled plasma samples from traumatic SCI patients (n=10, identification cohort). By performing SAS, we identified a panel of 19 antigenic targets to which the individual samples of the plasma pool showed antibody reactivity. Sequence analysis to identify the selected antigenic targets uncovered 5 known proteins, to which antibody reactivity has not been associated with SCI before, as well as linear peptides. Immunoreactivity against 9 of the 19 novel identified targets was validated in 41 additional SCI patients and an equal number of age- and gender-matched healthy subjects. Overall, we found elevated antibody levels to at least 1 of the 9 targets in 51% of our total SCI patient cohort (n=51) with a specificity of 73%. By combining 6 of these 9 targets into a panel, an overall reactivity of approximately half of the SCI patients could be maintained while increasing the specificity to 82%. In conclusion, our innovative high-throughput approach resulted in the identification of previously unexplored antigenic targets with elevated immunoreactivity in more than 50% of the SCI patients. Characterization of the validated antibody responses and their targets will not only provide new insight into the underlying disease processes of SCI pathology, but also significantly contribute to uncovering potential antibody biomarkers for SCI patients.

3.2 INTRODUCTION

Neuroinflammation is a key process in SCI pathophysiology that can persist for months or even years after primary trauma. Its strong dual character in SCI underscores the need for an in-depth understanding of the complex neuroinflammatory processes [137-139]. While the responses mediated by innate immune cells and T cells have been extensively studied, the exact contribution of B cells and the humoral response that is triggered after SCI remains elusive. In experimental SCI, B cells accumulated in the injured spinal cord, formed follicle-like structures and contributed to aggravated tissue damage [15]. B cell-knockout mice displayed a highly improved neurological recovery and a markedly less pronounced neuropathology after SCI compared to wild type (WT) mice [17]. SCI-induced B cell activation culminated in the production of pathologic and central nervous system (CNS)-reactive antibodies which were released in the blood stream and migrated to the lesion [15, 17]. Passive transfer of serum antibodies from SCI mice into naive/uninjured mice showed that these SCI-induced antibodies participated in neuroinflammatory responses and exerted a degenerative effect in the spinal cord by causing cell death and sustained neurological dysfunction [15, 17]. A proteomics study on spinal cord tissue in mice indicated that more than 50 different proteins were targeted by antibodies after SCI, however, up to now only glutamate receptor 2/3 and nuclear antigens have been described as antibody targets in SCI models [15, 140].

In human SCI pathology, increased antibody responses to a number of CNS proteins (glial fibrillary acidic protein (GFAP), myelin basic protein (MBP)), glycoproteins (myelin associated glycoprotein (MAG)), glycolipids (GM_1 gangliosides) and nuclear antigens have been detected. The antibody titers to several of those myelin components remained elevated until years after the initial trauma [23-27, 29, 141]. Interestingly, the titers of these antibodies seemed to correlate with clinical parameters (e.g. SCI complications) [23, 24, 27]. Identification of the full spectrum of antigenic targets of the SCI-induced antibody responses is indispensable to develop passive and active antibody-based therapeutics or diagnostic and prognostic agents.

To date, only antibody responses to target antigens described in other CNS disorders have been investigated in SCI pathology. This hypothesis-driven approach yielded only limited success in identifying clinically relevant antibody

responses. The heterogeneous nature of the SCI population further underscores the importance of an innovative and unbiased approach, to fully explore the complex information present in the antibody repertoire of SCI patients. SAS is a powerful high-throughput method based on cDNA phage display and subsequent selection on patient antibodies which enables the identification of a broad profile of antigenic targets [120, 129, 134]. By using a cDNA phage display library derived from the target tissue, a disease-relevant system that is fully representative for the heterogeneity present within the target tissue, is created. This approach allows the identification of not only known proteins, but also of unknown or uncharacterized proteins. SAS has been successfully applied in our lab to identify an elaborate panel of novel relevant antibody responses for various diseases, such as multiple sclerosis, clinically isolated syndrome and rheumatoid arthritis [128, 130, 142]. We have not only demonstrated the pathologic *in vivo* relevance of these antibody responses but, also their diagnostic and prognostic potential [143-145].

In the present study, we constructed a high quality cDNA expression library from human spinal cord tissues which allowed rapid isolation of novel antigenic targets and identified generic antibody responses by using plasma samples from SCI patients. Subsequently, detailed serological characterization of these antibody responses was assessed in SCI patients and healthy controls.

3.3 MATERIALS AND METHODS

3.3.1 Patient samples

Peripheral blood was collected from traumatic and pathologic SCI patients in Jessa Hospital (Hasselt, Belgium), University Hospitals Leuven (Leuven, Belgium), Adelante Rehabilitation Centre (Hoensbroek, The Netherlands), Hospital East-Limburg (Genk, Belgium), Antwerp University Hospital (Edegem, Belgium), Radboud University Medical Centre (Nijmegen, The Netherlands), Academic Hospital Maastricht and General Hospital Turnhout (Turnhout, Belgium). Samples of traumatic SCI patients were taken at hospitalization (T0) or 3 weeks (T1) after injury. Samples of pathologic SCI patients (e.g. stenosis, spinal disc herniation, compression caused by bleeding) were collected preoperatively (T0) and 3 weeks after surgery (T1). Patients with pre-existing autoimmune disorders were excluded from the study. Written informed consent was acquired from all participants after approval by the Medical ethics committee Hospital East-Limburg (B371201317091), Adelante (54-14/CK/JM) and Academic Hospital Maastricht (METC13-4-079). Blood samples were centrifuged for 10 min at 400 g. Plasma was collected and centrifuged for 10 min at 1500 g. After processing, plasma samples were aliquoted and stored at -80°C. Samples were processed and stored in collaboration with the University Biobank Limburg (UBiLim) and Biobank University Hospitals Leuven. A total of 51 SCI patients and 49 age- and gender-matched healthy controls were involved in the study. Healthy control plasma samples together with information on demographics, relevant health issues (e.g. allergy, infectious/autoimmune disorders, SCI, etc.), vaccination, concomitant medication, smoking status and medical history of family members were collected via UBiLim.

3.3.2 Construction of a human spinal cord (hSC) cDNA phage display library

Commercially obtained poly A+ RNA (size range of 0.2-10 kb, Clontech, Saint-Germain-en-Laye, France) from spinal cord tissue of 18 Caucasians (ages 25-63 years) was converted to double-stranded cDNA with EcoRI and XhoI adapters by using the Superscript Choice System for cDNA synthesis kit (Life Technologies, Gent, Belgium) as described previously [146]. Purified cDNA inserts were directionally ligated into our pVI phage display vectors, pSPVIA, pSPVIB and pSPVIC, each representing 1 of 3 different reading frames [134]. Ligation mixtures

were used to transform *Escherichia coli* (*E.coli*) TG1 cells (Lucigen, Middleton, United States) by electroporation to obtain hSC-pSPVIA, hSC-pSPVIB and hSC-pSPVIC libraries. Infection of the pSPVIA/B/C SC bacterial library with helper phage resulted in the formation of phage particles displaying the antigenic repertoire present in spinal cord tissue.

3.3.3 Serological antigen selection procedure

The SAS procedure was performed as described previously [130, 134]. In brief, an immunotube (Nunc, Roskilde, Denmark) was coated overnight at 4°C with 10 µg/ml rabbit anti-human Immunoglobulin G (IgG, Dako, Glostrup, Denmark) in coating buffer (0.1 M sodium hydrogen carbonate, pH 9.6). After washing with 0.1% (v/v) phosphate buffered saline-Tween20 (PBS-T, 50 mM Tris, 150 mM sodium chloride, pH 7.5) and PBS, the immunotube was blocked with 2% (w/v) skimmed milk powder in PBS (MPBS) for 2 h at room temperature (RT). Plasma samples of 10 traumatic SCI patients were pooled and pre-adsorbed against *E. coli* and phage components, as described previously [134]. For the first selection round, equal numbers of phage particles from each hSC cDNA phage display library (hSC-pSPVI-A, hSC-pSPVI-B and hSC-pSPVI-C) were pre-incubated with the pre-adsorbed SCI plasma pool in 2% MPBS for 1.5 h at RT on a rotating platform [147]. After washing the immunotube, the pre-incubated phage-plasma mix was transferred to the coated tube on a rotating platform, followed by standing conditions at RT. Non-bound phage were removed by extensive washing of the immunotube with 0.1% PBS-T and PBS. Bound phage were eluted by adding 100 mM triethylamide (Sigma-Aldrich, Bornem, Belgium) to the immunotube for 10 min on a rotating platform and neutralized with 1 M Tris-HCl (pH 7.4). The output of each selection round was amplified by infection of *E. coli* TG1 bacteria and plated on 2x YT agar plates containing ampicillin and glucose (16 g/l bacto-tryptone, 10 g/l yeast extract, 5 g/l NaCl, 15 g/l bacto-agar, ampicillin at 100 µg/ml, and glucose at 2%). Five consecutive selection rounds were performed. To identify enriched cDNA clones, individual colonies were selected and insert cDNA fragments were amplified with vector primers binding adjacent to the cDNA insert followed by restriction enzyme digestion (BstNI (Roche Diagnostics, Vilvoorde, Belgium) and NspI (NEB, Leiden, The Netherlands)). Enriched cDNA products representing identical cDNA clones were selected and identified by sequencing of the corresponding cDNA phage insert. Amino acid sequences of identified clones

were compared to public protein databases of the national center for biotechnology information (NCBI) with Basic Local Alignment Search Tool (BLAST) analysis.

3.3.4 Phage Enzyme Linked Immunosorbent Assay (ELISA)

Antibody reactivity levels of individual plasma samples against selected phage clones were measured by phage ELISA. Ninety-six-well flat-bottom plates (Greiner Bio-One, Wemmel, Belgium) were coated overnight at 4°C with 5 µg/ml anti-M13 antibody (GE Health care, Diegem, Belgium) in coating buffer. Plates were washed twice with PBS and blocked with 5% MPBS for 2 h at 37°C, while shaking. After washing three times with 0.1% PBS-T and once with PBS, polyethylene glycol-purified phage displaying the candidate antigen (7×10^{11} colony forming units/ml) or empty phage (negative control) were added and incubated for 1 h at 37°C under static conditions followed by 30 min at RT, while shaking. Plates were washed and plasma samples (1/100 in 5% MPBS) were incubated for 1 h at 37°C under static conditions followed by 30 min at RT, while shaking. Washing steps were repeated and horseradish peroxidase human IgG-Fc fragment cross-adsorbed antibody (1/50,000, Bethyl laboratories, Montgomery, USA) was added for 1 h shaking at RT. 3,3',5,5' tetramethyl-benzidine dihydrochloride (TMB, Thermo Scientific, Erembodegem, Belgium) solution was added after washing the plates and the reactions were incubated in the dark for 11 min. The color reaction was stopped by adding 1.8 N H_2SO_4. Optical density (OD) signals were measured at 450 nm in a Microplate reader Infinite M1000 Pro (TECAN, Männedorf, Switzerland). Samples were considered positive when the general reactivity (OD(specific phage)/OD(empty phage)) was higher than 1.5 and the OD-value of a specific signal was above 0.1. Samples were tested in duplicate in a single ELISA experiment and experiments were performed independently for at least two times. Polyreactive samples (reactive to the empty phage) were excluded from the analysis.

3.3.5 Statistical analysis

Statistical analysis was performed using GraphPad Prism 6 XML (Graph Pad software, La Jolla, California, USA). Fisher's exact test was applied for the analysis of associations between the presence of antibody reactivity directed to particular antigenic targets or panels of targets and SCI patients. A p-value of <0.05 was considered statistically significant.

3.4 RESULTS

3.4.1 Antibody profiling of SCI plasma samples using SAS

A high quality hSC cDNA phage display library was generated from human spinal cord tissue of 18 Caucasians. Human spinal cord cDNA fragments were cloned into the pVI phage display vectors in three reading frames, resulting in a total library size of 6.32 $x10^6$ independent clones. The spinal cord cDNA inserts ranged from 50 to >1300 base pairs. Details of the performed quality controls are described in chapter 2. Altogether, these results showed that the hSC cDNA phage display library had a high quality and diversity. Subsequently, this hSC cDNA phage display library was screened for antibody reactivity using a plasma pool consisting of 10 randomly selected traumatic SCI patients (identification cohort; mean age 48 years (range from 27 to 85 years); table 3.1). In the identification cohort, both samples collected at hospitalization (i.e. within 48 hours after traumatic injury; T0) and 3 weeks after injury (T1) were included. The majority of the patients were men (9/10) and had a cervical level injury (6/9). Both injury severity and type (compression, contusion, fracture or laceration) were highly diverse within the pool. By using a heterogeneous plasma pool, the general patient population was represented and the detection of patient-specific immunoreactivity was limited.

To analyze the overall antibody reactivity profile in SCI patients, SAS was used. Five consecutive selection rounds were performed. After characterization of the selection output, a total of 38 enriched phage clones were selected which represent putative antigenic targets present after SCI.

Table 3.1: Characteristics of traumatic SCI patients used for the SAS procedure (identification cohort)

Patient	Time of sampling (T)[a]	Age (years)	Gender[b]	Location of injury[c]	Type of tSCI[d]
SCI.1	T0	27	M	T5	Laceration
SCI.2	T0	29	M	T6-10	Fracture
SCI.3	T0	37	M	C4-6	Contusion
SCI.4	T0	43	M	C4-5	Contusion
SCI.5	T0	54	M	C6	Fracture
SCI.6	T0	67	M	NA[e]	Compression
SCI.7	T1	33	M	C6-T2	Contusion
SCI.8	T1	29	M	C4	Contusion
SCI.9	T1	73	F	C1	Compression
SCI.10	T1	85	M	C6	Contusion

[a]T0, at hospitalization; T1, 3 weeks after injury
[b]F, female; M, male
[c]C, cervical; T, thoracic
[d]tSCI, traumatic spinal cord injury
[e]Not available

3.4.2 Antibody reactivity is increased in plasma of traumatic SCI patients

To confirm that the enriched phage clones were selected based on specific interactions with SCI patient antibodies and to characterize the reactivity toward the identified clones, a pilot screen was performed on the individual plasma samples from the 10 traumatic SCI patients used in the SAS procedure (identification cohort) and an equal number of age- and gender-matched healthy controls. As shown in figure 3.1, 19 phage clones showed antibody reactivity in 9 of the 10 traumatic SCI plasma samples, while no or low reactivity was detected in healthy controls, which demonstrates that SCI-related antibodies were identified. The remaining phage clones displayed no reactivity in traumatic SCI patients or reactivity in the control samples. SCI-reactive antigenic targets were annotated an UH.SCI.number (Hasselt University, SCI, clone number). Based on the level and abundance of the antibody responses, our results show that traumatic SCI patients have an increased reactivity toward the selected antigenic targets compared to the healthy control group.

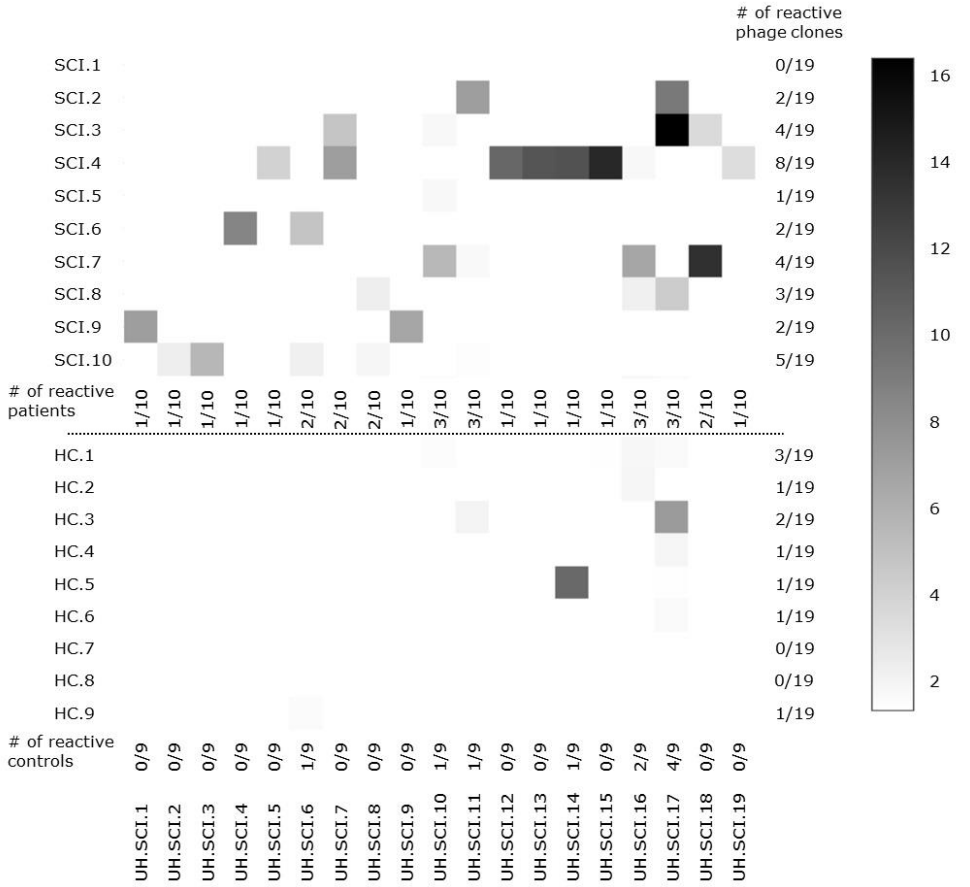

Figure 3.1: Increased antibody reactivity in plasma of traumatic SCI patients
Antibody reactivity toward the identified targets is increased in the individual traumatic SCI samples used in the SAS procedure (n=10) compared to healthy controls (HC, n=9). Samples were considered positive when the general reactivity (OD(specific phage)/OD(empty phage)) was higher than 1.5 and the specific signal was above 0.1. Antibody levels in positive samples are shown in a grey scale. Low antibody levels are indicated in light grey (ratio reactivity (OD(specific phage)/OD(empty phage)) is 2), high antibody levels are indicated in dark grey (ratio reactivity (OD(specific phage)/OD(empty phage)) ranged from 12 to 16). Samples were analyzed in duplicate in a single ELISA experiment and experiments were performed independently for at least 2 times.

3.4.3 Identity of antigens targeted by SCI-related antibodies

To gain insight into the antibody responses that are present after SCI, the targets of the selected antibody responses were identified using sequencing and the amino acid sequences of the 19 antigenic targets were compared to public protein

databases using BLAST analysis of NCBI (table 3.2). Five of the selected antigenic targets (UH.SCI.2, UH.SCI.5, UH.SCI.6, UH.SCI.7 and UH.SCI.19) encoded parts of known proteins: 26S proteasome non-ATPase regulatory subunit 4 (PSMD4), glyceraldehyde-3-phosphate dehydrogenase (GAPDH), myeloma-overexpressed gene 2 (MYEOV2), protein S100-B (S100B) and adipocyte enhancer-binding protein 1 (AEBP1). The remaining antigenic targets resulted from the expression of novel cDNA sequences, out of frame expression of known cDNAs or normally untranslated mRNA regions (e.g. 3'UTR regions). These expressed peptides likely form epitopes which structurally mimic *in vivo* antigens (mimotopes) and showed partial homology to proteins which might be implicated in brain disorders (e.g. ras/Rap GTPase-activating protein (SYNGAP1), to different known proteins (e.g. zinc finger protein 148 (ZN148) and receptor tyrosine-protein phosphatase eta (PTPRJ)), and to proteins with unknown function (e.g. transmembrane protein 236 (TMEM236)) [148]. Upon close examination of the different targets, it becomes clear that the identified antigenic targets are highly diverse with regard to their size (4 to 120 amino acids), sequence composition and amino acid characteristics (hydrophobic, polar or charged). This is also illustrated by the reactivity profile detected in an individual traumatic SCI patient (SCI.4), who shows specific and strong reactivity toward several targets (UH.SCI.5, UH.SCI.7, UH.SCI.12-15 and UH.SCI.19) which are diverse in sequence and structure characteristics. Altogether, our results demonstrate that antibody responses to a broad range of antigenic targets are present in SCI patients.

Table 3.2: Target identity of the SCI-related antibody responses

Clone	Translated cDNA product	Size (amino acids)	Homology on protein level
Coding			
UH.SCI.2	TEEDDYDVMQDPEFLQSVLENLPGVDPNNEAIRNAMGSLASQATKDGKKDKKEEDKK*	57	(56/56) 26S proteasome non-ATPase regulatory subunit 4 (PSMD4)
UH.SCI.5	HRVVDLMAHMASKE*	14	(13/13) Glyceraldehyde-3-phosphate dehydrogenase (GAPDH)
UH.SCI.6	TFPEGAGPYVDLDEAGGSTGLLMDLAANEKAVHADFFNDFEDLFDDDDIQ*	50	(49/50) Myeloma-overexpressed gene 2 protein (MYEOV2)
UH.SCI.7	HEFFEHE*	7	(7/7) Protein S100-B (S100B)
UH.SCI.19	PVETYTVNFGDF*	12	(11/11) Adipocyte enhancer-binding protein 1 (AEBP1)
Non-coding			
UH.SCI.1	IKTVTSQ*	7	(6/7) Transmembrane protein 236 (TMEM236)
UH.SCI.3	TNNFITSNKN*	10	(6/6) Calcium-activated chloride channel regulator 2 (CLCA2)
UH.SCI.4	PLKDIIDNI*	9	(6/6) Di-N-acetylchitobiase precursor (CTBS) (6/8) Poly(A)-specific ribonuclease PARN (PARN) (6/6) TBC1 domain family member 2B (TBC1D2B)
UH.SCI.8	NSSKTYVGTSDKVQTPSRDLGCPLGSHCSLSLLT*	34	No significant similarity found
UH.SCI.9	NSELLSNKSALHKFIKYAFWI*	21	(12/19) E3 ubiquitin-protein ligase HACE1 (HACE1)
UH.SCI.10	PFFTVPIPRPGA*	12	(8/8) F-box only protein 42 (FBXO42)
UH.SCI.11	EFFDNSRKVDD*	11	(6/8) Ras/Rap GTPase-activating protein SynGAP (SYNGAP1)
UH.SCI.12	NSKHSLKS*	8	(6/7) Zinc finger protein 148 (ZNF148)
UH.SCI.13	EDKT*	4	(4/4) Tax1-binding protein 3 (TAX1BP3)
UH.SCI.14	TQEGAGSERGVITTF*	15	(10/14) Receptor-type tyrosine-protein phosphatase eta (PTPRJ)
UH.SCI.15	TEGKEQERSDKDE*	13	(7/9) Espin (ESPN)
UH.SCI.16	QGEDKISVY*	9	(6/6) Midasin (MDN1)
UH.SCI.17	NSLHSLLGQKNND*	13	(10/13) Zinc finger protein 28 (ZNF28)
UH.SCI.18	QRLFRQSSSQELLGCGSKTLMGGEGWLLEEGRSQTGQTVLLTPSPAQRALPLWPLLQTPALTHTPLGLHSFALKDLPKSPFPCLASPLRRERYLQNWVGGMSMNCPSIWDMLHQSERENK	120	No significant similarity found

3.4.4 Validation of the identified antibody responses in SCI patients

Next, we addressed whether antibody reactivity toward the 19 novel antigenic targets was also present in a larger confirmatory cohort of SCI patients. Therefore, we screened 41 additional SCI patients from which samples collected within the same time range as the identification cohort samples were available. This allowed us to validate the identified antibody responses in a similar phase after injury. After large scale screening of the SCI patient samples and age- and gender-matched healthy controls, immunoreactivity against 9 of the 19 novel identified targets was validated. For 19/41 (46%) additional SCI patients, antibody reactivity was detected toward at least 1 of the 9 targets. The remaining targets were excluded because patient reactivity could not be confirmed in our validation cohort or high reactivity was detected in control samples.

Our total SCI cohort (identification and validation cohort) consisted of 51 SCI patients (82% males, mean age 57±16 years) and contained both traumatic and pathologic SCI patients. Furthermore, 49 age- and gender- matched controls (65% males, mean age 55±17 years) were included in the screening (table 3.3).

Table 3.3: Characteristics of the study populations

Cohort	Time of sampling (T)[a]	Mean age (in years)	Gender (F/M)[b]	AIS[c]	Location of injury[d]	tSCI/pSCI ratio[e]
Patients n=51	T0-T1	57	9/42	A-E	C-S	25/26
Healthy controls n=49	/	55	17/32	/	/	/

[a]T0, at hospitalization; T1, 3 weeks after injury or surgery
[b]F, female; M, male
[c]American Spinal Injury Association Impairment Scale
[d]C, cervical; S, sacral
[e]tSCI, traumatic spinal cord injury; pSCI, pathologic spinal cord injury

Of the total SCI cohort, 26/51 (51%) patients showed antibody reactivity to at least 1 of the 9 validated targets (table 3.4). The frequency of antibody reactivity against the individual targets within the SCI patients ranged from 4% to 20%. The highest reactivity and SCI-specificity was demonstrated using a panel of 6 targets. Immunoreactivity toward this SCI patient-associated antigen panel could be detected in approximately half of the SCI patients (47%) with an associated specificity of 82% (p=0.00145, table 3.4). For 1 of the individual antigenic targets, UH.SCI.9, a significant association was found between the presence of antibody

reactivity and SCI patients (p=0.0134; overall reactivity: 12%; specificity: 100%, table 3.4). Interestingly, while only traumatic SCI patients were included in the selection of SCI-related antibody responses, also 46% of the pathologic SCI patients showed increased immunoreactivity toward this panel of 6 novel identified targets (table 3.4).

Table 3.4: Antibody reactivity in the SCI cohort and age- and gender-matched healthy controls

Clone	Identification cohort (n=10)	Validation cohort (n=41)	Total cohort (n=51)			HC[c] (n=49)	Fisher's exact test (p-value)[d]
			tSCI[a] (n=25)	pSCI[b] (n=26)	Total (n=51)		
UH.SCI.1	1/10 (10%)	3/41 (7%)	2/25 (8%)	2/26 (8%)	4/51 (8%)	2/49 (4%)	ns
UH.SCI.2	1/10 (10%)	4/41 (10%)	2/25 (8%)	3/26 (12%)	5/51 (10%)	1/49 (2%)	ns
UH.SCI.7	2/10 (20%)	2/41 (5%)	2/25 (8%)	2/26 (8%)	4/51 (8%)	2/49 (4%)	ns
UH.SCI.8	2/10 (20%)	1/41 (2%)	2/25 (8%)	1/26 (4%)	3/51 (6%)	2/49 (4%)	ns
UH.SCI.9	1/10 (10%)	5/41 (12%)	3/25 (12%)	3/26 (12%)	6/51 (12%)	0/49 (0%)	0.0134
UH.SCI.11	3/10 (30%)	7/41 (17%)	5/25 (20%)	5/26 (19%)	10/51 (20%)	5/49 (10%)	ns
UH.SCI.12	1/10 (10%)	1/41 (2%)	1/25 (4%)	1/26 (4%)	2/51 (4%)	0/49 (0%)	ns
UH.SCI.13	1/10 (10%)	1/41 (2%)	1/25 (4%)	1/26 (4%)	2/51 (4%)	1/49 (2%)	ns
UH.SCI.15	1/10 (10%)	4/41 (10%)	3/25 (12%)	2/26 (8%)	5/51 (10%)	1/49 (2%)	ns
Total cohort	7/10 (70%)	19/41 (46%)	13/25 (52%)	13/26 (50%)	26/51 (51%)	13/49 (27%)	0.0073
Panel of 6 targets (bold)	6/10 (60%)	18/41 (44%)	12/25 (48%)	12/26 (46%)	24/51 (47%)	9/49 (18%)	0.00145

[a]tSCI, traumatic spinal cord injury
[b]pSCI, pathologic spinal cord injury
[c]HC, healthy control
[d]ns, not significant

Whether or not the presence of these identified antibody responses after SCI was determined by the time point of sampling, we compared the antibody reactivity in patient samples collected at hospitalization (T0) and at 3 weeks after injury (traumatic SCI) or surgery (pathologic SCI) (T1) (figure 3.2). Within the SCI cohort both traumatic and pathologic SCI patients showed antibody reactivity at hospitalization and 3 weeks after injury or surgery. Notably, most antibody positive patients exhibit reactivity at both time points of sampling. Altogether, immunoreactivity toward 9 novel identified antigenic targets was validated in both traumatic and pathologic SCI patients, which highlights the relevance of these novel identified antibody responses and their targets in inflammatory mechanisms present after damage to the spinal cord.

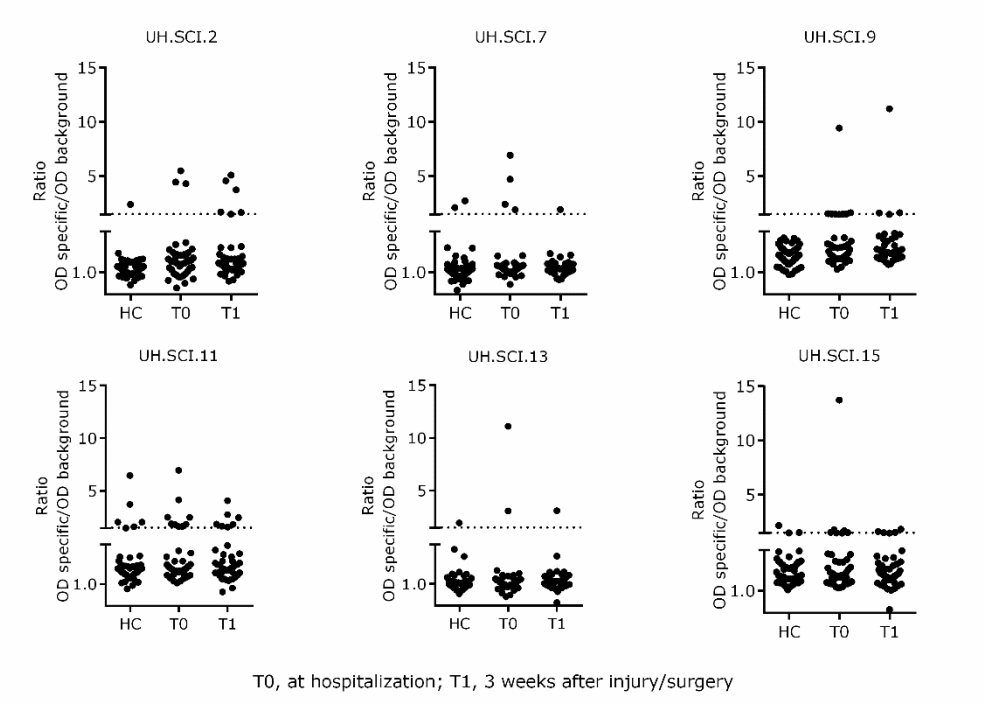

Figure 3.2: Antibody reactivity in SCI samples collected at hospitalization and 3 weeks after injury or surgery

Immunoreactivity toward the panel of 6 novel identified antigenic targets is found in samples collected at hospitalization (collected within 48 hours and maximum 4 days after injury, T0) and 3 weeks after injury or surgery (T1). Antibody reactivity is illustrated as the ratio (OD(specific phage)/OD(empty phage)). Samples were considered positive when the general reactivity (OD(specific phage)/OD(empty phage)) was higher than 1.5 and the

specific signal was above 0.1. Samples were analyzed in duplicate in a single ELISA experiment and experiments were performed independently for at least 2 times.

3.5 DISCUSSION

In the present study, the antibody signature of SCI patients was explored by using a powerful and unbiased high-throughput strategy, called SAS. By pooling plasma of 10 patients with highly diverse lesion characteristics (location, type and severity of the lesion), we analyzed the general antibody reactivity profile present in the heterogeneous SCI patient population. Our innovative and unbiased approach resulted in the identification of 19 distinct antigenic targets with increased reactivity in SCI patients compared to healthy controls. We confirmed reactivity toward 9 of the 19 targets in an additional cohort of 41 SCI patients, including both traumatic and pathologic SCI patients, and an equal number of age- and gender-matched healthy controls. Antibody reactivity against these 9 novel targets was found in 51% of the total SCI patient cohort. By combining 6 of these 9 targets into a panel, an overall reactivity of approximately 50% could be maintained while increasing the specificity to 82%.

We here report immunoreactivity toward various novel antigenic targets in SCI patients, identified via a powerful unbiased approach. A proteomics study using spinal cord tissue already indicated that over 50 distinct antigenic targets are present after SCI in mice [15, 140]. By using a tissue-specific cDNA library containing cDNA sequences encoding proteins with a nervous system-specific expression pattern or proteins involved in pathologic processes triggered after SCI, we created a relevant strategy to identify novel antibody targets in SCI [146]. Our results indicate that this highly diverse antibody profile is also present in SCI patients. Previously, hypothesis-driven studies only demonstrated elevated antibody responses toward MBP, MAG, GFAP, GM1 ganglioside and galactosylceramidase in sera of SCI patients and we now extend the antibody profile with responses directed against S100B, GAPDH, PSMD4, AEBP1 and, MYEOV2 [23-27, 29, 141]. The first novel identified target, S100B, is a dimeric calcium-binding protein localized predominantly in astroglial and Schwann cells and increased levels of this protein have been found in CSF and serum of SCI patients [71, 75, 81, 149]. While antibody responses directed against S100B were shown in CNS pathologies such as traumatic brain injury (TBI), they have not been reported in SCI patients before [150, 151]. S100B protein was detected in a very early stage after SCI with peak levels detectable already 6h after injury [152, 153]. Interestingly, in this study, antibody responses toward UH.SCI.7 (S100B) were already present in samples taken within

48 hours after injury. Target UH.SCI.5 partly encodes GAPDH which is a well-studied multidimensional protein involved in the homeostatic regulation and is often referred to as a "housekeeping" protein [154, 155]. In stroke models, nuclear GAPDH cascades are triggered leading to posttranscriptional modifications and allowing GAPDH to play a crucial role in brain damage [155, 156]. Because of the multifunctional involvement of GAPDH in the brain, it is not surprising that GAPDH might play a role in SCI pathology [155, 156]. PSMD4 is a non-ATPase subunit of the proteasomal 19S regulator which plays a key role in the recognition and processing of ubiquitylated proteins for proteolysis and AEBP1 may have a proinflammatory function and is involved in apoptosis and cell survival [157, 158]. The function of MYEOV2, on the other hand, is still unknown. Furthermore, 14 peptide sequences were identified which resulted from the expression of novel cDNA sequences, out of frame expression of known cDNAs or untranslated mRNA regions (e.g. 3'UTR regions) and probably comprise mimotopes. Overall, we identified antibody responses against a broad panel of targets which further underlines the strength of using an unbiased approach such as SAS.

During immune maturation, B cells are not exposed to the variety of unique CNS antigens expressed on neurons, oligodendrocytes, microglia and astrocytes causing a lack of tolerance against these CNS-specific proteins. Although evidence suggests that the blood-spinal cord barrier (BSCB) is more permeable than the blood-brain barrier (BBB), under normal conditions, an intact blood-CNS barrier protects neurons and glial cells from antibodies that cross-react with neurological tissue [159]. However, when the blood-CNS barrier is damaged, these circulating antibodies can infiltrate the CNS with the potential destruction of the neurologic tissue. A recent study showed that the lack of S100B compromises the BBB and allows access of CNS-reactive antibodies to the brain which generates pathological changes [160]. Upon SCI, the BSCB permeability is compromised as long as 56 days [161]. Antibodies against S100B might however prolong BSCB permeability resulting in a continued neuroinflammatory response. Yet, even after reconstitution of BSCB integrity, processes such as adsorptive endocytosis, active transport across the blood-CNS barrier and local antibody production can result in antibody accumulation in the injured spinal cord [15].

The antibody responses toward the novel identified targets were detected both in samples collected at hospitalization and 3 weeks after injury or surgery. The

mechanisms and different phases of antibody production after SCI have been investigated in SCI mouse models [15, 17]. It was suggested that after SCI and damage of the BSCB, CNS antigens are released into the bloodstream and drain into peripheral lymphoid tissues where they encounter the cells of the adaptive immune system. Newly formed IgG antibodies are typically formed 3 weeks after the insult [162]. The formation of new antibodies in SCI is supported by Ankeny et al. (2006) who showed that serum IgM levels are increased in SCI mice during the first 2 weeks after injury, while serum IgG_{2a} levels are delayed until week 2 and remained elevated up to 42 days post injury [15]. Besides newly formed immune responses, resting or memory B cells can become primed or re-activated by cognate antigens or polyclonal stimuli which has been suggested as a mechanism for antibody responses to CNS proteins in SCI pathology. Our results imply that both newly formed antibody responses and molecular mimicry mechanisms might be relevant in human SCI pathology.

Interestingly, while only traumatic SCI patients were used in the identification of the novel antibody responses, increased reactivity toward the identified antigenic targets was also evident in nearly half of the pathologic SCI patients. While traumatic SCI is an acute event, pathologic SCI is often a more chronic process. Since antibodies are stable, become amplified in the immune response and have a long half-life, their presence over time in pathology is not unexpected and highlights the relevance of these antibody responses in common inflammatory processes that are triggered after injury to the spinal cord.

Besides the potential relevance of the identified targets and their corresponding antibody responses in SCI pathophysiology, the discovery of these novel SCI-related antibody responses is also highly relevant from a clinical viewpoint. We here report individual antigenic targets with an overall reactivity varying from 4 to 20%, and with high specificity ranging from 90 to 100%, which are comparable to the previously reported antibody reactivity toward GM1 gangliosides, GFAP, MAG and MBP [23-26, 29]. One of our novel identified antigenic targets (UH.SCI.9) was significantly associated with SCI patients. By combining 6 antigenic targets in a SCI patient-associated panel, we found relevant immunoreactivity in 47% of the SCI patients with a 82% specificity. Multiplexing of inflammatory biomarkers in SCI pathology has been shown to be a valuable strategy to significantly improve the sensitivity rate while maintaining a high specificity [75]. Previous studies showed

that enhanced antibody levels correlated with complications in SCI patients [23, 24, 27]. So far, association of the novel antibodies with clinical parameters could not be determined as our SCI patient population is heterogeneous and a limited sample size was screened. Gender-related influences on the outcome after SCI have been reported with a better recovery in females. The improved recovery has, at least partly, been attributed to the regulation of the SCI-induced neuroinflammatory response by sex hormones [163, 164]. In our cohort, analyzing the validated antibody responses based on gender did not show any sex-related differences in antibody reactivity against the novel identified targets. Still, as antibodies have been suggested to represent better biomarkers than their antigen counterparts, and we find increased antibody responses already very early after the injury, the investigation of their potential as a prognostic biomarker for SCI patients is highly desirable [19, 165, 166].

In summary, the antibody reactivity profile after SCI in humans was explored by using an unbiased and powerful high-throughput technology based on phage display, which resulted in the identification of 9 novel antigenic targets with elevated immunoreactivity in SCI patients compared to healthy controls. By combining 6 of these 9 antigenic targets into a panel, an overall reactivity of nearly 50% could be detected with a specificity of 82%. Further characterization of both the SCI-related antibody responses and the corresponding targets will provide more insight into the role of the humoral immune component within SCI-induced neuroinflammation and their clinical relevance.

4

Development and optimization of peptide and protein ELISA for autoantibody testing in spinal cord injury patients

4.1 ABSTRACT

A spinal cord injury (SCI)-associated panel of 6 antigenic targets was identified using the serological antigen selection (SAS) procedure followed by phage enzyme-linked immunosorbent assay (ELISA) screening. As phage ELISA is a labor intensive method and requires specific biosafety measures, we aimed to translate the phage-mediated test into a high-throughput and sensitive peptide ELISA. Via phage-peptide competition ELISA, the target specificity of the antibody responses within our SCI-associated panel were confirmed. Subsequently, synthetic peptides corresponding to the SCI-peptides displayed on the phage surface were implemented in solid-phase ELISA. Custom in-house ELISA were successfully optimized for UH.SCI.2, UH.SCI.7, UH.SCI.11 and UH.SCI.13. Assay validation screening revealed UH.SCI.2 and UH.SCI.7 as the most interesting antigenic targets and demonstrated an increased sensitivity for our peptide ELISA in comparison with the corresponding phage and protein ELISA. Additionally, by using peptides and recombinant proteins in competition ELISA, we confirmed 26S proteasome non-ATPase regulatory subunit 4 (PSMD4) and protein S100-B (S100B) as the *in vivo* targets of UH.SCI.2 and UH.SCI.7 antibody responses, respectively. In conclusion, we developed high-throughput and clinically applicable peptide ELISA for detection of antibodies against the C-terminus of PSMD4 and S100B, which can be applied for large-scale screening of SCI patients and controls.

4.2 INTRODUCTION

As described in chapter 3, we discovered 19 novel antigenic targets in SCI patients using serological antigen selection (SAS) [167]. Six antigenic targets were combined into a SCI-associated panel for which an overall reactivity was detected in approximately half of the SCI patients and 18% of the healthy controls using phage ELISA. ELISA is used to detect and quantify biological molecules such as specific antigens or antibodies in a complex mixture, even at low concentrations. In clinical practice, ELISA is applied for diagnostic purposes, while in biomedical research this method is used as an analytical tool [168]. In order to detect antibodies in plasma or serum samples, the specific antigen is immobilized by adhering or capturing via an antigen-specific antibody (sandwich ELISA) onto the well surface. In our lab, antigens displayed on the phage surface are captured using a coating antibody directed against a phage coat protein in a phage ELISA format (figure 4.1a), while synthetic peptides or recombinant full length proteins are usually directly coated via solid-phase peptide or protein ELISA (figure 4.1b). Subsequently, a plasma/serum sample is added, allowing the formation of antigen-antibody complexes, which can be detected by an enzyme-coupled detection antibody. Upon addition of a chromogenic substrate, a visible color change is created, detected by a spectrophotometer and converted into a quantitative output. As phage ELISA is time consuming and working with phages requires appropriate biosafety measures, phage ELISA is not always applicable in a clinical setting. To this end, we aimed to translate the phage-mediated research test into a solid-phase peptide ELISA, which is a more clinically applicable high-throughput tool. First, target specificity of antibody responses within the SCI-associated panel toward each corresponding synthetic peptide was investigated using phage-peptide competition ELISA. Subsequently, these corresponding synthetic peptides were used to develop and optimize solid-phase peptide ELISA. BLAST analysis already demonstrated that UH.SCI.2 and UH.SCI.7 corresponded to C-terminal parts of 26S proteasome non-ATPase regulatory subunit 4 (PSMD4) and protein S100-B (S100B), respectively. Therefore, the second objective was to confirm the *in vivo* target identity of UH.SCI.2 and UH.SCI.7 antibody responses using recombinant peptides and proteins in a competition ELISA.

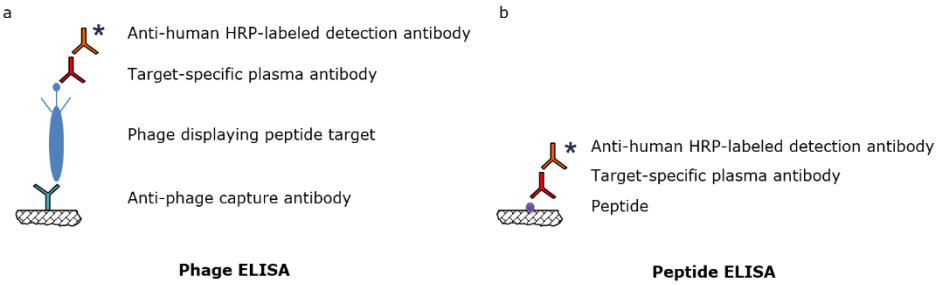

Figure 4.1: Schematic representation of the phage versus peptide ELISA

In phage ELISA, the well surface is coated with an anti-phage antibody which captures the phage clone of interest (a). In peptide ELISA, synthetic peptides are directly coated on the well surface (b). Subsequently, a plasma sample containing target-specific antibodies is added, resulting in the formation of an antigen-antibody complex which can be detected by an enzyme-coupled detection antibody (a and b). HRP, horseradish peroxidase.

4.3 MATERIALS AND METHODS

4.3.1 Competition assay

To confirm that the newly identified antibody responses were specifically directed toward the peptide displayed on the phage surface, phage-peptide competition ELISA were performed based on the phage ELISA set-up described in chapter 3. Plasma samples were pre-incubated with increasing concentrations (0-5 µg/ml) of the corresponding synthetic peptide (Biomatik, Delaware, USA) or as a negative control with an equal amount of control peptide (table 4.1).

Table 4.1: Peptide identities

Peptide name[a]	Peptide sequence[b]	Coating conditions
UH.SCI.2	TEEDDYDVMQDPEFLQSVLENLPGVDPNNEAIRNA MGSLASQATKDGKKDKKEEDKK	1 µg/ml in PBS
UH.SCI.7	*DLLENSRPRR*HEFFEHE	1 µg/ml in PBS
UH.SCI.9	*GPSRPDLLE*NSELLSNKSALHKFIKYAFWI*	/
UH.SCI.11	EFFDNSRKVDD*	5 µg/ml in PBS
UH.SCI.13	*IFQRIRGRVD*EDKT*	1 µg/ml in PBS
UH.SCI.15	*SSREFAAAS*TEGKEQERSDKDE*	/
Control peptide	WTKTPDGNFQLGGTEP	Similar to specific peptide

[a] Hasselt University.spinal cord injury.number of the clone
[b] Adaptor sequence (*in italic*) was added to allow coating of short peptides

4.3.2 Recombinant protein expression and purification

Recombinant human S100B (Histidine (His) tag at the N-terminus) was commercially obtained (Sino Biologicals Inc., Beijing, China). Full length human PSMD4 cDNA was cloned in the pBAD/Thio-TOPO vector (Invitrogen, Merelbeke, Belgium), expressed in LMG194 *E. coli* bacteria as a fusion protein with thioredoxin (THIO) at the N-terminal side and a His_6-tag at the C-terminus and purified using nickel-nitrilotriacetic acid sepharose beads (IBA, Leusden, the Netherlands), as described previously [5]. Recombinant PSMD4 protein expression and purity were analyzed by sodium dodecyl sulfate polyacrylamide gel electrophoresis (SDS-PAGE) and Coomassie brilliant blue staining (Phastgel Blue-R, GE Healthcare, Diegem, Belgium). Western blot using rabbit polyclonal anti-PSMD4 antibody (Abbexa, Cambridge, United Kingdom) was performed to confirm the protein identity. Recombinant expressed proteins (PSMD4 and THIO) were concentrated and dialyzed using iCON spin columns (Thermo Fisher Scientific, Erembodegem, Belgium) and protein concentrations were determined using the bicinchoninic acid (BCA) protein quantification kit (Thermo Fisher Scientific).

4.3.3 Peptide and recombinant protein ELISA

Antibody reactivity toward the novel antigenic targets was measured with solid-phase ELISA using synthetic peptide (table 4.1) or recombinant protein. Briefly, for peptide ELISA, polystyrene flat-bottom plates (Greiner Bio-one reference number 655161, Wemmel, Belgium) were coated with synthetic peptide (>85% purity, Biomatik) and control peptide (overnight at RT) in phosphate buffered saline (PBS), while for protein ELISA, high-binding ELISA plates (Greiner Bio-one, reference number 655092) were coated with 1 µg/ml recombinant produced PSMD4 and THIO (background signal) or 5 µg/ml S100B (Sino Biologicals Inc., Beijing, China) in coating buffer, overnight at 4°C. Coating conditions of the individual synthetic peptides were summarized in table 1. For both peptide and protein ELISA protocols, plates were washed twice with PBS containing 0.05% (v/v) and 0.1% (v/v) Tween-20, respectively. Next, plates were blocked with 2% skimmed milk powder in PBS (MPBS) for 2 h (37°C, shaking). After washing the plates three times, plasma samples (1:100 diluted in 2% MPBS) were incubated for 2 h (RT, shaking) and the amount of bound IgG was detected with rabbit anti-human IgG horseradish peroxidase (HRP)-labelled antibody (1:2000, Dako). The color reaction in peptide and protein ELISA was incubated for 11 min and 10 min, respectively, and stopped by adding 1.8 N H_2SO_4. Optical density (OD) signals were measured at 450 nm in a Microplate reader Infinite M1000 Pro (TECAN, Männedorf, Switzerland). Samples were tested in duplicate in a single ELISA experiment and experiments were performed independently for at least two times, except for S100B assays which were performed only once.

The *in vivo* identity of UH.SCI.2 and UH.SCI.7 was confirmed using a standard peptide ELISA and pre-incubation of antibody-positive and antibody-negative plasma samples with increasing amounts of corresponding protein (0-100 µg/ml).

4.3.4 Data analysis

For the phage and protein ELISA, results are reported by means of the ratio of the OD from the specific signal (specific phage or recombinant protein) and the OD from the background signal (empty phage or THIO). Samples were considered positive in the phage ELISA when the average reactivity (OD(specific phage)/OD(empty phage)) was higher than 1.5. For peptide ELISA, a serially-diluted positive plasma sample was included in the screening as a calibration curve to calculate arbitrary units (AU) for each individual sample and to assess the

interassay variability. The cut-off calculation for seropositivity in the peptide and protein ELISA is described in chapter 5. Positive samples were screened on control peptide to exclude polyreactive samples. Seropositive samples with an average reactivity (OD(specific peptide)/OD(control peptide)) lower than 1.5 were considered polyreactive (reactive to the control peptide) and were excluded from the analysis.

4.4 RESULTS

4.4.1 Confirmation of the antigenic specificity of SCI-associated antibodies to synthetic peptides

Before translation of our phage ELISA into a sensitive peptide ELISA, phage-peptide competition ELISA was used to determine whether the antibody responses that are directed against the peptides displayed on the phage surface, are also reactive against the corresponding synthetic peptide sequences (figure 4.2). For our SCI-associated panel, i.e. UH.SCI.2, UH.SCI.7, UH.SCI.9, UH.SCI.11, UH.SCI.13 and UH.SCI.15, pre-incubation with the highest amount of specific synthetic peptide reduced the OD signal of an antibody-positive sample to background reactivity (OD signal of an antibody-negative sample), demonstrating successful competition between the phage-displayed peptides and their corresponding synthetic peptides. OD signals of an antibody-negative sample or control peptide pre-incubation conditions remained stable. Altogether, these results confirm that the newly identified antibody responses within the SCI-associated panel are specifically directed against the peptide sequence displayed on the phage surface. Therefore, the corresponding synthetic peptides can be used directly to detect these antibody responses in a solid-phase peptide ELISA.

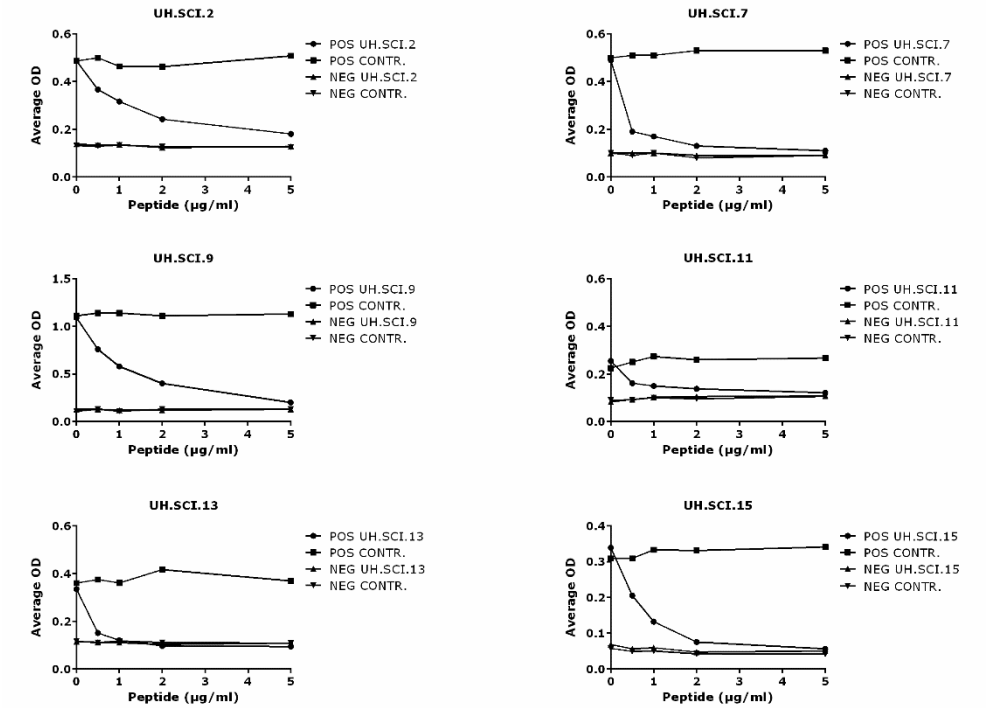

Figure 4.2: Competition assays for confirmation of target specificity

To investigate the target specificity of the newly identified antibody responses, competition ELISA was performed using a standard phage ELISA set-up. Before sample addition, antibody-positive (POS) or antibody-negative (NEG) plasma samples were pre-incubated with increasing amounts of specific synthetic peptide (UH.SCI.2, UH.SCI.7, UH.SCI.9, UH.SCI.11, UH.SCI.13 or UH.SCI.15; 0-5 µg/ml) or control peptide (negative control, CONTR., 0-5 µg/ml). Results were visualized as average optical density (OD) signals for each sample.

4.4.2 Peptide ELISA development and validation

The synthetic peptides of UH.SCI.2, UH.SCI.7, UH.SCI.9, UH.SCI.11, UH.SCI.13 and UH.SCI.15 were used to develop and optimize solid-phase peptide ELISA. During the optimization process, varying coating concentrations were tested (0-10 µg/ml) in PBS (figure 4.3) and coating buffer (data not shown). For UH.SCI.2, UH.SCI.7, UH.SCI.11 and UH.SCI.13 in PBS, immobilization of synthetic peptide could be shown via reactivity of an antibody-positive sample. Control conditions (e.g. antibody-negative sample and no sample) did not show immunoreactivity.

The optimal coating concentrations for these four peptides were determined based on the coating conditions with a clear difference between the reactivity of an antibody-positive and an antibody-negative sample and are summarized in table 4.1. For UH.SCI.9 and UH.SCI.15 coating, only limited immunoreactivity of an antibody-positive sample was observed, even with a coating concentration of 10 µg/ml. For these targets, further optimization was performed, such as testing of higher coating concentrations (10-25 µg/ml), coating buffers with varying pH and composition, different ELISA plates, coating temperature (4°C versus RT) as well as the addition of an adaptor sequence to increase the coating efficiency (data not shown). Despite these optimization steps, no optimal coating condition could be determined for UH.SCI.9 and UH.SCI.15.

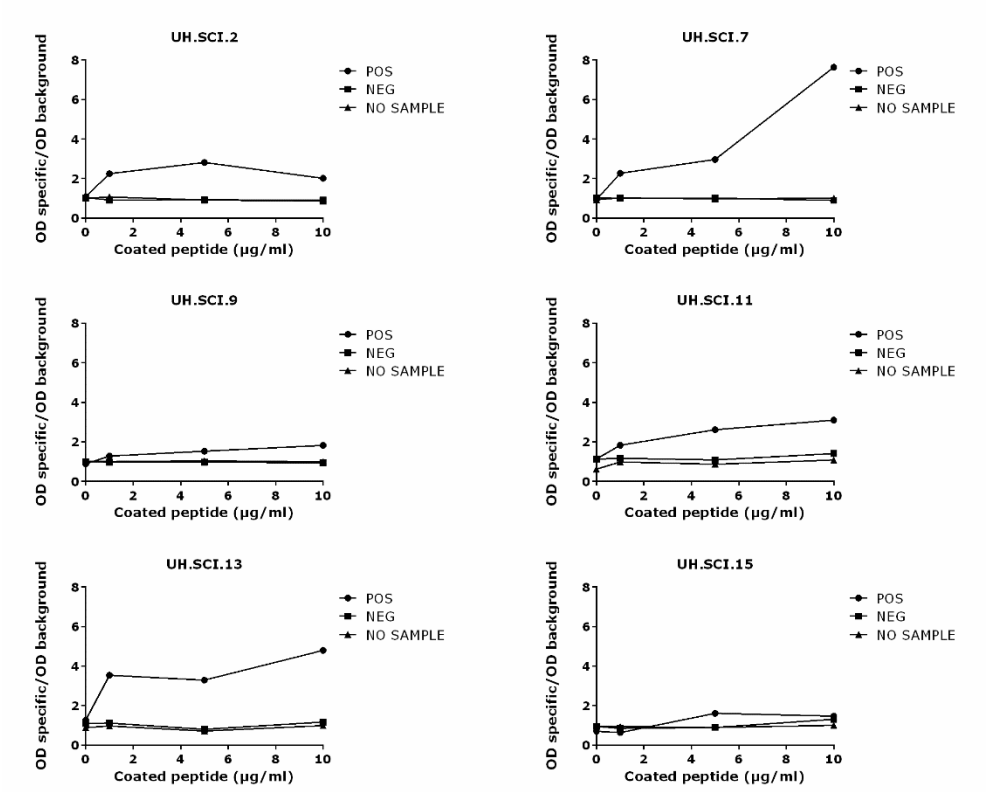

Figure 4.3: Coating optimization of the peptides of the SCI-associated panel

For each synthetic peptide (UH.SCI.2, UH.SCI.7, UH.SCI.9, UH.SCI.11, UH.SCI.13 and UH.SCI.15), varying coating concentrations (0-10 µg/ml) were tested in PBS. Immobilization of the synthetic peptide was detected using an antibody-positive sample (POS). An antibody-

negative (NEG) and no sample (NO SAMPLE) were included in the assay as negative control conditions. For the peptide ELISA optimization, immunoreactivity is visualized as the ratio of the optical density (OD) signal of the specific signal (synthetic peptide of interest) versus the OD signal of the background signal (control peptide).

In order to evaluate the performance of the newly developed peptide ELISA, most samples of the phage ELISA screening described in chapter 3 were also screened with our in-house peptide ELISA. Phage ELISA screening for UH.SCI.11 demonstrated high healthy control reactivity (chapter 3) and, therefore, UH.SCI.11 was excluded from the study. Screening with our optimized UH.SCI.13 ELISA demonstrated higher antibody reactivity in the HC group in comparison with the SCI cohort (data not shown), resulting in the exclusion of UH.SCI.13 for the validation screening with peptide ELISA. For UH.SCI.2 and UH.SCI.7, seropositive samples in phage and/or peptide ELISA are shown in figure 4.4. Most positive samples in the phage ELISA were also positive in the peptide ELISA and the relative amplitude of the signal was generally conserved. On the other hand, our peptide ELISA showed a higher sensitivity since additional antibody-positive samples were identified. Altogether, our results show that sensitive peptide ELISA were developed for UH.SCI.2 and UH.SCI.7 which allow large-scale screening of SCI patients and controls.

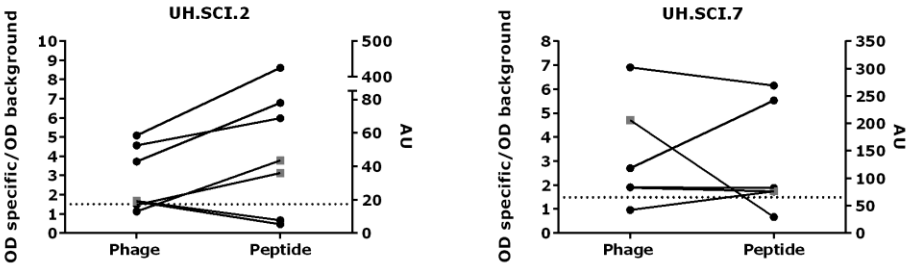

Figure 4.4: UH.SCI.2 and UH.SCI.7 phage versus peptide ELISA

The cohort in the phage ELISA screening (chapter 3) was also screened with our peptide ELISA. Positive samples in both or only one (grey squares) of the approaches were visualized in the graph. For phage ELISA, immunoreactivity is indicated by the ratio of the optical density (OD) signal of the specific signal (phage clone of interest) versus the background signal (empty phage). For peptide ELISA, arbitrary units (AU) were calculated for UH.SCI.2 and UH.SCI.7 antibodies using a calibration curve. Dots represent individual samples, the

lines connect the samples that are tested in both assays. The dashed horizontal line depicts the cut-off for seropositivity.

4.4.3 Confirmation of UH.SCI.2 and UH.SCI.7 *in vivo* target identity

Basic Local Alignment Search Tool (BLAST) analysis of UH.SCI.2 and UH.SCI.7 showed that both peptide sequences corresponded to the C-termini of respectively PSMD4 and S100B (figure 4.5a). To further confirm that antibodies against the UH.SCI.2 and UH.SCI.7 peptides are actually directed against these respective proteins, a peptide-protein competition ELISA was performed. Pre-incubation of antibody-positive plasma samples with increasing amounts of recombinant full length protein showed a decreasing OD signal (figure 4.5b), indicating successful competition between the synthetic peptide and the corresponding protein. For control conditions, the OD signal remained unchanged. Next, protein ELISA using recombinant PSMD4 and S100B were developed. To confirm the target specificity of UH.SCI.2 and UH.SCI.7 antibody responses, antibody-positive plasma samples in the peptide ELISA were also tested in the corresponding protein ELISA. As shown in figure 4.5c, seropositive samples in the peptide ELISA showed also immunoreactivity toward the corresponding protein. In comparison with the protein ELISA, the peptide ELISA showed a higher sensitivity, as demonstrated by the identification of more seropositive samples, but also by the proportional increase in antibody levels of seropositive samples. In conclusion, UH.SCI.2 and UH.SCI.7 antibody reactivity was found to correspond to PSMD4 and S100B antibody responses, respectively.

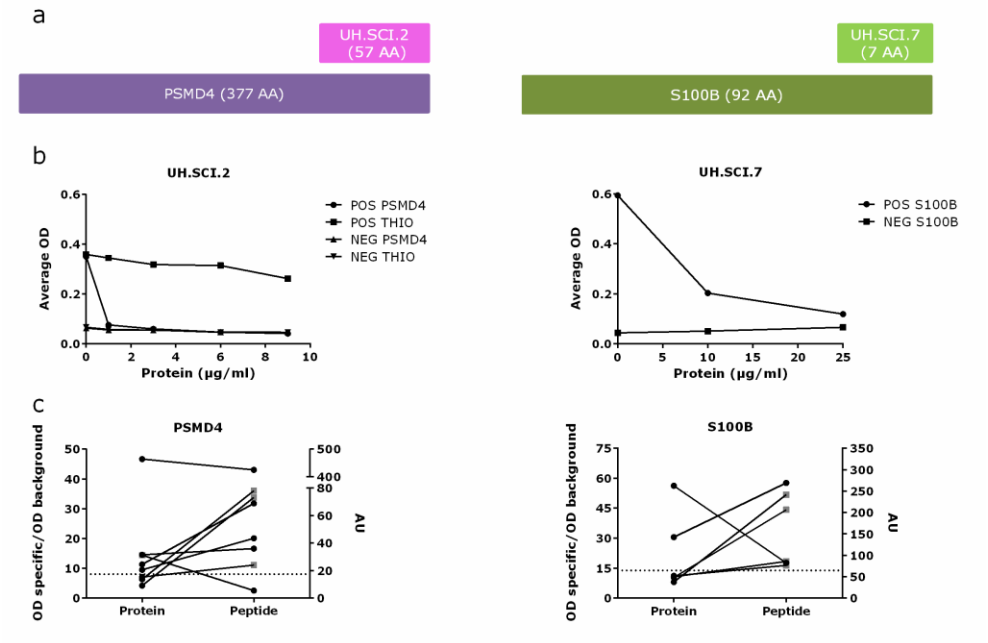

Figure 4.5: Confirmation of the *in vivo* target identity of UH.SCI.2 and UH.SCI.7

Basic Local Alignment Search Tool (BLAST) analysis demonstrated similarity between UH.SCI.2 and UH.SCI.7 and the C-termini of respectively PSMD4 and S100B (a). Competition assays with a standard peptide ELISA set-up were used to investigate the *in vivo* target identity of UH.SCI.2 and UH.SCI.7 antibody responses (b). Antibody-positive (POS) and antibody-negative (NEG) plasma samples were pre-incubated with increasing amounts of recombinant protein (0-25 µg/ml) before addition to plates coated with each respective peptide (1 µg/ml). PSMD4 is expressed as a fusion protein with Thioredoxine (THIO). Therefore, both a POS and NEG sample were pre-incubated with increasing amounts of THIO (0-9 µg/ml, negative control). Subsequently, antibody-positive samples in the peptide ELISA were also screened with the corresponding protein ELISA (c). Samples that were seropositive in only one of the two assays are indicated in grey squares. Antibody reactivity in the peptide and protein ELISA was expressed as arbitrary units (AU) or the ratio of the specific signal (OD recombinant protein) and the background reactivity (THIO or empty well), respectively. AA, amino acids.

4.5 DISCUSSION

Previously, we used a phage-mediated ELISA to explore immunoreactivity toward the newly identified antibody targets in SCI patients. As this approach is time consuming and requires specific biosafety measures, we aimed to convert the phage ELISA into a sensitive, high-throughput peptide ELISA. Specificity of the antibodies within the SCI-associated panel toward the respective displayed peptide sequences was confirmed and optimal coating conditions could be determined for UH.SCI.2, UH.SCI.7, UH.SCI.11 and UH.SCI.13 peptides. Extensive optimization of the UH.SCI.9 and UH.SCI.15 ELISA did not result in usable coating conditions. As UH.SCI.9 antibodies demonstrated a significant association with SCI patients in the phage ELISA screening (chapter 3), future optimization experiments should try other immobilization strategies like for example a streptavidin-biotin strategy to obtain target coating. UH.SCI.11 and UH.SCI.13 were excluded from the study, as both targets demonstrated high immunoreactivity in the HC group and are probably not SCI-specific. For PSMD4 (UH.SCI.2) and S100B (UH.SCI.7), peptide ELISA against their respective C-terminal peptides were successfully optimized. S100B antibody responses have already been described in traumatic brain injury (TBI) patients where they correlate with the severity of brain damage [150, 151]. Identification and detection of antibody responses with a described clinical relevance in similar neuroinflammatory disorders not only confirms the usefulness of phage display technology, but also validates the quality of our novel optimized peptide ELISA [150, 151]. Furthermore, in comparison with the corresponding phage and protein ELISA, our novel peptide ELISA is most suitable to perform large-scale screenings because of limited biosafety risks, cost- and time-efficiency and the improved sensitivity as higher signals were observed and additional antibody-positive samples were identified. Altogether, suitable robust peptide ELISA were optimized for detection of antibodies against PSMD4 and S100B in a research setting.

After indications by BLAST analysis in chapter 3, PSMD4 and S100B were now confirmed as the *in vivo* antibody targets of UH.SCI.2 and UH.SCI.7, respectively, and antibody reactivity against both full length recombinant proteins was demonstrated in SCI patients. S100B, a dimeric calcium-binding protein, is highly expressed in the cytoplasm and nucleus of astroglial cells of the brain (e.g.

astrocytes and in Schwann cells) and other tissues outside the central nervous system (CNS; e.g. bone marrow cells, chrondrocytes, lymphocytes, adipocytes and melanocytes) and can be released in the cerebrospinal fluid and blood [169, 170]. S100B has been described as a marker for damage to the blood-brain barrier (BBB), but is also involved in the development and recovery of the CNS after injury [170, 171]. Inhibition of S100B in a TBI model (controlled cortical impact model) using a neutralizing S100B antibody, demonstrated a significant reduction of the TBI-induced lesion volume, a better function of retention memory, reduced microglial activation, lower amounts of sensorimotor deficits and improved neuronal survival in the cortex [170]. These findings clearly show the degenerative role of increased S100B levels in TBI-induced neuroinflammation, cell loss and neurological dysfunction [170]. As these processes are also involved in SCI pathology, neutralizing S100B antibodies might have a beneficial role after SCI as well.

PSMD4 encodes two protein isoforms, for which the aliases antisecretory factor (AF) and angiocidin are often used [172]. The C-terminus of both isoforms shows 100% similarity with the UH.SCI.2 peptide. AF is shown to be involved in anti-inflammatory/secretory processes as well as the regulation of proteolytic processes in the proteasome [173, 174]. In the CNS, AF is located in blood vessels and perivascular cells which are essential in the initiation and regulation of inflammatory reactions [173]. In an experimental autoimmune encephalomyelitis (EAE) animal model, a redistribution of AF expression was demonstrated which seemed to correlate with the severity of disease. Neutralization of AF using TLD-1A8A antibodies in an EAE model aggravated the clinical severity and duration of the disease [175]. Together these observations indicate an anti-inflammatory and neuroprotective role of AF, while on the contrary, angiocidin was shown to promote a pro-inflammatory cytokine profile and antigen presentation in MS pathology (*in vitro*) [176]. As a contradictory role for the PSMD4 protein isoforms in neuroinflammatory conditions has been described, the effect of PSMD4 antibody responses in SCI is even harder to predict. Up to now, only a small fraction of the antibody repertoire in SCI patients has been identified and the targets of our identified antibody responses represent different functions dependent on the protein isoform, concentration and microenvironment, therefore, it is not clear

whether these antibodies will exert an pronounced beneficial or detrimental effect in SCI pathological processes.

In conclusion, high-throughput and clinically applicable peptide ELISA were optimized for the detection of PSMD4 and S100B antibodies. Further characterization of PSMD4 and S100B antibodies in SCI pathology is warranted to reveal their clinical and biological relevance.

5

PSMD4 and S100B autoantibodies in spinal cord injury patients

5.1 ABSTRACT

Using a phage display approach, we recently identified PSMD4 and S100B as autoantibody targets in spinal cord injury (SCI) patients. In the current study, we aimed to further characterize the clinical relevance of these autoantibodies in SCI pathology. Therefore, peptide ELISA were developed to screen for antibody reactivity in a SCI patient cohort (n=175, containing follow-up samples of traumatic and pathologic SCI patients post-injury/surgery), healthy controls (n=94) and patients with distinct pathologies (stroke (n=27), multiple sclerosis (MS, n=54) and rheumatoid arthritis (RA, n=57)). Using our in-house optimized peptide ELISA, similar immunoreactivity was found within healthy controls (PSMD4 4% and S100B 5%) and our SCI patient cohort (PSMD4 4% and S100B 6%), irrespective of the cause of pathology or time post-injury. Analysis of PSMD4 and S100B immunoreactivity in healthy controls and follow-up samples from an early SCI cohort (samples collected within 1 year after injury) showed that these autoantibodies were already present before injury and remained stable throughout the follow-up period after SCI. To investigate the disease specificity of these autoantibodies, stroke, MS and RA patient samples were screened, which demonstrated that PSMD4 and S100B autoantibodies were not SCI specific and were also not induced by other neuroinflammatory or autoimmune conditions. In conclusion, an in-depth characterization of PSMD4 and S100B autoantibody responses showed similar reactivity within healthy controls, SCI and neuroinflammatory or autoimmune disorders. Both autoantibodies are probably part of the autoantibody reactivity in a percentage of the general population, and are not induced by SCI. Nonetheless, they still might contribute to degenerative or recovery processes under pathological conditions.

5.2 INTRODUCTION

Damage to the spinal cord affects motor, sensory and/or autonomic functions. Based on neurological symptoms observed using the American Spinal Injury Association impairment scale (AIS) and magnetic resonance imaging (MRI), the diagnosis of spinal cord injury (SCI) can be made and the location of the lesion in the spinal cord can be determined. A reliable prognosis prediction is more challenging as the current prognostic tools have various limitations and give only limited information on the severity of the lesion [177, 178]. Therefore, there is a clear need for novel clinically relevant disease markers that can contribute to SCI prognosis.

Previously, we identified novel antibody targets in SCI patients using serological antigen selection based on cDNA phage display (chapter 3). For two of the newly identified antibody targets, PSMD4 and S100B, we optimized C-terminal peptide ELISA and confirmed the *in vivo* target identity (chapter 4). In order to investigate the clinical relevance of PSMD4 and S100B autoantibodies in SCI pathology, we first validated the prevalence of these autoantibody responses in SCI patients. Therefore, a large SCI cohort (n=175) was screened for PSMD4 and S100B autoantibodies using our in-house peptide ELISA. Additionally, the stability of these autoantibodies over time after SCI was investigated by screening follow-up samples of our early SCI cohort (samples collected <1 year after injury) and an independent chronic SCI cohort (samples collected >1 year after injury). Additionally, to examine whether these autoantibodies are primarily formed after SCI, we compared PSMD4 and S100B reactivity and levels in healthy controls and SCI samples collected at hospitalization (T0) and 3 weeks after injury/surgery (T1). Next, the presence and levels of PSMD4 and S100B autoantibodies were analyzed for correlations with general patient characteristics and prognostic parameters. Finally, we assessed the disease specificity of PSMD4 and S100B autoantibodies by screening age- and gender-matched healthy controls, as well as other pathologies such as stroke, MS and RA.

5.3 MATERIALS AND METHODS

5.3.1 Patient samples

SCI patient cohort

For our early SCI cohort (<1 year after injury), peripheral blood from traumatic and pathologic SCI patients was collected in Adelante Rehabilitation Centre (Hoensbroek, The Netherlands), Jessa Hospital (Hasselt, Belgium), University Hospitals Leuven (Leuven, Belgium), Academic Hospital Maastricht (Maastricht, The Netherlands), Hospital East-Limburg (Genk, Belgium), Antwerp University Hospital (Edegem, Belgium), General Hospital Turnhout (Turnhout, Belgium) and Radboud University Medical Centre (Nijmegen, The Netherlands). SCI patients with pre-existing autoimmune disorders were excluded from the study. This study was approved by the institutional ethics committees and written informed consent was acquired from all participants. Samples were processed and stored in collaboration with University Biobank Limburg (UBiLim) and Biobank University Hospitals Leuven. Additional SCI samples (samples collected within 30 days after SCI or >1 year after SCI) were kindly provided by Prof. dr. Georgene W. Hergenroeder (University of Texas Health Science Center at Houston-McGovern Medical School, Houston, Texas, USA). Characteristics of the total SCI population were summarized in table 5.1. In order to investigate the time range during which PSMD4 and S100B autoantibodies were present after SCI, samples of traumatic SCI (tSCI) patients were taken at hospitalization (T0) and at 3 weeks (T1), 6 weeks (T2), 12 weeks (T3) and 18 weeks (T4) after injury. Samples of pathologic SCI (pSCI) patients (e.g. stenosis, spinal disc herniation, compression caused by bleeding and oncologic pathology/metastasis) were collected preoperatively (T0) and at 3 weeks (T1), 6 weeks (T2), 12 weeks (T3) and 18 weeks (T4) after surgery.

Control populations

To investigate the disease specificity of PSMD4 and S100B autoantibodies, healthy controls and other neuroinflammatory (stroke) or autoimmune conditions (MS and RA patients) were included in the study. The healthy control group was age- and gender-matched with the SCI patients on a group level. The age and gender of MS, stroke and RA patient groups were selected to represent the respective patient population characteristics and patients were treated according to a

standard treatment regimen. Characteristics of the healthy controls, stroke, MS and RA populations were summarized in table 5.1. Plasma samples from healthy controls, RA and MS patients were collected via UBiLim. Stroke samples were kindly provided by Prof. dr. Luisa M. Villar (Ramón y Cajal Hospital, Madrid Spain).

Table 5.1: Characteristics of the study populations

Cohort	No.	Mean age (in years)	Gender (F/M)[b]	AIS[c]	Location of injury[d]	pSCI/tSCI ratio[e]
SCI patient population						
SCI patients (<1 year after SCI)[a]	116	55 ± 16	22/89	A-E	C-S	46/65
Chronic SCI patients (> 1 year after SCI)	59	44 ± 14	15/44	A-D	C-L	0/59
Control groups						
Healthy controls	94	54 ± 17	24/70	/	/	/
Stroke	27	54 ± 16	11/16	/	/	/
Multiple sclerosis (MS)	54	46 ± 14	39/15	/	/	/
Rheumatoid artritis (RA)	57	53 ± 14	45/12	/	/	/

[a] Missing data of 5 samples
[b] F, female; M, male
[c] American Spinal Injury Association Impairment Scale
[d] C, cervical; L, lumbal; S, sacral
[e] tSCI, traumatic spinal cord injury; pSCI, pathologic spinal cord injury

5.3.2 Peptide ELISA

Antibody reactivity toward PSMD4 and S100B was measured with our ELISA using synthetic C-terminal peptide, as described in chapter 4. Briefly, for peptide ELISA, polystyrene flat-bottom plates (Greiner Bio-one reference number 655161, Wemmel, Belgium) were coated with 1 µg/ml synthetic peptide (>85% purity, Biomatik) and control peptide in phosphate-buffered saline (PBS; 50 mM Tris, 150 mM sodium chloride, pH 7.5), overnight at room temperature (RT). Plates were washed twice with PBS containing 0.05% (v/v) Tween-20 and blocked with 2% (w/v) skimmed milk powder in PBS (MPBS) for 2 hours (h) (37°C, shaking). After washing the plates three times, plasma samples (1:100 diluted in 2% MPBS) were incubated for 2 h (RT, shaking). Washing steps were repeated and the amount of bound IgG was detected with rabbit anti-human IgG horseradish peroxidase-labelled antibody (1:2000, Dako). After incubation with 3,3',5,5' tetramethyl-benzidine dihydrochloride (TMB) for 11 min, the color reaction was stopped by addition of 1.8 N H_2SO_4. Optical density (OD) signals were measured at 450 nm in a Microplate reader Infinite M1000 Pro (TECAN, Männedorf, Switzerland). Samples were tested in duplicate in a single ELISA experiment and experiments were performed independently for at least two times.

5.3.3 Data analysis

For peptide ELISA, a serially-diluted positive plasma sample was included in the screening as a calibration curve to calculate arbitrary units (AU) for each individual sample, thereby allowing the comparison of antibody levels. The calibration curve was also used to assess the interassay variability. To determine the cut-off, healthy control samples with a reactivity lower than average plus three times standard deviation were used. Using these values, the cut-off for seropositivity was calculated based on the average reactivity in the remaining healthy control group plus three times standard deviation. Positive samples were also screened on control peptide to exclude polyreactive samples. Seropositive samples with an average reactivity ratio (OD(specific peptide)/OD(control peptide)) lower than 1.5 were considered polyreactive (reactive to the control peptide) and were excluded from the analysis.

Statistical analysis was performed using JMP version Pro 12 (SAS Institute Inc, Cary, North Carolina, USA). Linear regression models were used to investigate the effect of continuous dependent variables (e.g. antibody levels). Ordinal logistic regression models were used to study ordinal dependent variables (e.g. immunoreactivity). For all statistical tests, a p-value of <0.05 was considered statistically significant.

5.4 RESULTS

5.4.1 PSMD4 and S100B autoantibody prevalence in SCI patients

In order to characterize PSMD4 and S100B autoantibodies in SCI pathology, a large SCI cohort was analyzed for both antibody responses using our in-house peptide ELISA. Primary PSMD4 and S100B autoantibody responses were studied in SCI samples collected at least 3 weeks after injury (≥T1). The early SCI cohort consisted of 65 traumatic and 46 pathologic SCI patients, but for 8 early tSCI patients, only a sample collected at hospitalization was available, causing the exclusion of these patients in figure 5.1a. Screening of the early SCI cohort confirmed the seroprevalence within SCI patients and showed comparable antibody reactivity (PSMD4 4-7%; S100B 4-9%) and levels, irrespective of the cause of pathology (figure 5.1a). In order to gain insight into the presence over time of these antibody responses after SCI, follow-up samples of our early SCI cohort and an independent cohort of 59 chronic tSCI patients (>1 year after SCI) were evaluated for PSMD4 and S100B autoantibodies. Although limited in number, the follow-up samples from early seropositive SCI patients shown in figure 5.1b, indicate that PSMD4 and S100B autoantibodies can already be detected at hospitalization (T0, collected within 1 week after SCI) and that they remain constant after SCI. Furthermore, PSMD4 and S100B autoantibody reactivity and levels were similar between early (<1 year after SCI; PSMD4 4%; S100B 9%) and chronic (>1 year after SCI; PSMD4 3%; S100B 5%) tSCI patients (Figure 5.1a). These preliminary observations suggest that PSMD4 and S100B autoantibodies are not part of a primary antibody response triggered by SCI pathological processes (figure 5.1b). This is further supported by a similar seroprevalence and antibody levels between healthy controls (PSMD4 4%; S100B 5%) and tSCI samples collected at hospitalization (T0; PSMD4 2%; S100B 7%)) or ≥3 weeks after injury (≥T1; PSMD4 4%; S100B 9%) (figure 5.1c). Similar results at both time points of sampling were obtained for pSCI patients (data not shown). For the remaining part of the study, the first time point of sampling was used for each SCI patient. Finally, we observed that all seropositive healthy controls were older than 55 years.

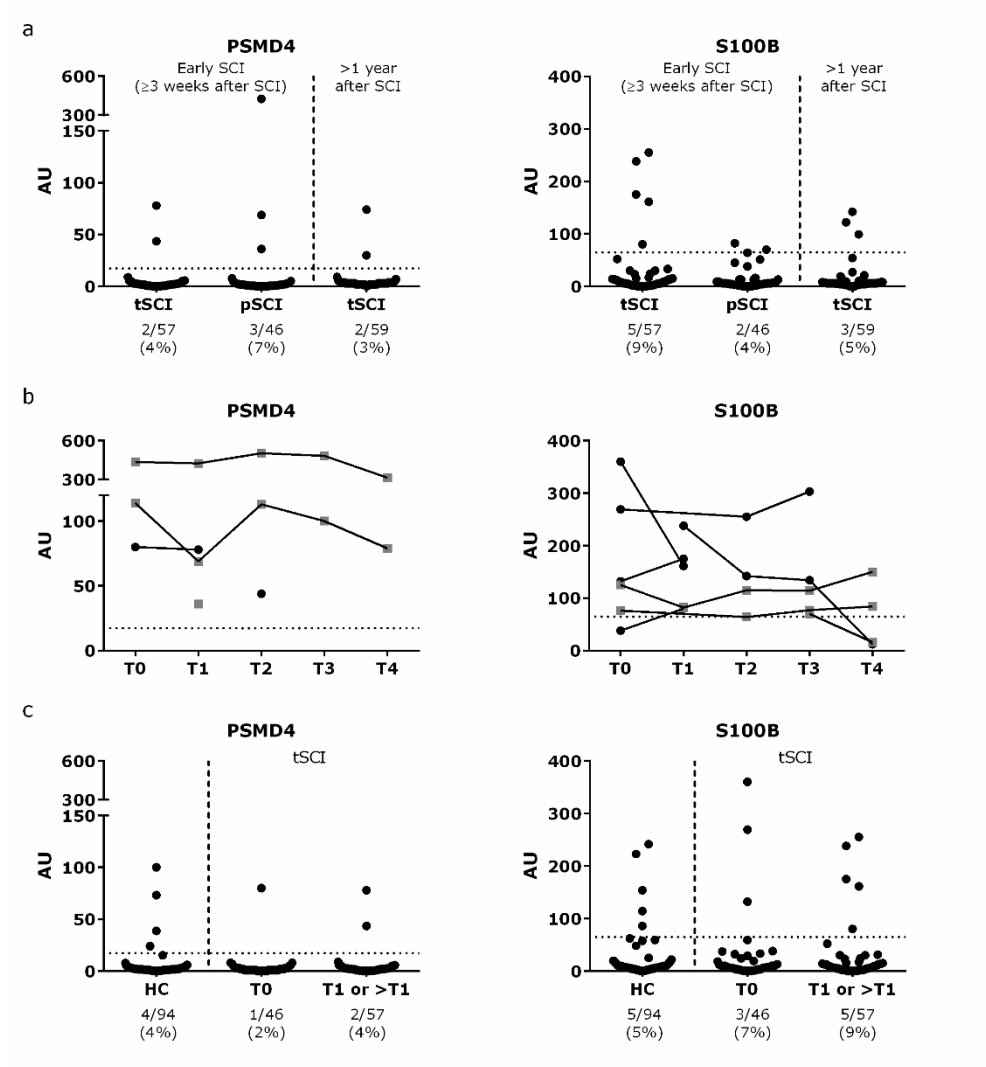

Figure 5.1: PSMD4 and S100B autoantibody responses in SCI patients

Plasma samples from SCI patients (46 pathological SCI (pSCI), 65 early traumatic SCI (tSCI) and 59 chronic traumatic SCI) were screened for PSMD4 and S100B autoantibody reactivity using peptide ELISA (a). Early SCI antibody responses were studied in samples collected at least 3 weeks after injury (≥T1). For 8 early tSCI patients, only a sample collected at hospitalization was available, causing the exclusion of these patients in graph a. Subsequently, PSMD4 and S100B antibody responses were investigated in follow-up samples of the early SCI cohort (b; tSCI patient samples are indicated in black; pSCI patient samples are indicated in grey squares). Samples of tSCI patients were taken at hospitalization (T0, collected within 1 week after SCI) and at 3 (T1), 6 (T2), 12 (T3) and 18 weeks (T4) after injury. Samples of pSCI patients were collected preoperatively (T0) and at

3 (T1), 6 (T2), 12 (T3) and 18 weeks (T4) after surgery. The PSMD4 and S100B seroprevalence and antibody levels were compared between healthy controls (HC) and tSCI samples collected at T0 and ≥T1 (c). Arbitrary units (AU) were calculated for PSMD4 and S100B autoantibodies using a calibration curve (a-c). Dots represent individual samples. The dashed horizontal line depicts the cut-off for seropositivity (based on antibody reactivity in the HC group) in the PSMD4 and S100B peptide ELISA and was set at 17.3 and 64.8 AU, respectively.

5.4.2 Exploration of the clinical relevance of PSMD4 and S100B autoantibodies in SCI patients

To explore the clinical relevance of PSMD4 and S100B autoantibodies, correlations between these antibody responses and general patient characteristics such as age and gender (figure 5.2a/b) or prognostic parameters such as injury severity (based on the AIS classification) and location of the lesion were studied. PSMD4 autoantibodies were not correlated with the general patient characteristics or prognostic parameters. For S100B autoantibody levels, a correlation with age was demonstrated ($p=0.03103$), while no correlation could be found for gender, AIS and the location of the injury.

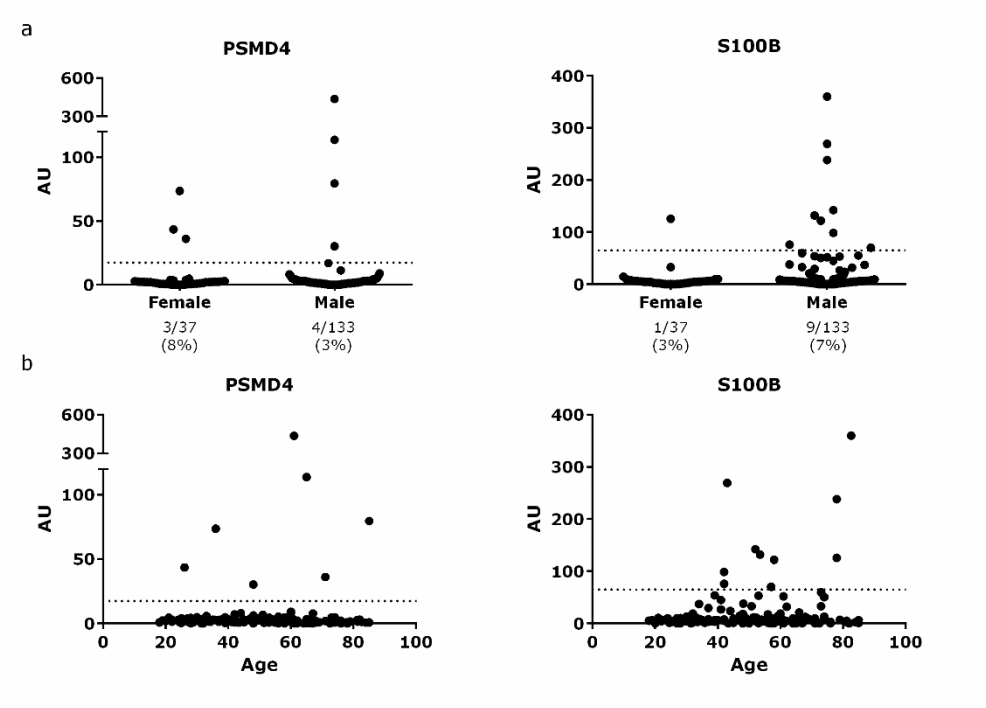

Figure 5.2: PSMD4 and S100B autoantibody responses in SCI patients: influence of gender and age

Correlations between PSMD4/S100B antibody reactivity and the gender (a) or age (b) of SCI patients (early traumatic and pathologic SCI patients and chronic SCI patients). Arbitrary units (AU) were calculated for PSMD4 and S100B autoantibodies using a calibration curve. Dots represent individual samples. The dashed horizontal line depicts the cut-off for seropositivity (based on antibody reactivity in the HC group) in the PSMD4 and S100B peptide ELISA and was set at 17.3 and 64.8 AU, respectively.

5.4.3 PSMD4 and S100B autoantibody specificity

In order to understand the potential relevance of PSMD4 and S100B autoantibodies in SCI, we addressed whether both autoantibody responses were present in similar pathology-induced neuroinflammatory (e.g. stroke) or autoimmune conditions (e.g. MS and RA patients). Therefore, 27 stroke, 54 MS and 57 RA patients were analyzed for the presence of autoantibodies toward PSMD4 and S100B (figure 5.3). Within the SCI patient population an effect of age on S100B autoantibody levels was observed, therefore, also age and gender influences on antibody reactivity were tested within the different study populations

and corrected for if necessary. All study populations (healthy controls, MS and RA patients) except stroke, showed PSMD4 immunoreactivity (2-5%), which is in the same range as the autoantibody reactivity in the SCI cohort (4%). While, healthy controls, MS and RA patients (5-7%) demonstrated a comparable prevalence of S100B autoantibodies (6%) as SCI patients, stroke patients did show 15% autoantibody reactivity toward S100B.

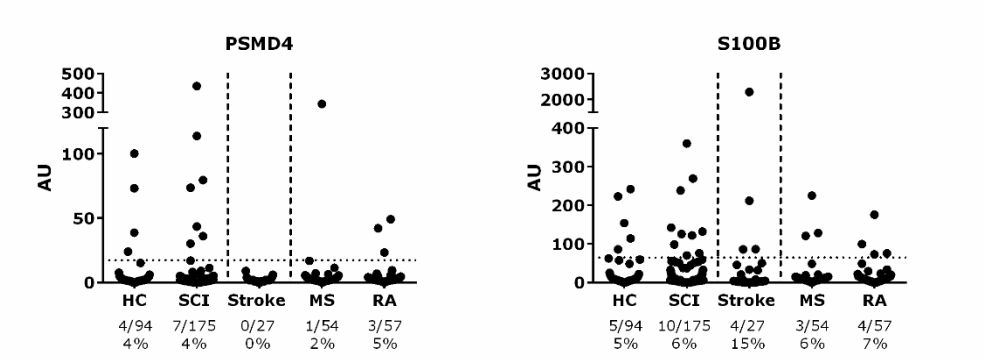

Figure 5.3: PSMD4 and S100B autoantibodies in neuroinflammatory and autoimmune disorders

Plasma samples of 94 healthy controls (HC), 175 spinal cord injury (SCI; early traumatic SCI, pathologic SCI and chronic traumatic SCI patients), 27 stroke, 54 multiple sclerosis (MS) and 57 rheumatoid arthritis (RA) patients were analyzed for the presence of PSMD4 and S100B autoantibody responses. Arbitrary units (AU) were calculated for PSMD4 and S100B autoantibodies using a calibration curve. Dots represent individual samples. The dashed horizontal line depicts the cut-off for seropositivity (based on antibody reactivity in the HC group) in the PSMD4 and S100B peptide ELISA and was set at 17.3 and 64.8 AU, respectively.

5.5 DISCUSSION

We here report the prevalence and specificity of PSMD4 and S100B autoantibodies in SCI patients and control groups. When analyzing the seroprevalence of PSMD4 and S100B autoantibodies in SCI patients, a similar autoantibody reactivity was demonstrated within the SCI subpopulations irrespective of the cause of pathology or time post-injury. Furthermore, these autoantibodies were also detected in healthy controls and other neuroinflammatory and autoimmune disorders, showing that they are not SCI specific. As the diagnosis of SCI is mostly straightforward and based on neurological symptoms and MRI images, the clinical significance of these autoantibody responses is less focused on their specificity. Next to the location of the lesion, also the injury severity is essential for an accurate prognosis prediction. Current prognostic tools provide only limited information on the severity and, therefore, there is a need for disease markers that can contribute to a better outcome prediction. In order to investigate the clinical relevance of PSMD4 and S100B autoantibodies, we investigated the correlations between these autoantibodies and general patient characteristics (age, gender) or prognostic parameters (AIS and injury location). Although 175 SCI patients were included in the study, only a limited number of patients showed autoantibody reactivity and clinical data was not always available, making correlations challenging. So far, no association between PSMD4 autoantibodies and general patient characteristics or clinical prognostic parameters was demonstrated. For S100B autoantibody levels a significant correlation was found with the age of the patient. Additionally, all seropositive healthy controls were older than 55 years. These observations are not unexpected as aging has shown to induce an increase in the generation of autoantibodies [179]. Furthermore, S100B autoantibodies have already been described for their clinical relevance in traumatic brain injury (TBI) and in this study S100B autoantibodies were found in related neuroinflammatory conditions such as stroke and SCI, which underscores the importance of a further characterization of their clinical role within neuroinflammatory pathologies [18, 19].

It has been suggested that after SCI and rupture of the blood-spinal cord barrier (BSCB), central nervous system (CNS) antigens are released from damaged tissue into the blood stream where they may trigger the activation of adaptive immune cells (e.g. T and B lymphocytes). B cell activation and differentiation into plasma

cells subsequently culminates in the production of pathologic antibodies and based on this hypothesis, it is expected that newly formed antibodies are present 3 weeks after the insult (peak of IgG production) [15, 17, 162, 180]. In our study, we found that primary antibody responses against PSMD4 and S100B were not generated, neither re-induced, following injury to the spinal cord. Therefore, PSMD4 and S100B immunoreactivity and autoantibody levels as seen in healthy controls and SCI patients, probably reflect reactivity in a limited percentage of the general population. By screening other study populations such as stroke, MS and RA patients, similar PSMD4 and S100B autoantibody reactivity and levels were demonstrated, suggesting that these autoantibody responses are also not induced by neuroinflammation or autoimmunity. Regardless of the origin of these autoantibody responses themselves, it is possible that they can affect the pathological or repair processes following SCI. Still, we would anticipate a pathogenic role for these autoantibody responses in spinal cord dysfunction only when accompanied by BSCB disruption, allowing the antibodies to infiltrate the spinal cord parenchyma.

As PSMD4 and S100B autoantibody responses were found in our healthy control cohort (respectively 4% and 5%) and other study populations, they probably represent a part of the natural autoantibody profile or are formed as response to exogenous targets and show reactivity to PSMD4 and S100B via molecular mimicry. Relatively constant levels and affinities of natural IgG autoantibodies toward S100B have been detected in serum of healthy adults [181]. Both PSMD4 and S100B are expressed in the CNS, which normally is considered 'immune privileged' due to an intact BSCB. In both traumatic and pathologic SCI conditions, the BSCB is damaged and thereby allows access for these autoantibodies to their CNS targets. In this way, (naturally occurring) autoantibodies still might contribute to pathological processes in CNS disorders, which emphasizes the need to elucidate the role of specific autoantibodies in SCI pathology [30, 161]. That S100B came up as an autoantibody target from our serological antigen selection, is especially interesting since S100B is considered a marker for blood-brain barrier damage, and repeated exposure to increased S100B levels has been shown to result in the development of an autoimmune response [151, 182]. Although increased S100B levels have been detected after SCI, our data demonstrate the presence of S100B autoantibodies in SCI patients, but no autoantibody (re-)induction [71, 75, 81, 149].

Whether this is due to the immunosuppressive effect that is seen after SCI or the single exposure to increased protein levels is not clear [183-185]. In order to investigate the hypothesis that repeated exposure to increased protein levels results in autoantibody production, other CNS pathologies with multiple triggers for protein expression such as TBI or epilepsy should be analyzed for the presence and induction of autoimmune responses.

In conclusion, our data demonstrate that PSMD4 and S100B autoantibody responses are present in SCI patients and healthy controls as well as in other neuroinflammatory and autoimmune pathologies. At present, there is no clear link between the presence of PSMD4 autoantibodies and general patient characteristics or clinical prognostic parameters for SCI. For S100B autoantibody levels, a correlation with the age of SCI patients was detected. As S100B autoantibodies have already been described for their clinical relevance in TBI and these autoantibodies were detected in SCI and stroke, the clinical relevance of these autoantibodies should be characterized further within neuroinflammatory pathologies. Furthermore, future studies are required to elucidate whether these immune responses have a biological relevance within SCI pathological processes.

6

Biological characterization of PSMD4 autoantibody responses in spinal cord injury

6.1 ABSTRACT

Autoantibodies against 26S proteasome non-ATPase regulatory subunit 4 (PSMD4) were detected in spinal cord injury (SCI) patients. In this study, we aim to further characterize the role of PSMD4 and autoantibodies against PSMD4 in SCI pathology. The expression pattern of PSMD4 was studied in the spinal cord of human and mice, and blood samples of naive and SCI mice were analyzed for PSMD4 antibody formation using our in-house PSMD4 ELISA. The pathological role of PSMD4 autoantibodies in SCI was explored using passive transfer of polyclonal rabbit PSMD4 autoantibodies in a T-cut hemisection mouse model. In normal human and mouse spinal cord tissue, PSMD4 expression was found in endothelial, neuronal and glial cells. In mice, PSMD4 gene expression was significantly increased in the acute and subacute phase after SCI and returned to basal levels in the early stage of the chronic remodelling phase. PSMD4 protein expression remained stable throughout a 28 day period after SCI. Furthermore, no PSMD4 antibody formation was detected in our SCI mouse model. Passive-transfer of polyclonal rabbit PSMD4 autoantibodies in a SCI mouse model did not show a detrimental or beneficial effect on the functional recovery of SCI mice. Further characterization of PSMD4 and PSMD4 autoantibodies is necessary to elucidate the biological relevance in SCI pathology.

6.2 INTRODUCTION

Antibodies have been shown to contribute to degenerative processes after spinal cord injury (SCI) [17]. Yet, the role of distinctive antigen-specific antibody responses in SCI pathology remains elusive. Previously, we detected UH.SCI.2 antibodies in SCI patients and identified 26S proteasome non-ATPase regulatory subunit 4 (PSMD4) as the *in vivo* target of UH.SCI.2 antibody responses. PSMD4 is often described under its aliases antisecretory factor (AF) and angiocidin which are formed by alternative splicing. Both isoforms are highly similar in sequence and overall structure, but differ by the addition of a three amino acid GER sequence at position 255 in the protein (figure 6.1) [172]. The UH.SCI.2 peptide sequence previously identified in our study (chapter 3) is located at the C-terminus of PSMD4 and has 100% similarity with both protein isoforms.

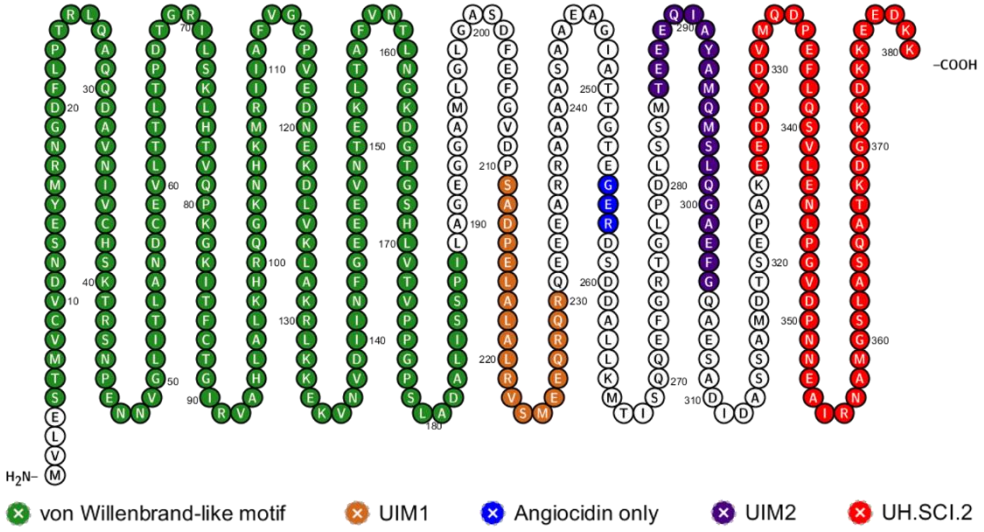

Figure 6.1: Amino acid sequence of PSMD4/AF, angiocidin and UH.SCI.2

Amino acid sequences of PSMD4/antisecretory factor (AF), angiocidin and UH.SCI.2 visualized using Protter (http://wlab.ethz.ch/protter/start/). Functional motifs, such as the von Willebrand-like motif and ubiquitin-interacting motifs (UIM), are indicated on the PSMD4 amino acid sequence.

PSMD4 is present in nearly all cell types and tissues of the body as a part of the 26S proteasome. In addition, PSMD4 is also found in a free form in the cytoplasm and nucleus or in the extracellular environment (e.g. plasma) [173]. The proteasome

is involved in the clearing of misfolded or damaged proteins or proteins that are no longer required and as such has important functions in biological processes such as cell cycle progression, apoptosis or DNA repair mechanisms [186]. Specifically, PSMD4 regulates proteolytic processes in the proteasome by binding polyubiquitin, a degradation signal on proteins, via its ubiquitin-interacting motifs (UIM) at the C-terminal end [173]. On the N-terminus, PSMD4 contains a von Willenbrand-like motif which is involved in the anti-inflammatory and anti-secretory functions [173, 174]. In healthy individuals, PSMD4 is thought to be present in an inactive state. Upon exposure to bacterial toxins or defined dietary compounds, a mild inflammatory response is initiated. This inflammation is suggested to induce post-translational modifications (e.g. proteolysis, glycosylation, phosphorylation) or conformational changes in the PSMD4 structure, influencing which motif becomes available [174, 187]. In line with an inflammatory function, PSMD4 is expressed by immune cells (e.g. macrophages, B cells and dendritic cells) and *in vitro* studies demonstrated a role of PSMD4 in the modulation of memory/effector T cell proliferation [188]. In the central nervous system (CNS), PSMD4 is located in blood vessels and perivascular cells which are essential in the initiation and regulation of inflammatory reactions [173]. Experimental autoimmune encephalomyelitis (EAE) resulted in an increased PSMD4 expression in the perivascular cells and additional PSMD4 expression in parenchymal microglia and infiltrating leukocytes [175]. Furthermore, the PSMD4 expression pattern in the CNS of EAE mice was suggested to correlate with the severity of disease [175]. Inhibition of PSMD4 expression using TLD-1A8A antibodies in an EAE model aggravated the clinical severity and duration of the disease [175]. Besides its beneficial role in EAE, protective effects of PSMD4 have also been reported in a rat model for intracranial hypertension and focal brain injury [189, 190]. Angiocidin, on the other hand, is described as a tumor and vascular associated protein, which is mainly studied in different types of cancer (e.g. lung, colon, prostate and breast) because of its inhibitory effect on angiogenesis and its involvement in tumor progression mechanisms [191]. Angiocidin is able to bind to tumor matrix proteins such as thrombospondin-1, which is important in the homing of leukocytes in the tumor. This finding suggests that angiocidin might be involved in the activation mechanisms of leukocytes [192]. Furthermore, it has been shown that angiocidin induces monocyte-to-macrophage differentiation and pro-

inflammatory cytokine secretion. Both characteristics result in an improved antigen presentation by monocytes and direct or indirect tumor cell destruction by functional macrophages [193, 194]. Additionally, an *in vitro* study in MS pathology demonstrated similar pro-inflammatory effects for angiocidin [176].

Previously, we found PSMD4 autoantibodies in SCI patients. Up to now, a contradictory role for the PSMD4 protein isoforms has been described. In this study, we aimed to investigate the biological relevance of PSMD4 and PSMD4 autoantibody responses in SCI pathology. First, the PSMD4 expression pattern was investigated in human and mice spinal cord. Subsequently, the formation of PSMD4 autoantibodies was explored after induction of a dorsal T-cut hemisection injury in mice. Finally, the biological relevance of PSMD4 autoantibodies was investigated by performing a passive transfer experiment of rabbit antibodies directed against the C-terminus of mouse PSMD4 in a SCI animal model. By investigating the biological relevance of PSMD4 autoantibody responses and PSMD4, more insight into the role of antibodies in SCI pathology will be obtained.

6.3 MATERIALS AND METHODS

6.3.1 Animal experiments

Experimental SCI

C57BL/6j mice (Janvier, Le Genest-Saint-Isle, France) were used for the *in vivo* experiments and housed in a conventional animal facility at Hasselt University under regulated conditions (i.e. in a temperature-controlled room (20 ± 3°C) on a 12 h light-dark schedule and with food and water *ad libitum)*. All procedures were approved by the local animal ethics committee of Hasselt University and were performed according to the guidelines described in Directive 2010/63/EU on the protection of animals used for scientific purposes.

A hemisection injury was applied in female, 9- to 10-week-old mice, as previously described [195-202]. Briefly, mice were anesthetized and the spinal cord was exposed by performing a partial laminectomy at thoracic level 8. Subsequently, iridectomy scissors were used to induce a bilateral hemisection injury in the spinal cord with the transection of the left and right dorsal funiculus, the dorsal horns and the ventral funiculus as a consequence. Induction of a T-cut hemisection causes a complete transection of the dorsomedial and ventral corticospinal tract and disturbs several other descending and ascending tracts (figure 6.2). After suturing of the muscles, the back skin was closed with wound clips (Autoclip ®, Clay-Adams Co., Inc.). The aftercare consisted of the administration of glucose solution (20%) to compensate for any blood loss during surgery, incubation in a temperature-controlled chamber (33°C) until thermoregulation was established and manually voiding the bladder until spontaneous return of the micturition reflex.

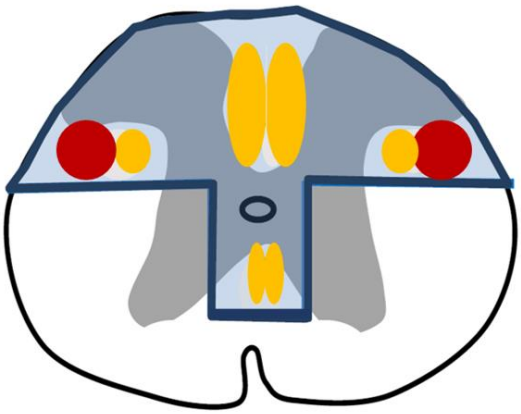

Figure 6.2: Schematic representation of a T-cut hemisection SCI in rodents (coronal view)

The transected area of the spinal cord after a T-cut lesion is indicated in blue. The corticospinal tract and the rubrospinal tracts are indicated in yellow and red, respectively. Image modified from Tuszynski and Steward, 2012 [201].

Basso Mouse Scale (BMS) for locomotion evaluation

In order to investigate the functional recovery after induction of a T-cut hemisection, locomotor recovery was evaluated by a blinded investigator using the BMS locomotor rating scale [60]. The BMS is a 10-point scale (9=normal locomotion; 0 =complete hind limb paralysis) in which mice are scored based on forelimb and hindlimb coordination during sustained locomotion, trunk stability, paw orientation and tail position in an open field during a 4-minute interval [60, 61]. The first week after injury, mice were scored daily and from the start of the second week until the end of the observation period (28 days post-injury (dpi)), mice were scored every second day. Mice with a BMS-score of ≥2 directly after surgery were excluded from the study.

Intraspinal antibody injections

To investigate the biological relevance of PSMD4 autoantibodies in SCI pathology, polyclonal rabbit anti-C-terminal mouse PSMD4 antibodies were produced (Eurogentec, Seraing, Belgium). Mice with a hemisection injury were divided into three treatment groups, those receiving an intraspinal injection of vehicle control (phosphate buffered saline (PBS), 0.01% thimerosal and 0.1% bovine serum albumin (BSA)), isotype control antibodies (rabbit IgG/IgM in PBS, 0.01%

thimerosal and 0.1% BSA) or C-terminal mouse PSMD4 antibodies (in PBS, 0.01% thimerosal and 0.1% BSA). Intraspinal antibody injections were performed 2 mm rostral to the lesion site using a motorized stereotactic injection pump (Stoelting, Dublin, Ireland) with a 33-gauge needle attached to a 10 µl Hamilton syringe as described before [17]. The needle was stereotactically positioned into the spinal cord at a depth of 1 mm and 0.5 µg of antibodies in a volume of 1 µl were injected over a 4 minutes (min) time period. The antibody concentration injected in the spinal cord was based on a similar passive transfer experiment reported by Ankeny et al [17]. In order to allow a proper distribution of the bolus injection, the needle was kept in place for an additional 4 min.

6.3.2 RNA isolation and RT-qPCR

Spinal cord tissue was collected from naive and SCI mice (5 mm cranial and 5 mm caudal to the lesion center) at different time points (2, 7 and 28 dpi) to study PSMD4 mRNA levels. mRNA was isolated using the Paris Kit (Fisher Scientific, Erembodegem, Belgium), according to the manufacturer's protocol with minor modifications. A chloroform incubation step was added in the protocol to eliminate fat/cholesterol from the spinal cords to ameliorate the RNA isolation [203]. The reverse transcription system (Quanta Biosciences, Gaithersburg, USA) was used to convert RNA into cDNA using the iCYCLER (Biorad Laboratories N.V., Temse, Belgium). Quantitative PCR reaction mix consisted of fast SYBR green master mix (Applied biosystems, Gaasbeek, Belgium), 300 nM forward and reverse primer (table 6.1), RNase free water and 10 ng template cDNA and was performed by a StepOnePlus detection system (Applied Biosystems, Gaasbeek, Belgium) using universal cycling conditions (40 cycles of 15 s at 95°C and 1 s at 60°C). All PCR reactions were done in triplicate. Primers were designed using PrimerBank (https://pga.mgh.harvard.edu/primerbank/). The RT-qPCR data were normalized according to the method described by Vandesompele et al. (2002), by geometric averaging of multiple internal control genes [204]. Processing of raw data and calculation of normalized relative quantities were done by using an improved version of the ΔΔCt method [205]. The mRNA expression levels were expressed relative to the basal condition (naive mice). The two most stable housekeeping genes out of five for the different experiments were cyclophilin A (CYCA) and tyrosine 3-monooxygenase/tryptophan 5-monooxygenase activation protein, zeta polypeptide (YWHAZ).

Table 6.1: Primer sequences

Gene	Forward primer	Reverse primer
PSMD4[a]	5'-GACCCGGAGTTCCTTCAGAG-3'	5'-CAGAGCCCCCATGACACTTC-3'
Reference genes		
CYCA[b]	5'-GCGTCTCCTTCGAGCTGTT-3'	5'-AAGTCACCACCCTGGCA-3'
YWHAZ[c]	5'-GCAACGATGTACTGTCTCTTTTGG-3'	5'-GTCCACAATTCCTTTCTTGTCATC-3'

[a]26S proteasome non-ATPase regulatory subunit 4
[b]Cyclophilin A
[c]Tyrosine 3-monooxygenase/tryptophan 5-monooxygenase activation protein, zeta polypeptide

6.3.3 Western blot

Total protein concentrations of SCI tissue, isolated one cm around the lesion (5 mm cranial and 5 mm caudal), were measured using the Pierce™ BCA Protein Assay kit (Thermo Scientific, Belgium). Protein samples (30 µg) were separated by 12% sodium dodecyl sulfate polyacrylamide gel at 200 V and blotted onto a 100% methanol-activated polyvinylidene fluoride membrane (Millipore, Overijse, Belgium) for 90 min at 350 mA. Membranes were blocked for 2 hours (h) in 5% (w/v) skimmed milk powder in PBS (MPBS, 50 mM Tris, 150 mM sodium chloride, pH 7.5) followed by overnight incubation with rabbit anti-PSMD4 antibody (1:1000, Abexxa Catalogue number abx000984, Cambridge, United Kingdom)) in 5% MPBS, at 4°C. Next, membranes were washed for 30 min (two times short, 15 min, two times 5 min) with 0.1% (v/v) PBS Tween-20 (PBS-T) and incubated with goat anti-rabbit IgG horseradish peroxidase (HRP) labelled antibody (1:1500; Dako, Heverlee, Belgium) for 1 h at room temperature (RT). Pierce™ ECL Western blotting Substrate (Thermo Fisher Scientific, Erembodegem, Belgium) was used for signal detection and images were taken using ImageQuant LAS 4000 Mini (Thermo Fisher Scientific, Erembodegem, Belgium). After visualization of PSMD4 protein expression, primary and secondary antibodies were removed by mild stripping buffer incubation for two times 5-10 min, followed by washing steps with PBS-T. Blocking steps were repeated and membranes were incubated with mouse anti-beta(β)-actine antibody (1:3000, 47778, Santa Cruz, USA) at 4°C, while shaking, as an internal loading control. After washing the membranes, rabbit anti-mouse HRP labelled antibody (1:1500; P0449, Dako, Heverlee, Belgium) was incubated for 1 h at RT. Washing steps were repeated and chemiluminescent signal detection was performed as described above.

6.3.4 Peptide and recombinant protein ELISA

In order to investigate the induction of antibody responses against C-terminal or full length PSMD4 after SCI, peripheral blood from female naive and SCI C57BL/6j mice was collected. Samples of naive mice were taken between the age of 9 and 68 weeks. Samples of SCI mice were taken between the age of 14 and 16 weeks. Blood samples were centrifuged for 10 min at 400 g. Plasma was collected, aliquoted and stored at -20°C.

Antibody reactivity toward C-terminal and full length PSMD4 was measured with solid-phase ELISA using synthetic C-terminal peptide or recombinant PSMD4 protein, as described in chapter 4 with minor modifications. Briefly, for peptide ELISA, polystyrene flat-bottom plates (Greiner Bio-one, Wemmel, Belgium) were coated with 10 µg/ml synthetic peptide (more than 85% purity, Biomatik/Gentaur Europe, Kampenhout, Belgium) and control peptide in PBS, overnight at RT, while for protein ELISA, high binding ELISA plates (Greiner Bio-one) were coated with 10 µg/ml recombinantly produced PSMD4 and thioredoxin (THIO, control signal) in coating buffer (0.1 M sodium hydrogen carbonate, pH 9.6), overnight at 4°C. After blocking the plates, plasma samples were diluted 1:50 in 2% MPBS and incubated for 2 h (RT, shaking). The color reaction in peptide and protein ELISA was incubated for 15 min. Samples were tested in duplicate in a single ELISA experiment.

6.3.5 Immunohistochemistry

Normal human and EAE mouse spinal cord paraffin coupes were kindly provided by Prof. Jack van Horssen of Hasselt University and VU University Medical Center Amsterdam and Suzan Wetzels of Hasselt University, respectively. Tissue sections of human and mouse spinal cord were deparaffinized and endogenous peroxidase was deactivated by incubation with 0.3% methanol for 10 min. After washing the sections with PBS and Milli-Q water, antigen retrieval was performed by addition of pre-warmed 10 mM sodium-citrate buffer with 0.05% Tween-20 for 30 min. Wash steps were repeated and sections were blocked with 100% protein block (serum free; Dako, Heverlee, Belgium) for 30 min at RT. Blocking solution was removed and sections were incubated overnight at 4°C with rabbit anti-PSMD4 antibody (1:400, Abbexa, Cambridge, United Kingdom) in PBS with 1% protein block and 0.05% Triton X-100. After washing the sections, swine anti-rabbit biotinylated antibody (1:400, Dako, Heverlee, Belgium) in PBS with 10% protein

block was incubated for 1 h at RT followed by addition of streptavidin/HRP (1:400) in PBS with 10% protein block for 30 min at RT. 3, 3'-diaminobenzidine (DAB, Dako, Heverlee, Belgium) staining was incubated for 1 min, followed by a hematoxylin counterstaining for 5 min. Sections were dehydrated by incubation in increasing alcohol series and xylene and mounted with DPX non aqueous mounting medium. Images were taken with the Leica DM2000 LED and a Leica MC170 HD camera (Leica microsystems, Diegem, Belgium) or Nikon Eclipse 80i microscope and a Nikon Digital sight DS-SM camera (Nikon Instruments Europe B.V., Brussels, Belgium).

In order to collect cryosections for immunohistochemistry purposes, mice were sacrificed with a lethal injection of Dolethal and transcardially perfused with Ringer solution containing heparin and subsequently with 4% paraformaldehyde (PFA) in PBS (pH 7.4). Dissected spinal cords were incubated with 5% sucrose in 4% PFA followed by 30% sucrose in PBS. Dehydrated tissues were embedded in Tissue-Tek O.C.T. Compound (Sakura, Berchem, Belgium) and frozen in liquid-nitrogen cooled isopentane. Serial sagittal cryosections (10 µm thick) were obtained and blocked with 10% protein block in PBS containing 0.5% Triton X-100 for 30 min at RT. Subsequently, the cryosections were incubated with the primary antibodies rabbit anti-PSMD4 (1:1000, Abbexa, Cambridge, United Kingdom) or mouse anti-GFAP (glial fibrillary acidic protein, 1:500, Sigma, Diegem, Belgium) and rat anti-MBP (myelin basic protein; 1:250, Wako, Neuss, Germany) in PBS with 1% protein block (serum free; Dako, Heverlee, Belgium) and 0.05% Triton X-100 overnight at 4°C in a humidified chamber. After washing the cryosections three times 10 min in PBS, GFAP/MBP stainings were incubated with goat anti-mouse Alexa 568 (1:250, Thermo Fisher Scientific, Belgium) and goat anti-rat Alexa 488 (1:250, Thermo Fisher Scientific, Belgium) in PBS with 1% protein block and 0,05% Triton X-100. Washing steps were repeated and 4',6-diaminodino-2-phenylindole (DAPI) counterstaining was performed for 10 min followed by mounting of the cryosections. Images were taken with a Nikon Eclipse 80i microscope and a Nikon digital sight camera DS-2MBWc (Nikon Instruments Europe B.V., Brussels, Belgium) or a Leica DM4000 B LED microscope and a Leica DFC 450c camera (Leica microsystems, Diegem, Belgium).

For the PSMD4/neuronal nuclei (NeuN) double staining, PSMD4 incubated cryosections were washed and incubated with mouse anti-NeuN antibody (1:100,

Merck, Overijse, Belgium) in PBS for 1.5-2 h at RT. Washing steps were repeated and a mixture of goat anti-mouse Alexa 488 (1:300, Invitrogen) and goat anti-rabbit Alexa 555 (1:600, Invitrogen) in PBS containing 10% protein block and 0.05% Triton X-100 were pre-incubated for 1 h at RT and subsequently added to the cryosections for 1 h at RT. After washing the cryosections, DAPI counterstaining was performed for 10 min at RT followed by a Sudan Black staining (Sigma-Aldrich, Overijse, Belgium) for 10 min to reduce the background signal. Cryosections were washed in 70% ethanol and eight times in PBS and mounted with fluorescent mounting medium (Dako, Heverlee, Belgium). Images were taken as described before.

6.3.6 Data analysis

For the peptide and protein ELISA, results were reported by means of the ratio of the OD from the specific signal (C-terminal or full length PSMD4) and the OD of the control signal (control peptide or THIO). Samples were considered positive when the general reactivity (OD(C-terminal or full length PSMD4)/OD(control peptide or THIO)) was higher than 1.5.

Lesion size (anti-GFAP immunofluorescence) and demyelinated area (anti-MBP immunofluorescence) were quantified on 3-7 serial sections per animal (vehicle control: n=2, isotype control antibodies: n=3, C-terminal mouse PSMD4 antibodies: n=1) using ImageJ open source software, as described in [202].

Statistical analysis was performed using GraphPad Prism 6 XML (Graph Pad software, La Jolla, California, USA). PSMD4 mRNA and protein levels were compared between the different time points after injury by performing a Mann-Whitney U testing or the Kruskal Wallis test followed by Dunn's multiple comparison test. Functional recovery evaluation via the BMS (*in vivo*) was analyzed using two-way ANOVA for repeated measurements with a bonferonni post hoc test for multiple comparisons. For all statistical tests, a p-value of <0.05 was considered statistically significant.

6.4 RESULTS

6.4.1 PSMD4 is expressed by endothelial, neuronal and glial cells in the spinal cord

In order to understand the role of PSMD4 in SCI, we first assessed the expression pattern of PSMD4 in human and mice spinal cord tissue. In human tissue, PSMD4 expression was found in cells lining the spinal central canal and blood vessels, which likely represent ependymal or endothelial cells, respectively (figure 6.3). Additionally, also a subset of cells located in the white matter and the dorsal and ventral horn of the spinal cord expressed PSMD4. In the white matter, PSMD4-positive cells hold a glial-like phenotype. In the grey matter, PSMD4-positive cells demonstrate a large cell body with neuritis, suggestive of motor and sensory neurons of the ventral and dorsal horn, respectively. In non-lesion grey matter of spinal cord tissue from EAE mice, PSMD4-positive cells with a neuronal morphology were detected (figure 6.4a). As shown in figure 6.4b, PSMD4/NeuN double-staining of non-lesion spinal cord tissue of SCI mice confirmed the neuronal phenotype (NeuN-positive) of PSMD4-positive cells. Furthermore, also cells positive for only PSMD4 were visible in the overlap picture, indicating that PSMD4 was also expressed by other cell types, presumably glial cells, in the spinal cord parenchyma.

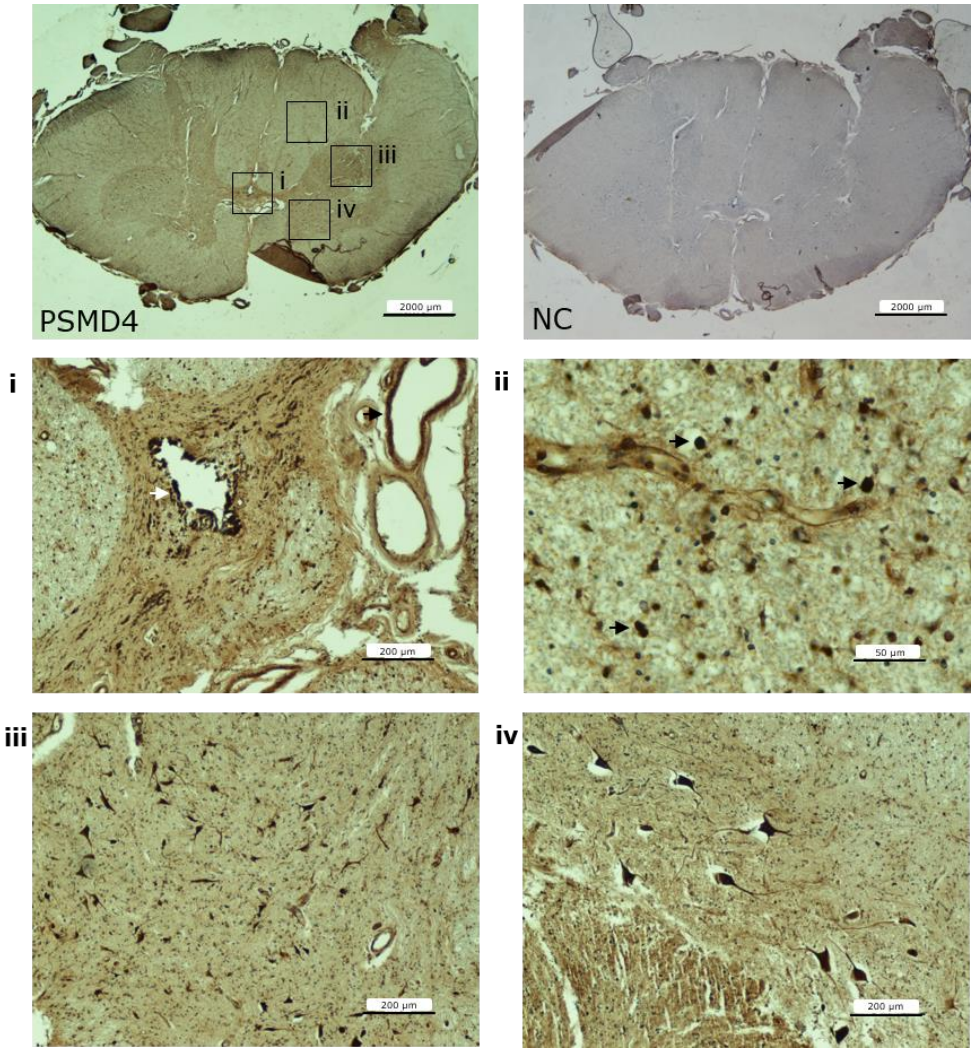

Figure 6.3: PSMD4 expression in human spinal cord tissue

PSMD4 staining in normal human spinal cord tissue was performed with DAB (brown) followed by an haematoxylin counterstaining (blue). Arrowheads indicate the spinal central canal (i, white), a blood vessel (i, black), glial cells (ii, black) and sensory (iii) and motor (iv) neurons. NC, negative control (no primary antibody).

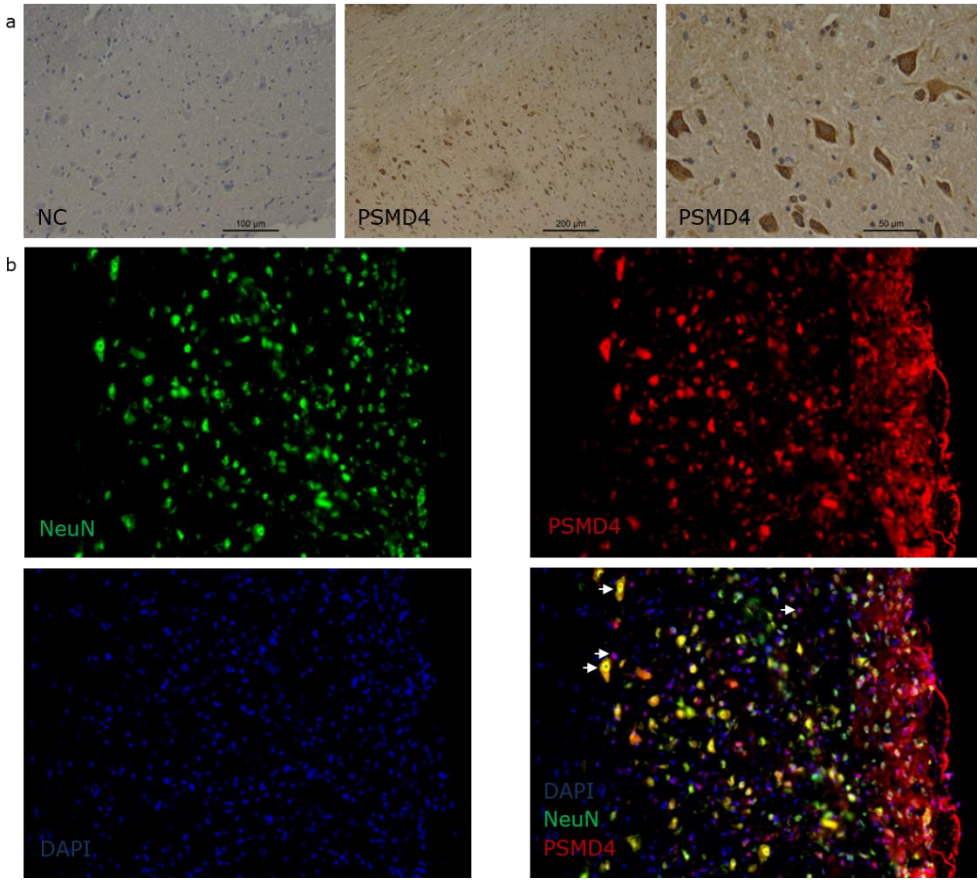

Figure 6.4: PSMD4 expression in mouse spinal cord tissue

PSMD4 expression in normal appearing spinal cord tissue of EAE mice (a). Staining was performed with DAB (brown) followed by an haematoxylin counterstaining (blue) (a). PSMD4 staining using fluorescently labeled secondary antibodies in normal spinal cord tissue of SCI mice (b). To characterize the PSMD4-positive cells, mouse SCI spinal cord was double-stained with PSMD4 and neuronal nuclei (NeuN). Arrowheads in the overlap figure indicate single- and double-positive cells for PSMD4 and/or NeuN. Pictures of fluorescent stainings were taken at a 20x magnification. NC, negative control (no primary antibody); DAPI, 4',6-Diamidino-2-Phenylindole.

6.4.2 PSMD4 protein expression and PSMD4 antibody production were not induced after SCI in mice

Next, we investigated whether PSMD4 expression was increased in the acute (2 dpi), the subacute (7 dpi) and at the early stage of the chronic remodeling phase (28 dpi) in a T-cut hemisection mouse model. Gene expression analysis showed a significant induction of PSMD4 mRNA 2 dpi compared to baseline levels, which remained elevated (although at lower levels) at 7 dpi and returned to basal levels at day 28 post-SCI (figure 6.5a, $p<0.05$). However, PSMD4 protein levels remained unchanged over a period of 28 dpi (figure 6.5b). Next, both undamaged and lesion spinal cord tissue of SCI mice were stained for PSMD4. In the undamaged tissue of the spinal cord, a clear cellular PSMD4 staining was present, while in the lesion site, a more diffuse PSMD4 staining pattern was observed with less PSMD4-positive cells (Figure 6.5c). In **chapter 3**, we reported the presence of PSMD4 autoantibodies in SCI patients and healthy controls. We now screened plasma samples of naive (n=10) and SCI mice (n=12, 28 dpi) for the presence of antibodies against C-terminal peptide and full length human PSMD4. As shown in figure 6.5d, 1 of the 10 naive mice demonstrated borderline anti-PSMD4 reactivity and there was no induction of these antibody responses after SCI in mice.

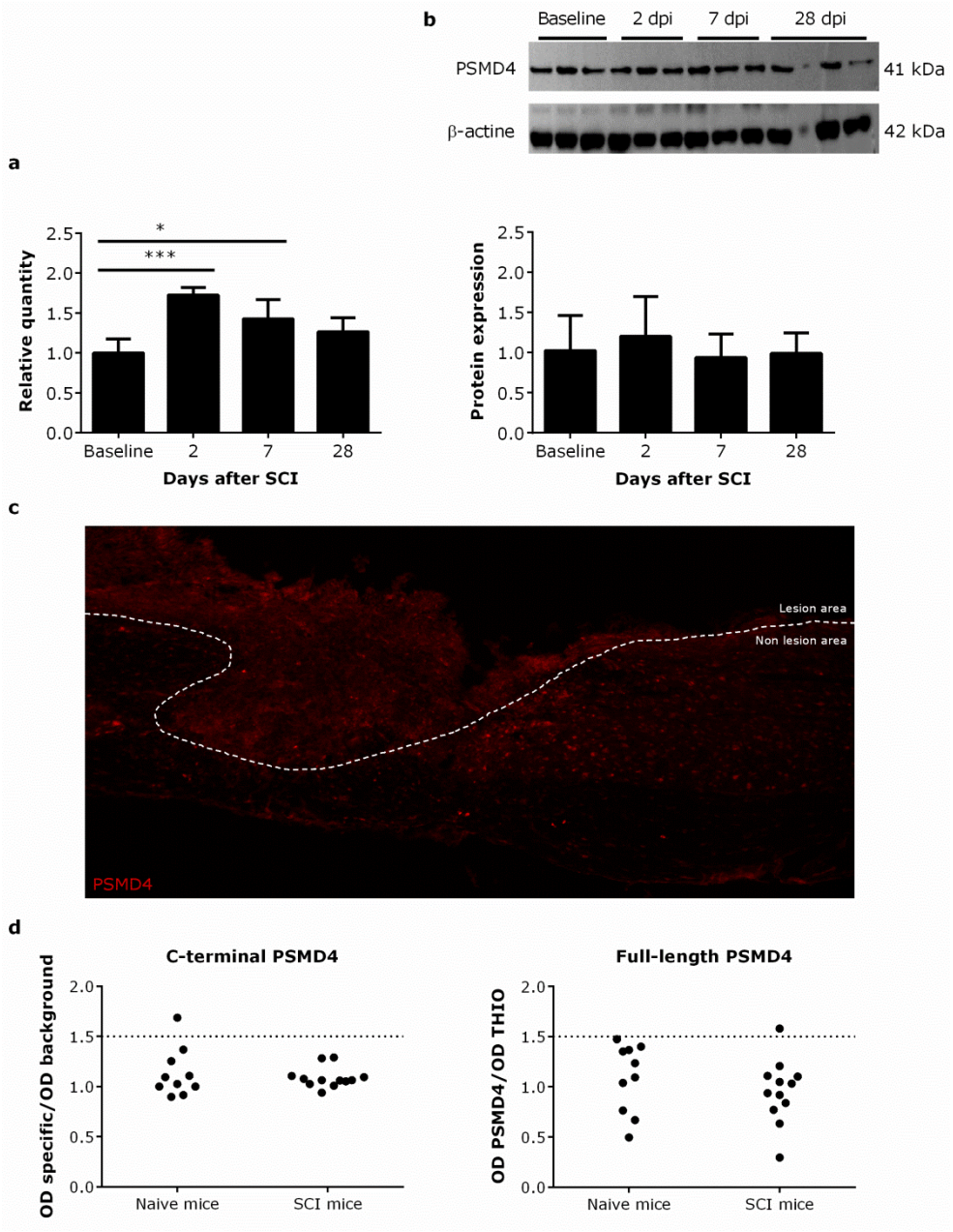

Figure 6.5: PSMD4 and PSMD4 antibodies in SCI mice

PSMD4 gene (a) and protein (b) expression was investigated in spinal cord tissue collected from naive mice (qPCR n=8 and western blot n=10, baseline) and 2 (qPCR n=4 and western blot n=7), 7 (qPCR n=8 and western blot n=8) and 28 (qPCR n=4 and western blot n=7) days post-injury (dpi). The mRNA expression levels were normalized to the 2 most stable housekeeping genes (cyclophilin A (CYCA) and tyrosine 3-monooxygenase/tryptophan 5-

monooxygenase activation protein, zeta polypeptide (YWHAZ)) and expressed relative to the basal condition (naive mice). PSMD4 protein expression was normalized to β-actine. PSMD4 gene and protein expression levels were compared between the different time points after injury by performing a Mann-Whitney U testing or the Kruskal Wallis test followed by Dunn's multiple comparison test. For all statistical tests, a p-value of <0.05 was considered statistically significant (*, $p<0.05$; ***, $p<0.001$). PSMD4 staining in spinal cord tissue (collected 1 week post-injury) of SCI mice (c, 5x magnification). The lesion area is indicated with a dashed line. C-terminal and full length PSMD4 antibody induction was studied in naive (n= 10) and SCI mice (n= 12) (d). Antibody reactivity was visualized in the ratio of the optical density (OD) from the specific signal (C-terminal peptide or full length PSMD4) and the OD from the control signal (control peptide or THIO).

6.4.3 The pathologic role of antibodies against the C-terminus of mouse PSMD4 in SCI pathology

To address whether PSMD4 autoantibody responses have a pathologic effect in SCI pathology, a dorsal T-cut hemisection was induced in female wild-type mice in conjunction with an intraspinal injection of antibodies against the C-terminus of mouse PSMD4, isotype control antibodies or vehicle control. Functional recovery was evaluated up to 28 dpi (figure 6.6a). Our study included 13 animals in each treatment group. Two animals of different groups (C-terminal mouse PSMD4 antibody group and vehicle control group) died the day of surgery. Animals with severe weight loss post-injury and/or the absence of locomotor recovery after 10 dpi were excluded from the study. All three groups experienced severe hind limb paralysis up to 10 dpi and showed only limited recovery toward the end of the observation period, with no difference in functional recovery between the three groups. Histological analyses of the lesion size (GFAP staining) and demyelinated area (MBP staining) on spinal cord tissue of recovering mice demonstrated similar results for all three groups (figure 6.6b/c).

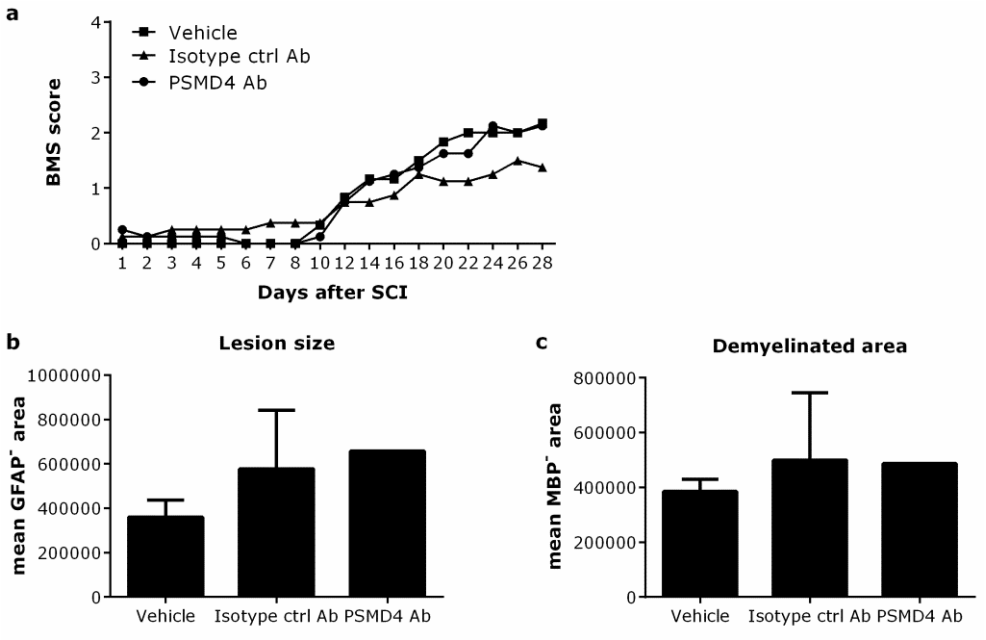

Figure 6.6: Effect of C-terminal mouse PSMD4 antibodies in a SCI mouse model

C57BL/6j mice with an T-cut hemisection lesion were intraspinally injected with vehicle control (n=3), isotype control antibodies (isotype ctrl Ab, n=4) and C-terminal PSMD4 antibodies (PSMD4 Ab, n=4). Functional recovery was evaluated for 28 days post-injury using the Basso Mouse score (BMS) (a). Spinal cord sections of recovering mice (vehicle: n=2, isotype ctrl Ab: n=3, PSMD4 Ab n=1) were stained for glial fibrillary acidic protein (GFAP) and myelin basic protein (MBP) to quantify the lesion size (b) and demyelinated area (c), respectively.

6.5 DISCUSSION

In the current study, we characterized the biological relevance of PSMD4 and PSMD4 autoantibodies in SCI pathology. Distinct cell types, such as endothelial, neuronal and glial cells, were found to express PSMD4 in the spinal cord, representing potential targets of PSMD4 autoantibodies after disruption of the blood-spinal cord barrier (BSCB). These observations are based on cell morphology and location in the tissue, and thus further confirmation of cell type expression is required using specific markers. In this context, we did validate the neuronal phenotype of PSMD4-positive cells. Our histological observations are in line with the study of Johansson et al. (2008) which showed PSMD4 expression in neurons and epithelial cells of the choroid plexus in rat brain [206]. Jennische et al. (2006) generated polyclonal antibodies against PSMD4, which recognized neurons with an epitope-specific subcellular staining pattern. This finding indicates that PSMD4 is present in the CNS in different conformational variants [174]. After SCI in mice, cellular PSMD4 expression was mainly found outside the lesion site, suggesting that PSMD4 autoantibodies might thus affect healthy spinal cord tissue after disruption of the BSCB. Furthermore, in healthy individuals, PSMD4 was suggested to be present in an inactive state. Upon environmental changes and induction of a mild-inflammatory response, post-translational modifications or conformational changes occur, which converts PSMD4 into an active form [187, 207]. Since SCI has a significant impact on the body, the activation state of PSMD4 after SCI should be analyzed as well. Additionally, as PSMD4 might be present in varying conformations or with post-translational modifications, antibody responses directed against epitopes located in modified sites of the protein might not be selected during the SAS procedure or measured with our PSMD4 ELISA. Future experiments should explore the PSMD4 structure after SCI in order to gain more insight into the role of PSMD4 in SCI pathology.

Next, we investigated the expression levels of PSMD4 after SCI to gain further insight into the function of this protein in SCI pathology. At mRNA level, PSMD4 gene expression showed a significant induction in the acute (2 dpi) and subacute phase (7 dpi) after injury in mice, pointing to the activation of pathways with PSMD4 involvement. Gene expression levels returned to basal levels in the early stage of the chronic remodeling phase (28 dpi). Despite the induction of PSMD4 at transcriptional level after SCI, on protein level, PSMD4 expression remained

constant during a time period of 28 dpi. Our observations are in contrast with the study of Davidson et al. (2004), which showed that EAE induction in rats resulted in a reduced PSMD4 gene expression level preceding the onset of clinical symptoms (day 2 after EAE induction), followed by increased gene expression until resolution of the disease [175]. These opposing findings regarding PSMD4 expression observed in SCI and EAE might be explained by the nature of the pathologies (chronic versus acute inflammation), the species (rat versus human) and different techniques that were used to investigate PSMD4 expression.

PSMD4 autoantibodies were detected in SCI patients and healthy controls (chapter 3). In mice, PSMD4 antibody reactivity was found in only 1 in 10 of the controls and these antibodies were not induced after SCI. As the serum IgG half-life in mice is shorter than in humans, 28 dpi might be too late to detect the induction of newly formed PSMD4 antibodies in mice [208]. A full kinetic study covering the different phases after SCI (acute, subacute and chronic phase) is needed in order to study SCI-induced antibody responses. Ankeny et al. (2009) demonstrated that SCI-induced antibodies exert neurotoxic effects in the spinal cord of naive mice [17]. At present, it is not known which proteins these antibodies are targeting and the role of antigen-specific antibodies in SCI pathology has not been studied. As we found PSMD4 autoantibodies after SCI in patients, we performed a passive transfer experiment with C-terminal mouse PSMD4 antibodies in a SCI mouse model. Our preliminary results demonstrated no effect of C-terminal mouse PSMD4 antibodies on the functional recovery after SCI. Due to the small final sample size, the passive transfer experiment should be repeated in order to assess the role of PSMD4 autoantibodies in SCI pathology. The induction of two lesions in the spinal cord (e.g. T-cut hemisection injury in combination with the intraspinal injection of antibodies) might explain both the absence of recovery and the severe weight loss causing the exclusion of animals from the study. Therefore, future experiments should focus on injecting antibodies in the spinal cord of naive mice in order to study the pathogenicity of these antibodies. Alternatively, PSMD4 antibodies can be injected peripherally after SCI as a disrupted BSCB increases the permeability of the spinal cord. In this case, sufficient infiltration of PSMD4 antibodies might be limited and variable between the different animals in the study, yet, this experimental setup would actually mimic the human situation to a better extent.

PSMD4 is shown to exert protective effects in rats with intracranial hypertension and focal brain injury [189, 190]. Furthermore, PSMD4 is expressed in immune cells and *in vitro* studies demonstrated an immune modulatory effect on effector/memory T cells and their cytokine profile. Therefore, inhibition of PSMD4 expression was expected to have an pro-inflammatory effect on the neuroinflammatory response after SCI [175]. Inhibition of PSMD4 in cultured T cells resulted in the expression of pro-inflammatory cytokines. This finding was further supported by an increased severity of the disease course after injection of PSMD4 antibodies in an EAE model [175]. Based on these results, blocking of PSMD4 expression induces a pro-inflammatory micro-environment, which might contribute to additional damage within the spinal cord and further loss of functionality. Up to now, only a degenerative effect of SCI-induced antibody responses has been described, while antibodies might also contribute in recovery processes. Further characterization of the role of antibodies in SCI pathology will give more insight into the neuroinflammatory response and might contribute to the development of novel treatment strategies.

In conclusion, PSMD4 was expressed in blood vessels, the spinal central canal and glial and neuronal cells of the spinal cord. As these components might be targeted by PSMD4 autoantibodies after disruption of the BSCB, further characterization of PSMD4 autoantibodies in SCI pathology is essential.

7

SUMMARY, GENERAL DISCUSSION & FUTURE PERSPECTIVES

7.1 Summary and general discussion

Spinal cord injury (SCI) is a sudden and unexpected condition resulting in temporary or permanent disruption of motor, sensor and/or autonomic functions [1, 2]. As the patients' quality of life is dramatically affected and current treatment strategies are unable to induce complete neurological or functional recovery, an accurate diagnosis and prognosis prediction is essential [5]. The diagnosis of SCI is mostly straightforward and based on neurological symptoms and magnetic resonance imaging (MRI). A reliable prognosis prediction is more challenging as the current prognostic tools have various limitations and give only limited information on the severity of the lesion [177, 178]. Therefore, the identification of disease markers that can support the current prognostic tools is warranted. Furthermore, clinically relevant markers that are associated with the disease can give more insight into the pathological processes after SCI and can contribute to the development of novel treatment strategies.

Recent studies highlight the pivotal role of B cells and antibodies in SCI-induced neuroinflammation [15, 17]. Animal models have shown that B cells and antibodies clearly contribute to aggravated tissue damage and impaired neurological recovery after SCI [15, 17]. However, the identity of SCI-induced antibody targets remains unclear. In SCI patients, elevated levels of antibodies to several central nervous system (CNS) lipids and proteins such as GM1 gangliosides and myelin-associated glycoprotein have been detected in serum [23, 24, 26, 27, 29, 104]. Despite these findings, there is no substantial evidence yet for a relevant role of B cells and antibodies in SCI-induced disease processes in humans. Therefore, a comprehensive analysis of patient samples is needed to establish the true prevalence, specificity and pathogenic relevance of SCI-induced antibodies in humans.

The goal of this study was to determine the antibody reactivity profile after SCI using serological antigen selection (SAS) in order to identify novel disease markers for SCI patients and to discover biologically relevant antibody responses. Two of the newly identified antigenic targets, UH.SCI.2 and UH.SCI.7, correspond to parts of the proteins 26S proteasome non-ATPase regulatory subunit 4 (PSMD4) and protein S100-B (S100B), respectively. For both antigenic targets we confirmed the *in vivo* identity. Using our in-house optimized peptide ELISA, PSMD4 and S100B autoantibodies were further characterized within SCI patients and other

study populations for their clinical relevance. Subsequently, we explored the biological relevance of PSMD4 and PSMD4 autoantibodies in SCI pathology. The main study results are described and discussed in this chapter.

AIM 1: Discovery of novel disease markers for SCI patients by application of the SAS procedure

Knowledge about the antibody profile of patients with a SCI remains incomplete. The presence of a limited number of antibody responses related to CNS pathologies has been studied in SCI patients [23, 24, 26, 27, 29]. Only 1 study analyzed the antibody profile of SCI patients using a proteomic approach (2D western blot followed by liquid chromatography coupled with mass spectrometry) and identified antibody responses toward glial fibrillary acidic protein (GFAP) [25]. Therefore, we aimed to identify novel antigenic targets in SCI patients using SAS.

To apply the SAS procedure, a cDNA phage display library was constructed from normal human spinal cord tissue (**chapter 2**). This library contained cDNA inserts involved in a variety of general biological processes as well as neuroinflammatory-related processes which are expected to be triggered by an SCI, such as the immune response, response to stress and apoptosis. Although our cDNA library was generated from normal, undamaged human spinal cord, it also gave a good representation of the *in vivo* antigenic targets expected to be present in the damaged spinal cord. Screening the human spinal cord cDNA phage display library with pooled plasma samples from traumatic SCI patients (n=10, identification cohort) resulted in the identification of 19 novel antigenic targets to which the individual samples of the plasma pool showed antibody reactivity and to which no or low reactivity was detected in age- and gender matched healthy subjects (**chapter 3**). Five of these antigenic targets demonstrated sequence similarity with known proteins, to which antibody reactivity has not been associated with SCI before. The remaining targets originated from the 3'UTR region of mRNA or genomic/ribosomal RNA whose out-of-frame translation resulted in random peptides. Screening of these 19 antigenic targets against a small independent SCI cohort (n=51) and age- and gender-matched healthy subjects (n=49) revealed validated immunoreactivity against 9 of the 19 novel identified targets. In this initial SCI cohort, antibody reactivity to at least one out of these nine targets was detected in 51% of the SCI cohort with a specificity of 73%. Validated antigenic

targets with unique patient reactivity, low to moderate sensitivity and high specificity were combined into a panel of 6 targets. Within this panel, an overall reactivity of approximately half of the SCI patients could be maintained while increasing the specificity to 82%. The clinical relevance of this panel and the individual targets should be explored further in a larger SCI cohort.

AIM 2: Clinical validation of the novel identified antibody responses

Current diagnostic and prognostic tools have various limitations and give only limited information on the severity of a SCI. Therefore, there is a clear need for novel clinically relevant disease markers that can contribute to SCI diagnosis and prognosis. As we identified an SCI-associated panel of 6 antigenic targets, we aimed to validate the clinical relevance of these candidate disease markers in SCI patients.

In **chapter 4**, we successfully translated the phage-mediated ELISA for 4 (UH.SCI.2, UH.SCI.7, UH.SCI.11 and UH.SCI.13) of the 6 antigenic targets into a peptide ELISA, which is a more clinically applicable high-throughput tool. High healthy control reactivity was detected for UH.SCI.11 and UH.SCI.13, resulting in the exclusion of both targets. The peptide ELISA for the remaining two antigenic targets (UH.SCI.2 and UH.SCI.7) demonstrated an improved sensitivity compared to phage ELISA as higher signals were observed and additional antibody-positive samples were identified. Basic local alignment search tool (BLAST) analysis demonstrated similarity of the UH.SCI.2 (56/56 100%) and UH.SCI.7 (7/7 100%) peptides with the C-termini of respectively PSMD4 and S100B. Synthetic peptides corresponding to the phage-displayed peptide sequences and recombinant full length proteins were used to confirm PSMD4 and S100B as *in vivo* targets of UH.SCI.2 and UH.SCI.7 antibodies, respectively. Subsequently, we focused further on the clinical characterization of PSMD4 and S100B autoantibodies in SCI patients (**chapter 5**). Using our peptide ELISA, we validated the prevalence of PSMD4 and S100B autoantibody reactivity in SCI patients and studied their disease specificity by screening healthy controls and other neuroinflammatory or autoimmune populations (e.g. stroke, multiple sclerosis (MS) and rheumatoid arthritis (RA) patients). Screening of our SCI cohort demonstrated similar autoantibody reactivities, irrespective of the cause of pathology (traumatic or pathologic) or time post-injury (weeks to months or >1 year post-injury). PSMD4

and S100B autoantibodies were already present in the acute phase after SCI and remained unchanged during a follow-up period of 5 months, indicating that these autoantibodies are not (re-)induced after SCI or surgery on the spinal cord. Indeed, screening of healthy controls showed similar immunoreactivities compared to the SCI cohort. Additionally, PSMD4 and S100B autoantibodies were also detected in stroke, MS and RA patients, confirming that these autoantibodies are not specific for SCI patients and also other neuroinflammatory or autoimmune conditions did not induce these autoantibody responses. Altogether, both autoantibody responses seem to be part of the antibody reactivity present in a small part of the general population. Nevertheless, since their targets are expressed in the spinal cord, these autoantibodies might still contribute to degenerative or recovery processes after SCI. Therefore, their biological role within SCI pathology should be explored further.

AIM 3: Characterization of the biological relevance of PSMD4 autoantibodies in SCI

Passive transfer of murine SCI-induced antibodies was shown to exert neurotoxic effects in the spinal cord of naive mice [17]. However, the antibody targets in these animal experiments were not known. On the other hand, for a few antibody responses in SCI patients, such as myelin basic protein, myelin associated glycoprotein and GM1 gangliosides, the targets are known, but their biological effect in SCI pathology has not been studied. For S100B autoantibodies, a link with the severity of traumatic brain injury (TBI) pathology in patients has already been described, while PSMD4 autoantibodies were only explored in an EAE animal model [150, 151, 175]. As we detected PSMD4 autoantibodies in SCI patients, we aimed to characterize PSMD4 and PSMD4 autoantibody responses for their biological relevance in SCI pathology.

In **chapter 6**, we investigated the tissue expression of PSMD4 in the spinal cord under uninjured conditions and after SCI. Under normal conditions, PSMD4 was found to be expressed by cells lining the spinal central canal and blood vessels, by glial cells in the white matter and by neuronal cells in the dorsal and ventral horn of human spinal cord tissue. Similar neuronal PSMD4-positive cells were found in spinal cord tissue of mice by a PSMD4/neuronal nuclei (NeuN) double-staining. Still, also non-neuronal cell types of the spinal cord have PSMD4

expression. As PSMD4 was present in the spinal cord under uninjured conditions, we investigated whether PSMD4 expression changed upon SCI. PSMD4 gene expression levels were significantly increased during the acute and subacute phase after SCI and restored to baseline levels after 1 week post-injury. At the protein level, PSMD4 expression remained unchanged over a period of 28 days post-injury, which was confirmed by a PSMD4 staining of the lesion site. As PSMD4 autoantibody reactivity was demonstrated in SCI patients and healthy controls (**chapter 3-5**), we screened blood samples of naive and SCI mice for antibody reactivity toward C-terminal or full length PSMD4, but no PSMD4 antibody formation was detected. The second aim of **chapter 6** was to investigate whether PSMD4 autoantibodies have a pathological effect after SCI. Therefore, a passive transfer experiment of C-terminal mouse PSMD4 autoantibodies was performed in a T-cut hemisection SCI animal model. Our preliminary results did not show an effect - either detrimental or beneficial - of PSMD4 autoantibodies on the functional recovery of SCI mice. However, because PSMD4 is expressed by important CNS structures and, after SCI, PSMD4 autoantibodies have access to the CNS, further characterization of PSMD4 and PSMD4 autoantibodies is necessary to elucidate their biological relevance in SCI pathology.

Do our newly identified antibody responses have diagnostic/prognostic potential in SCI patients?

In this study, only PSMD4 and S100B autoantibodies have been studied for their clinical relevance in SCI patients and, at present, we could not find clinical correlations between these autoantibodies and the current prognostic tools (**chapter 5**). Despite the clear need for disease markers to support the diagnosis and prognosis in SCI patients, only a few studies have been performed to investigate antibodies as candidate biomarkers in SCI patients [23-29]. Up to now, only 1 study demonstrated a correlation between GM1 ganglioside IgG autoantibodies and medical complications in SCI patients (neuropathic pain and urinary tract infections) [23]. Most studies were not able to identify candidate disease markers with a good sensitivity and correlated clinical relevance because they consisted of only small numbers of SCI subjects, did not include control subjects or compared distinct time points of sampling.

We found that PSMD4 and S100B autoantibodies are not induced upon injury, but since their targets are expressed throughout the spinal cord, they might still contribute to neuroinflammatory responses upon breach of the blood-spinal cord barrier (BSCB) after SCI. Therefore, the presence of these autoantibodies in SCI patients may give clinically relevant information. Our patient cohort is large compared to other biomarker studies in the field of SCI as we screened 175 SCI subjects with follow-up samples included for 66 SCI patients. Still, the heterogeneity of the SCI patient population, the detection of low amounts of seropositivity for PSMD4 and S100B and the lack of clinical data for some patients limited our analysis. At this point, we could not find correlations between PSMD4 or S100B autoantibody responses and clinical parameters. For future experiments, it might be beneficial to perform an additional positive selection round in the SAS procedure using an independent SCI pool to increase seropositivity of the identified antibody targets.

As the patient population is highly diverse, identification of a single biomarker that can reflect the full spectrum of the injury response is challenging. Therefore, Kwon et al. proposed the strategy to compose a panel of putative structural and inflammatory CSF biomarkers (e.g. S100B, GFAP and IL-8) which was demonstrated to correlate with lesion severity [75]. In our study, a panel of 6 antigenic targets was identified using SAS technology which showed a significant

association between the presence of at least 1 antibody response of the panel and SCI patients (**chapter 3**). In order to explore the disease marker potential of this panel, further optimization of the UH.SCI.9 and UH.SCI.15 peptide ELISA and large-scale screening of SCI patient cohorts with complete corresponding clinical data is essential.

Although we could not find clinical correlations with PSMD4 and S100B autoantibodies in SCI patients, antibodies have proven their biomarker potential in the diagnosis and prognosis for many autoimmune disorders such as MS and RA [209]. Whether antibodies can serve as disease markers in neuroinflammatory CNS disorders is still emerging. In TBI, several autoantibodies (anti-S100B, glial fibrillary acidic protein, myelin basic protein and phospholipids antibodies) have shown to correlate with clinical parameters (e.g. severity, outcome measure, complications) [151, 210, 211]. As most of these antibodies were also detected in SCI patients, a further clinical characterization of these antibody responses and the identification of the complete antibody profile within SCI patients is warranted.

Is there a difference in immunoreactivity between traumatic or pathologic SCI patients?

Although the SAS procedure was performed with a plasma pool of traumatic SCI patients, the newly identified antigenic targets also showed antibody reactivity in pathologic SCI patients (**chapter 3** and **5**). We included pathologic SCI patients in this study assuming that spinal surgery or pathology can breach the BSCB or influence its permeability, allowing antibody infiltration to the CNS. As a consequence, this could potentially induce a neuroinflammatory response similar to the response induced after traumatic conditions. As our data indicate that PSMD4 and S100B autoantibodies are present in a percentage of the general population, it is not surprising that also pathologic SCI patients demonstrate PSMD4 and S100B autoantibody reactivity. Although our pathologic samples are mostly collected around the time of spinal surgery, most of these patients already have a chronic pathology of the spinal cord. Therefore, we expected a difference in antibody reactivity in comparison with our early traumatic SCI patients, which have a more acute pathology. At present, pathologic SCI patients demonstrate similar PSMD4 and S100B antibody levels in comparison with traumatic SCI patients. As our pathologic SCI patient population is heterogeneous and limited in

sample size, the antibody profile in traumatic and pathologic SCI patients should be studied further. By increasing the number of patients within pathology groups, individual immune responses can be investigated for correlations with specific disease mechanisms.

Does the current SAS-based antibody profiling strategy allow the identification of primary antibody responses after SCI?

In **chapter 5**, we demonstrated similar antibody reactivity toward the newly identified antigenic targets in healthy controls and in the acute phase (T0) and 3 weeks (T1) after SCI, indicating that these autoantibody responses were already present before injury and were not (re)-induced after SCI. Initially, we aimed to identify newly formed antibody responses after SCI, as it was hypothesized that after BSCB disruption, CNS antigens are released into the circulation where they would trigger an adaptive immune response. Activation of B cells and differentiation into plasma cells resulting in the production of pathogenic antibodies has been shown in an SCI mouse model [15, 17]. Additionally, increased serum IgM levels were found in SCI mice during the first 2 weeks after injury, while serum IgG_{2a} levels were delayed until week 2 and remained elevated up to 42 days post-injury [15]. Up to now, a detailed characterization of the course of antibody responses in SCI patients was not performed. In our study, we only collected a sample at admission (T0) and 3 weeks after injury (T1). Future experiments might consider the collection of more samples in the early phase after SCI, so that the first time point of antibody detection can be determined as well as the course of the antibody response. For the SAS procedure, a pool of traumatic SCI patient samples collected at hospitalization (collected approximately 1 week after injury) or 3 weeks after injury was used. As 6 of the 10 samples in the SAS pool had been collected at T0, this might have limited the possibility to find primary antibody responses that are induced by the injury itself. Future experiments with the aim to identify newly formed antibody responses in traumatic SCI patients should select only blood samples collected 2-3 weeks post-injury, as this is the time range that newly formed IgG responses are present in the blood. Additionally, to reduce the identification of antigenic targets representing an aspecific antibody profile, negative selection can be performed

using healthy control samples, or when available, baseline samples of the same traumatic SCI patients.

Can antibodies present before injury contribute to pathological processes?

PSMD4 and S100B autoantibodies appear to be part of the antibody profile present in a small percentage of the population (**chapter 5**). Although autoreactive IgG responses are often described as a serological hallmark of several autoimmune disease, they can also be found in healthy controls and their formation is further induced with aging [179]. Nagele et al. (2013) investigated the antibody profile in healthy controls (n=57) using human protein microarrays and demonstrated abundant IgG autoantibodies in all subjects [212]. Whether these detected IgG autoantibodies are specific and able to bind their target in an *in vivo* situation is not clear, but with such a high prevalence of autoreactive antibodies in healthy persons, it is clear that not all autoantibodies will cause (overt) pathology. This can be explained by the fact that these autoantibodies might not have direct access to their targets because they are for instance intracellular or located in an inaccessible part of the body, like the CNS. For example, anti-N-methyl-D-aspartate receptor (NMDAR) autoantibodies showed a comparable seroprevalence (±10%), titer and *in vitro* functionality in neuropsychiatric patients and healthy controls [213, 214]. Still, these autoantibodies have been shown to be involved in pathological processes as more neurological abnormalities were observed in seropositive patients with a history of blood-brain barrier damage and an impact of NMDAR autoantibodies was observed on the lesion size evolution in ischemic stroke patients [213, 215]. Therefore, when an SCI causes disruption of the BSCB in persons who are already positive for PSMD4 or S100B autoantibodies, these autoantibodies can enter the CNS. As both PSMD4 and S100B are expressed by important structures and cells of the spinal cord, these autoantibodies might still contribute to pathological conditions and should be studied further for their biological relevance in SCI pathology.

What would the role of antibodies in SCI pathology processes be?

In a mouse model of SCI, it has been reported that B cells were activated and differentiated into plasma cells, which resulted in the production of pathogenic

antibodies [17]. At present, most evidence points toward a detrimental role of antibodies in SCI pathology, while antibodies might also contribute to the recovery process, for example via clearing of damaged tissue or inhibition of pro-inflammatory factors. Whether antibodies have a detrimental or beneficial effect is dependent on the antigen they are targeting. Therefore, information on the role of specific antibodies in SCI pathology can contribute in the development of novel treatment strategies, as antibodies with a beneficial effect can be administered in SCI patients and detrimental antibodies can be targeted by neutralization strategies.

Do S100B autoantibodies contribute to SCI pathological processes?

S100B is a calcium-binding protein concentrated in astrocytes and other glial cells, but it has also been detected outside the CNS. Under physiological concentrations, S100B is involved in processes related to cell proliferation, survival and differentiation as well as the regulation of cellular calcium homeostasis, while higher S100B concentrations exert a pro-inflammatory effect and contribute to neuronal dysfunction or cell death [216, 217]. After injury to the spinal cord, increased S100B levels were detected in CSF and serum [71, 75, 81, 149]. Therefore, inhibition of S100B in traumatic CNS conditions was expected to have beneficial effects and indeed, inhibition of S100B via neutralizing antibodies demonstrated a protective effect in a TBI model (controlled cortical impact) [170]. As a similar neuroinflammatory response develops after SCI and increased, although not significant, S100B levels have been shown to be present in SCI patients, we might expect that S100B autoantibodies have a protective effect in SCI patients as well [18, 28-30]. In order to investigate the biological role of S100B autoantibodies in SCI pathology, a similar research strategy can be used as described for PSMD4 autoantibodies. However, for S100B autoantibody passive-transfer experiments we should carefully consider the concentration of antibody that will be administered in order to only neutralize the harmful effects of S100B.

Are PSMD4 autoantibodies involved in SCI pathological processes?

PSMD4 exerts anti-inflammatory effects and neutralization of PSMD4 in EAE resulted in a more severe disease course [175]. As PSMD4 autoantibodies were detected in SCI patients (**chapter 4** and **5**) and PSMD4 expression is

demonstrated in different structures and cells of the spinal cord (**chapter 6**), we investigated the biological relevance of PSMD4 autoantibodies in pathological processes of SCI. Therefore, a passive-transfer experiment was performed in a T-cut hemisection mouse model using rabbit polyclonal antibodies raised against the C-terminus of mouse PSMD4. Based on our preliminary results, PSMD4 autoantibodies did not show a detrimental or beneficial effect on the functional recovery of SCI mice. Besides the functional evaluation, there were no differences in lesion size and demyelinated area between the treatment groups. However, as our sample size was small, the passive-transfer experiment should be repeated to reveal a possible involvement of PSMD4 autoantibodies in SCI pathology. In this study, we used a T-cut hemisection animal model, which is valuable to investigate the effect of PSMD4 autoantibodies on functional recovery and anatomic regeneration, however, in humans, contusion lesions are the most common type of SCI [218]. Future experiments should consider the use of a contusion SCI animal model, which gives a better representation of human injury biomechanics and neuropathology [218]. Furthermore, PSMD4 autoantibodies already seem to be present before injury, therefore, peripheral injection of PSMD4 autoantibodies in mice before the injury might give a better representation of what happens in SCI patients. As the BSCB is damaged in SCI mice, peripherally injected PSMD4 autoantibodies are also expected to infiltrate the spinal cord and contribute to SCI pathology. This mode of administration might also reduce secondary damage caused by the antibody injection in the spinal cord tissue itself, which possibly also causes a partial lesion. Still, whether PSMD4 autoantibodies can cause direct or indirect neurotoxic effects can be studied via direct injection of these antibodies in spinal cords of naive mice followed by a histological evaluation of the injection site and neuroinflammatory parameters.

In conclusion, in this thesis we explored the antibody profile present in SCI patients using SAS technology. Novel antibody targets were identified, which were not reported in SCI patients before. Further characterization of 2 of the coding antigenic targets revealed the *in vivo* target of UH.SCI.2 and UH.SCI.7 antibody responses, namely PSMD4 and S100B, respectively. Validation screening in a larger SCI cohort, healthy controls and other study populations demonstrated that these antibody responses are already present before the injury and are part of

the antibody profile present in a small percentage of the population. As both PSMD4 and S100B are expressed in the spinal cord and the BSCB is disrupted after SCI, these antibodies gain access to the CNS and can still contribute to SCI pathology. Therefore, PSMD4 and S100B antibody responses should be explored further for their biological role in SCI pathology.

8

Nederlandse samenvatting

Het oplopen van ruggenmergschade is meestal het gevolg van een plotse en onverwachte gebeurtenis en zorgt voor een tijdelijke of permanente verstoring van bewegings-, gevoels- en/of autonome functies (bijvoorbeeld controle over de ademhaling, urineblaas of darm) [1, 2]. De meest voorkomende traumatische oorzaken van ruggenmergschade zijn valpartijen, ongevallen met motorvoertuigen, sportactiviteiten en geweld. Daarnaast zijn er ook pathologische oorzaken die schade aan het ruggenmerg kunnen veroorzaken, zoals infectieziekten, tumoren, musculoskeletale ziekten of vasculaire aandoeningen [2-4]. De levenskwaliteit van de patiënt wordt, onafhankelijk van de oorzaak, drastisch aangetast en de huidige behandelingsstrategieën geven slechts een beperkt neurologisch of functioneel herstel [5]. Hierdoor is een vroege, nauwkeurige diagnose en prognose van groot belang. De diagnose van een ruggenmergletsel is relatief eenvoudig te stellen middels neurologische symptomen en MRI-beelden. De prognose daarentegen is moeilijker te bepalen aangezien de huidige parameters verschillende beperkingen vertonen en slechts beperkte informatie geven omtrent de ernst van de laesie [177, 178]. Nieuwe ziektemerkers of biomerkers zijn dan ook nodig om de prognose vlugger en duidelijker te specifiëren. Een biomerker is gedefinieerd als: 'Een kenmerk dat objectief gemeten en geëvalueerd kan worden als een indicator van normale biologische of pathogene processen of farmacologische reacties op therapeutische interventies' [62]. Verder kunnen biomerkers meer inzicht geven in de pathologische processen die ontstaan na ruggenmergschade, waardoor ze ook van belang zijn voor de ontwikkeling van nieuwe therapieën.

Het initieel letsel aan het ruggenmerg veroorzaakt schade aan neuronale cellen en hun axonen. Vervolgens wordt secundaire schade veroorzaakt door een cascade van pathologische veranderingen, gekenmerkt door neuroinflammatie en omvat de instroom en activatie van immuuncellen, waaronder B-cellen. Studies rond ruggenmergschade in diermodellen toonden aan dat B-cellen en de door hen geproduceerde antilichamen bijkomende schade kunnen veroorzaken en herstelprocessen verstoren. Waartegen de antilichamen in deze diermodellen gericht zijn, is momenteel nog grotendeels ongekend [15, 17]. In serum van patiënten met een ruggenmergletsel werden verhoogde antilichaamniveaus gedetecteerd tegen enkele centraal zenuwstelsel (CZS) antigenen, zoals GM1 gangliosiden en myeline-geassocieerd glycoproteïne [23, 24, 26, 27, 29, 104]. Toch zijn er nog geen

duidelijke aanwijzingen die aantonen dat B-cellen en antilichamen rechtstreeks betrokken zijn in ruggenmergschadeprocessen in de mens. Een gedetailleerde analyse van patiëntenstalen is nodig om de prevalentie, specificiteit en pathogene relevantie van ruggenmergschade-geïnduceerde antilichamen bij de mens te bepalen.

Het doel van deze studie was het bestuderen van het antilichaamprofiel in patiënten met ruggenmergschade door gebruik te maken van de serologische antigen-selectie (SAS) procedure. Zo willen we antilichamen identificeren die mogelijk een klinische of biologische relevantie hebben binnen de pathologie van ruggenmergschade. Twee van de geïdentificeerde antilichaamtargets, UH.SCI.2 en UH.SCI.7, toonden overeenkomst met respectievelijk 26S proteasoom non-ATPase regulerende subeenheid 4 (PSMD4) en proteïne S100-B (S100B). Voor beide targets werd de *in vivo* identiteit bevestigd. Door middel van onze in-huis geoptimaliseerde peptide ELISA werd de klinische relevantie van PSMD4- en S100B-autoantilichamen verder bestudeerd bij patiënten met een ruggenmergletsel. Tot slot werd de biologische relevantie van PSMD4 en PSMD4-autoantilichamen eveneens bestudeerd in de pathologie van ruggenmergschade.

Deel 1: Identificatie van nieuwe ziektemerkers voor ruggenmergschade-patiënten met behulp van de SAS procedure

De kennis omtrent het antilichaamprofiel in patiënten met een ruggenmergletsel blijft onvolledig. Enkele antilichaamresponsen die reeds beschreven zijn in CZS-pathologie werden ook bestudeerd voor hun aanwezigheid in ruggenmergschadepatiënten. Slechts één studie analyseerde het antilichaamprofiel in deze patiëntenpopulatie door gebruik te maken van proteomicatechnieken en identificeerde antilichamen gericht tegen gliaal fibrillair zuur eiwit [25]. Om het antilichaamprofiel in ruggenmergschadepatiënten verder te exploreren, maakten wij gebruik van de SAS-procedure. Hiervoor werd een cDNA expressiebibliotheek gemaakt van gezond humaan ruggenmergweefsel (**hoofdstuk 2**). Screening van deze cDNA bibliotheek met een pool van plasmastalen verkregen van traumatische ruggenmergschadepatiënten (n=10, identificatiecohort) resulteerde in de identificatie van 19 nieuwe antilichaamtargets. Deze targets toonden antilichaamreactiviteit in de individuele stalen van het identificatiecohort, terwijl geen of weinig antilichaamreactiviteit

werd gedetecteerd in gezonde controles (**hoofdstuk 3**). Vijf van deze 19 peptide-sequenties toonden overeenkomst met gekende proteïnen waartegen antilichaamreactiviteit voorheen nog niet geassocieerd was met ruggenmergschadepathologie. De overige antilichaamtargets zijn willekeurige peptiden die verkregen werden door expressie van niet-coderende mRNA regio's of genomisch/ribosomaal RNA. Screening van deze 19 antilichaamtargets in onafhankelijke cohorten van patiënten en gezonde controles toonde immunoreactiviteit tegen 9 van 19 antilichaamtargets. In dit ruggenmergschadecohort (n=51) werd antilichaamreactiviteit tegen minstens één van de negen targets gedetecteerd in 51% van de ruggenmergschadepatiënten met een specificiteit van 73%. Gevalideerde antilichaamtargets met unieke patiëntenreactiviteit (lage tot gemiddelde sensitiviteit en hoge specificiteit) werden gecombineerd in een panel van 6 kandidaat merkers. Dit panel kon een antilichaamreactiviteit in ongeveer 50% van de ruggenmergschadepatiënten behouden, terwijl de specificiteit verhoogde naar 82%. De klinische relevantie van dit panel en de individuele antilichaamtargets dient echter verder bestudeerd te worden in een groter cohort van ruggenmergschadepatiënten.

Deel 2: Klinische validatie van de nieuw geïdentificeerde antilichaamresponsen

De huidige diagnostische en prognostische parameters voor ruggenmergschade geven slechts beperkte informatie omtrent de ernst van de schade in het ruggenmerg. Hierdoor is er een duidelijke nood aan nieuwe ziektemerkers die kunnen bijdragen aan een vroege, betrouwbare prognose van ruggenmergletsels. Voorheen identificeerden we een panel van zes antilichaamtargets die een associatie vertoonde met ruggenmergletselpatiënten. Vervolgens bestudeerden we de klinische relevantie van deze kandidaat ziektemerkers in ruggenmergletselpatiënten. Hiervoor werd eerst de faag ELISA omgezet in een meer klinisch toepasbare peptide ELISA. Een geoptimaliseerde peptide ELISA werd bekomen voor vier van de zes antilichaamtargets (UH.SCI.2, UH.SCI.7, UH.SCI.11 en UH.SCI.13). UH.SCI.11 en UH.SCI.13 vertoonden hoge gezonde controlereactiviteit en werden uitgesloten in de verdere studie. Peptide ELISA voor UH.SCI.2 en UH.SCI.7 resulteerden in hogere reactiviteitssignalen en de identificatie van extra seropositieve stalen in vergelijking met de faag ELISA. Dit

geeft aan dat de peptide ELISA een verbeterde sensitiviteit heeft in vergelijking met de faag ELISA. Sequentieanalyse toonde gelijkenis aan tussen de UH.SCI.2 en UH.SCI.7 peptiden en het C-terminale uiteinde van PSMD4 en S100B, respectievelijk. Recombinante proteïnen van volledige lengte en synthetische peptiden overeenkomstig met de peptidesequenties die op het faagoppervlak tot expressie werden gebracht, werden gebruikt om PSMD4 en S100B als *in vivo* targets van UH.SCI.2 en UH.SCI.7 antilichamen te bevestigen. Vervolgens werd er een klinische karakterisatie uitgevoerd voor PSMD4- en S100B-autoantilichamen in ruggenmergletselpatiënten (**hoofdstuk 5**). Door gebruik te maken van onze peptide ELISA konden we de prevalentie van PSMD4- en S100B-autoantilichamen valideren in ruggenmergletselpatiënten en bepaalden we de ziektespecificiteit door gezonde controles en andere neuroinflammatoire (pathologische hersenschade zoals een beroerte) of auto-immune populaties (multiple sclerose (MS), reumatoïde artritis (RA)) te testen. Gelijkaardige autoantilichaamreactiviteit werd gedetecteerd in gezonde controles en ruggenmergletselpatiënten, onafhankelijk van de oorzaak van de pathologie (traumatisch of pathologisch) of tijd na schade (binnen 1 jaar of >1 jaar na schade). PSMD4- en S100B-autoantilichamen zijn reeds aanwezig in de eerste dagen na ruggenmergschade en blijven onveranderd tijdens een opvolgperiode van 5 maanden, wat erop wijst dat deze autoantilichamen niet ge(re)ïnduceerd worden na ruggenmergschade of een operatie aan het ruggenmerg. Daarnaast werden PSMD4- en S100B-autoantilichamen ook gedetecteerd in pathologische hersenschade en MS en RA patiënten, wat bevestigt dat deze autolichamen niet specifiek zijn voor SCI-patiënten en dat ook andere neuroinflammatoire of auto-immune condities de autoantilichaamresponsen niet induceren. Samengevat blijken beide autoantilichaamresponsen deel uit te maken van het antilichaamprofiel aanwezig in een beperkt deel van de algemene populatie. Toch kunnen deze autoantilichaamresponsen nog bijdragen aan schade- of herstelprocessen, waardoor hun biologische rol in de pathologie van ruggenmergschade verder bestudeerd dient te worden.

Deel 3: Biologische karakterisatie van PSMD4-autoantilichamen in ruggenmergschadepathologie

Via passieve overdracht van ruggenmergletsel-geïnduceerde antilichamen in het ruggenmerg van naïeve muizen werd het schadelijke karakter van deze antilichamen reeds gesuggereerd [17]. Tot hiertoe werden de effecten van antilichaamresponsen aanwezig in ruggenmergschadepatiënten echter nog niet bestudeerd in de pathologie. Voor S100B-autoantilichamen werd reeds een link aangetoond met de ernst van traumatische hersenschadepathologie in patiënten, terwijl PSMD4-autoantilichamen enkel verkend werden in een MS-diermodel [150, 151, 175]. Daarom bestudeerden we de biologische relevantie van PSMD4 en PSMD4-autoantilichamen in ruggenmergschadepathologie. Onder normale omstandigheden werd PSMD4 teruggevonden in de cellen die het centrale kanaal en de bloedvaten omlijnen. Verder werd PSMD4 eveneens tot expressie gebracht in gliale en neuronale cellen van de witte stof en de dorsale en ventrale hoorn van humaan ruggenmergweefsel. Gelijkaardige PSMD4-positieve neuronale cellen werden ook teruggevonden in het ruggenmerg van muizen. Het neuronaal fenotype van deze cellen werd bevestigd door middel van een PSMD4/NeuN dubbelkleuring, die eveneens aangaf dat ook andere celtypes in het ruggenmerg PSMD4 tot expressie brengen. Aangezien PSMD4 aanwezig is in normaal, onbeschadigd ruggenmergweefsel werd het effect van schade op PSMD4-expressie in het ruggenmerg onderzocht. PSMD4-genexpressie niveaus waren significant verhoogd tijdens de acute en subacute fase na het toebrengen van een ruggenmergletsel in muizen en herstelde na 1 week weer naar hun basiswaarden. PSMD4-proteïneniveaus bleven onveranderd gedurende een periode van 28 dagen na schade. Aangezien PSMD4-autoantilichaamreactiviteit werd aangetoond in ruggenmergletselpatiënten en gezonde controles, screenden we ook bloedstalen van naïeve muizen en muizen met een ruggenmergletsel voor reactiviteit tegen PSMD4. PSMD4-antilichaamreactiviteit was afwezig in beide groepen. Tot slot bestudeerden we het effect van PSMD4-autoantilichamen in een muismodel voor ruggenmergschade. Onze preliminaire resultaten toonden geen positief of negatief effect van PSMD4-autoantilichamen op het functioneel herstel in muizen met een ruggenmergletsel. Omwille van limitaties in de dierstudie, zoals het beperkt functioneel herstel en het gewichtsverlies, kan er geen sluitende conclusie genomen worden omtrent het effect van deze antilichamen op

ruggenmergschadepathologie. Een herhaling van het experiment is daarom aangewezen.

In deze thesis werd het antilichaamprofiel van ruggenmergschadepatiënten geanalyseerd door middel van de SAS-technologie. Nieuwe antilichaamtargets met antilichaamreactiviteit in ruggenmergschadepatiënten werden geïdentificeerd. Verdere karakterisatie van twee van de coderende antilichaamtargets resulteerde in de bevestiging van de *in vivo* targetidentiteit van UH.SCI.2- en UH.SCI.7-antilichaamresponsen, namelijk PSMD4 en S100B. Validatiescreening van een groot SCI cohort, gezonde controles en andere controle studiepopulaties toonden dat deze antilichaamresponsen waarschijnlijk deel uit maken van het antilichaamprofiel van een klein deel van de algemene populatie en dat deze antilichamen niet gevormd worden onder invloed van ruggenmergschade. Aangezien PSMD4 en S100B beiden tot expressie worden gebracht in het ruggenmerg en de bloed-ruggenmerg-barrière verstoord is na ruggenmergschade, krijgen deze antilichamen onder deze omstandigheden toegang tot het CZS. Hierdoor kunnen PSMD4- en S100B-autoantilichamen alsnog bijdragen tot pathologische processen en is een verdere biologische karakterisatie aangewezen. Het bestuderen van antilichamen binnen ruggenmergschadepathologie zal meer inzicht verschaffen in de neuroinflammatoire processen die ontstaan na schade aan het ruggenmerg, wat essentieel is voor de ontwikkeling van nieuwe behandelingen.

References

1. Majdan M, Brazinova A, Mauritz W. Epidemiology of traumatic spinal cord injuries in Austria 2002-2012. European spine journal : official publication of the European Spine Society, the European Spinal Deformity Society, and the European Section of the Cervical Spine Research Society. 2016;25(1):62-73.
2. Organization WH. International Perspectives on Spinal Cord Injury. 2013.
3. Nijendijk JH, Post MW, van Asbeck FW. Epidemiology of traumatic spinal cord injuries in The Netherlands in 2010. Spinal cord. 2014;52(4):258-63.
4. Center NSCIS. Facts and Figures at a Glance. AL: University of Alabama at Birmingham2016.
5. Jazayeri SB, Beygi S, Shokraneh F, Hagen EM, Rahimi-Movaghar V. Incidence of traumatic spinal cord injury worldwide: a systematic review. European spine journal : official publication of the European Spine Society, the European Spinal Deformity Society, and the European Section of the Cervical Spine Research Society. 2015;24(5):905-18.
6. Singh A, Tetreault L, Kalsi-Ryan S, Nouri A, Fehlings MG. Global prevalence and incidence of traumatic spinal cord injury. Clinical epidemiology. 2014;6:309-31.
7. Varma AK, Das A, Wallace Gt, Barry J, Vertegel AA, Ray SK, et al. Spinal cord injury: a review of current therapy, future treatments, and basic science frontiers. Neurochemical research. 2013;38(5):895-905.
8. Ryan Salewski HEaMGF. Neural Stem/Progenitor Cells for Spinal Cord Regeneration, Trends in Cell Signaling Pathways in Neuronal Fate Decision. Dr Sabine Wislet-Gendebien (Ed), InTech. 2013.
9. Anwar MA, Al Shehabi TS, Eid AH. Inflammogenesis of Secondary Spinal Cord Injury. Frontiers in cellular neuroscience. 2016;10:98.
10. Irene Paterniti EEaSC. Role of the Neuroinflammation in the Degree of Spinal Cord Injury: New Therapeutic Strategies, Recovery of Motor Function Following Spinal Cord Injury. Dr Heidi Fuller (Ed), InTech. 2016.
11. Medicine Io. Spinal cord injury: Progress, Promise, and Priorities. Washington, DC: The National Academies Press; 2005.
12. Ruff CA, Fehlings MG. Neural stem cells in regenerative medicine: bridging the gap. Panminerva Med. 2010;52(2):125-47.
13. Paola Suárez-Meade and Antonio Ibarra (2016). Protective Role of the Immune System in Spinal Cord Injury: Immunomodulation with Altered Peptide Ligands RoMFFSC.
14. Kigerl KA, Gensel JC, Ankeny DP, Alexander JK, Donnelly DJ, Popovich PG. Identification of two distinct macrophage subsets with divergent effects causing either neurotoxicity or regeneration in the injured mouse spinal cord. The Journal of neuroscience : the official journal of the Society for Neuroscience. 2009;29(43):13435-44.
15. Ankeny DP, Lucin KM, Sanders VM, McGaughy VM, Popovich PG. Spinal cord injury triggers systemic autoimmunity: evidence for chronic B lymphocyte activation and lupus-like autoantibody synthesis. J Neurochem. 2006;99(4):1073-87.
16. Wu B, Matic D, Djogo N, Szpotowicz E, Schachner M, Jakovcevski I. Improved regeneration after spinal cord injury in mice lacking functional T- and B-lymphocytes. Experimental neurology. 2012;237(2):274-85.
17. Ankeny DP, Guan Z, Popovich PG. B cells produce pathogenic antibodies and impair recovery after spinal cord injury in mice. J Clin Invest. 2009;119(10):2990-9.
18. Casili G, Impellizzeri D, Cordaro M, Esposito E, Cuzzocrea S. B-Cell Depletion with CD20 Antibodies as New Approach in the Treatment of Inflammatory and Immunological Events Associated with Spinal Cord Injury. Neurotherapeutics : the journal of the American Society for Experimental NeuroTherapeutics. 2016;13(4):880-94.
19. Lucin KM, Sanders VM, Jones TB, Malarkey WB, Popovich PG. Impaired antibody synthesis after spinal cord injury is level dependent and is due to sympathetic nervous system dysregulation. Experimental neurology. 2007;207(1):75-84.

20. Riegger T, Conrad S, Schluesener HJ, Kaps HP, Badke A, Baron C, et al. Immune depression syndrome following human spinal cord injury (SCI): a pilot study. Neuroscience. 2009;158(3):1194-9.
21. Salazar-Camarena DC, Ortiz-Lazareno PC, Cruz A, Oregon-Romero E, Machado-Contreras JR, Munoz-Valle JF, et al. Association of BAFF, APRIL serum levels, BAFF-R, TACI and BCMA expression on peripheral B-cell subsets with clinical manifestations in systemic lupus erythematosus. Lupus. 2016;25(6):582-92.
22. Saltzman JW, Battaglino RA, Salles L, Jha P, Sudhakar S, Garshick E, et al. B-Cell Maturation Antigen, A Proliferation-Inducing Ligand, and B-Cell Activating Factor Are Candidate Mediators of Spinal Cord Injury-Induced Autoimmunity. J Neurotraum. 2013;30(6):434-40.
23. Davies AL, Hayes KC, Dekaban GA. Clinical correlates of elevated serum concentrations of cytokines and autoantibodies in patients with spinal cord injury. Arch Phys Med Rehabil. 2007;88(11):1384-93.
24. Hayes KC, Hull TC, Delaney GA, Potter PJ, Sequeira KA, Campbell K, et al. Elevated serum titers of proinflammatory cytokines and CNS autoantibodies in patients with chronic spinal cord injury. J Neurotrauma. 2002;19(6):753-61.
25. Hergenroeder GW, Moore AN, Schmitt KM, Redell JB, Dash PK. Identification of autoantibodies to glial fibrillary acidic protein in spinal cord injury patients. Neuroreport. 2016;27(2):90-3.
26. Mizrachi Y, Ohry A, Aviel A, Rozin R, Brooks ME, Schwartz M. Systemic humoral factors participating in the course of spinal cord injury. Paraplegia. 1983;21(5):287-93.
27. Taranova NP, Makarov A, Amelina OA, Luchakova OS, Loboda EB, Leikin IB. The production of autoantibodies to nerve tissue glycolipid antigens in patients with traumatic spinal cord injuries. Zh Vopr Neirokhir Im N N Burdenko. 1992(4-5):21-4.
28. Yokobori S, Zhang ZQ, Moghieb A, Mondello S, Gajavelli S, Dietrich WD, et al. Acute Diagnostic Biomarkers for Spinal Cord Injury: Review of the Literature and Preliminary Research Report. World Neurosurg. 2015;83(5):867-78.
29. Zajarias-Fainsod D, Carrillo-Ruiz J, Mestre H, Grijalva I, Madrazo I, Ibarra A. Autoreactivity against myelin basic protein in patients with chronic paraplegia. European spine journal : official publication of the European Spine Society, the European Spinal Deformity Society, and the European Section of the Cervical Spine Research Society. 2012;21(5):964-70.
30. Ulndreaj A, Tzekou A, Mothe AJ, Siddiqui AM, Dragas R, Tator CH, et al. Characterization of the Antibody Response after Cervical Spinal Cord Injury. J Neurotrauma. 2017;34(6):1209-26.
31. Davies AL, Hayes KC, Dekaban GA. Clinical correlates of elevated serum concentrations of cytokines and autoantibodies in patients with spinal cord injury. Archives of physical medicine and rehabilitation. 2007;88(11):1384-93.
32. Chari A, Hentall ID, Papadopoulos MC, Pereira EA. Surgical Neurostimulation for Spinal Cord Injury. Brain sciences. 2017;7(2).
33. Martin G. Brodwin FWS, John Howard, Erin R. Brodwin. Elliott & Fitzpatrick, Inc. 2009.
34. Munce SE, Straus SE, Fehlings MG, Voth J, Nugaeva N, Jang E, et al. Impact of psychological characteristics in self-management in individuals with traumatic spinal cord injury. Spinal cord. 2016;54(1):29-33.
35. Schaefer DM, Flanders AE, Osterholm JL, Northrup BE. Prognostic significance of magnetic resonance imaging in the acute phase of cervical spine injury. Journal of neurosurgery. 1992;76(2):218-23.
36. Thuret S, Moon LDF, Gage FH. Therapeutic interventions after spinal cord injury. Nat Rev Neurosci. 2006;7(8):628-43.
37. Flanders AE, Spettell CM, Tartaglino LM, Friedman DP, Herbison GJ. Forecasting motor recovery after cervical spinal cord injury: value of MR imaging. Radiology. 1996;201(3):649-55.

38. Miyanji F, Furlan JC, Aarabi B, Arnold PM, Fehlings MG. Acute cervical traumatic spinal cord injury: MR imaging findings correlated with neurologic outcome--prospective study with 100 consecutive patients. Radiology. 2007;243(3):820-7.
39. Lammertse D, Dungan D, Dreisbach J, Falci S, Flanders A, Marino R, et al. Neuroimaging in traumatic spinal cord injury: an evidence-based review for clinical practice and research. The journal of spinal cord medicine. 2007;30(3):205-14.
40. Brown PJ, Marino RJ, Herbison GJ, Ditunno JF, Jr. The 72-hour examination as a predictor of recovery in motor complete quadriplegia. Arch Phys Med Rehabil. 1991;72(8):546-8.
41. Marino RJ, Graves DE. Metric properties of the ASIA motor score: subscales improve correlation with functional activities. Arch Phys Med Rehabil. 2004;85(11):1804-10.
42. Scholtes F, Theunissen E, Phan-Ba R, Adriaensens P, Brook G, Franzen R, et al. Post-mortem assessment of rat spinal cord injury and white matter sparing using inversion recovery-supported proton density magnetic resonance imaging. Spinal cord. 2011;49(3):345-51.
43. Navarro R, Juhas S, Keshavarzi S, Juhasova J, Motlik J, Johe K, et al. Chronic spinal compression model in minipigs: a systematic behavioral, qualitative, and quantitative neuropathological study. J Neurotrauma. 2012;29(3):499-513.
44. Ahuja CS, Nori S, Tetreault L, Wilson J, Kwon B, Harrop J, et al. Traumatic Spinal Cord Injury-Repair and Regeneration. Neurosurgery. 2017;80(3S):S9-S22.
45. Cristante AF, Barros Filho TE, Marcon RM, Letaif OB, Rocha ID. Therapeutic approaches for spinal cord injury. Clinics (Sao Paulo). 2012;67(10):1219-24.
46. Dietz V. Neuronal plasticity after a human spinal cord injury: positive and negative effects. Experimental neurology. 2012;235(1):110-5.
47. Wilson JR, Forgione N, Fehlings MG. Emerging therapies for acute traumatic spinal cord injury. CMAJ : Canadian Medical Association journal = journal de l'Association medicale canadienne. 2013;185(6):485-92.
48. Domingo A, Al-Yahya AA, Asiri Y, Eng JJ, Lam T, Rehabil SCI. A Systematic Review of the Effects of Pharmacological Agents on Walking Function in People with Spinal Cord Injury. J Neurotraum. 2012;29(5):865-79.
49. Harvey LA. Physiotherapy rehabilitation for people with spinal cord injuries. Journal of physiotherapy. 2016;62(1):4-11.
50. Nas K, Yazmalar L, Sah V, Aydin A, Ones K. Rehabilitation of spinal cord injuries. World journal of orthopedics. 2015;6(1):8-16.
51. Silva NA, Sousa N, Reis RL, Salgado AJ. From basics to clinical: a comprehensive review on spinal cord injury. Progress in neurobiology. 2014;114:25-57.
52. Kabu S, Gao Y, Kwon BK, Labhasetwar V. Drug delivery, cell-based therapies, and tissue engineering approaches for spinal cord injury. J Control Release. 2015;219:141-54.
53. Rahimi-Movaghar MS-AaV. Animal Models in Traumatic Spinal Cord Injury, Topics in Paraplegia: InTech; 2014.
54. Hill RL, Zhang YP, Burke DA, Devries WH, Zhang Y, Magnuson DS, et al. Anatomical and functional outcomes following a precise, graded, dorsal laceration spinal cord injury in C57BL/6 mice. J Neurotrauma. 2009;26(1):1-15.
55. Cheriyan T, Ryan DJ, Weinreb JH, Cheriyan J, Paul JC, Lafage V, et al. Spinal cord injury models: a review. Spinal cord. 2014;52(8):588-95.
56. Onifer SM, Rabchevsky AG, Scheff SW. Rat models of traumatic spinal cord injury to assess motor recovery. ILAR journal. 2007;48(4):385-95.
57. Handbook of Clinical Neurology .25. Injuries of Spine and Spinal-Cord - Vinken,Pj, Bruyn,Gw. Psychol Med. 1978;8(3):531-.
58. Loske P, Boato F, Hendrix S, Piepgras J, Just I, Ahnert-Hilger G, et al. Minimal essential length of Clostridium botulinum C3 peptides to enhance neuronal regenerative growth and connectivity in a non-enzymatic mode. J Neurochem. 2012;120(6):1084-96.
59. Steward O, Willenberg R. Rodent spinal cord injury models for studies of axon regeneration. Experimental neurology. 2017;287(Pt 3):374-83.

60. Basso DM, Fisher LC, Anderson AJ, Jakeman LB, McTigue DM, Popovich PG. Basso mouse scale for locomotion detects differences in recovery after spinal cord in ury in five common mouse strains. J Neurotraum. 2006;23(5):635-59.
61. Sheets AL, Lai PL, Fisher LC, Basso DM. Quantitative evaluation of 3D mouse behaviors and motor function in the open-field after spinal cord injury using markerless motion tracking. PloS one. 2013;8(9):e74536.
62. Atkinson AJ, Colburn WA, DeGruttola VG, DeMets DL, Downing GJ, Hoth DF, et al. Biomarkers and surrogate endpoints: Preferred definitions and conceptual framework. Clin Pharmacol Ther. 2001;69(3):89-95.
63. Kochanek PM, Berger RP, Bayir H, Wagner AK, Jenkins LW, Clark RS. Biomarkers of primary and evolving damage in traumatic and ischemic brain injury: diagnosis, prognosis, probing mechanisms, and therapeutic decision making. Current opinion in critical care. 2008;14(2):135-41.
64. Pouw MH, Hosman AJ, van Middendorp JJ, Verbeek MM, Vos PE, van de Meent H. Biomarkers in spinal cord injury. Spinal cord. 2009;47(7):519-25.
65. Kwon BK, Casha S, Hurlbert RJ, Yong VW. Inflammatory and structural biomarkers in acute traumatic spinal cord injury. Clinical chemistry and laboratory medicine : CCLM / FESCC. 2011;49(3):425-33.
66. Yokobori S, Zhang Z, Moghieb A, Mondello S, Gajavelli S, Dietrich WD, et al. Acute Diagnostic Biomarkers for Spinal Cord Injury: Review of the Literature and Preliminary Research Report. World Neurosurg. 2013.
67. Bandyopadhyay S, Hennes H, Gorelick MH, Wells RG, Walsh-Kelly CM. Serum neuron-specific enolase as a predictor of short-term outcome in children with closed traumatic brain injury. Academic emergency medicine : official journal of the Society for Academic Emergency Medicine. 2005;12(8):732-8.
68. Loy DN, Sroufe AE, Pelt JL, Burke DA, Cao QL, Talbott JF, et al. Serum biomarkers for experimental acute spinal cord injury: rapid elevation of neuron-specific enolase and S-100beta. Neurosurgery. 2005;56(2):391-7; discussion -7.
69. Nagy G, Dzsinich C, Selmeci L, Sepa G, Dzsinich M, Kekesi V, et al. Biochemical alterations in cerebrospinal fluid during thoracoabdominal aortic cross-clamping in dogs. Annals of vascular surgery. 2002;16(4):436-41.
70. Cao F, Yang XF, Liu WG, Hu WW, Li G, Zheng XJ, et al. Elevation of neuron-specific enolase and S-100beta protein level in experimental acute spinal cord injury. Journal of clinical neuroscience : official journal of the Neurosurgical Society of Australasia. 2008;15(5):541-4.
71. Pouw MH, Kwon BK, Verbeek MM, Vos PE, van Kampen A, Fisher CG, et al. Structural biomarkers in the cerebrospinal fluid within 24 h after a traumatic spinal cord injury: a descriptive analysis of 16 subjects. Spinal cord. 2014;52(6):428-33.
72. Ahadi R, Khodagholi F, Daneshi A, Vafaei A, Mafi AA, Jorjani M. Diagnostic Value of Serum Levels of GFAP, pNF-H, and NSE Compared With Clinical Findings in Severity Assessment of Human Traumatic Spinal Cord Injury. Spine. 2015;40(14):E823-30.
73. Wolf H, Krall C, Pajenda G, Leitgeb J, Bukaty AJ, Hajdu S, et al. Alterations of the biomarker S-100B and NSE in patients with acute vertebral spine fractures. The spine journal : official journal of the North American Spine Society. 2014;14(12):2918-22.
74. Kulbe JR, Geddes JW. Current status of fluid biomarkers in mild traumatic brain injury. Exp Neurol. 2015.
75. Kwon BK, Stammers AM, Belanger LM, Bernardo A, Chan D, Bishop CM, et al. Cerebrospinal fluid inflammatory cytokines and biomarkers of injury severity in acute human spinal cord injury. J Neurotrauma. 2010;27(4):669-82.
76. Shiiya N, Kunihara T, Miyatake T, Matsuzaki K, Yasuda K. Tau protein in the cerebrospinal fluid is a marker of brain injury after aortic surgery. The Annals of thoracic surgery. 2004;77(6):2034-8.
77. Jafari SS, Maxwell WL, Neilson M, Graham DI. Axonal cytoskeletal changes after non-disruptive axonal injury. Journal of neurocytology. 1997;26(4):207-21.
78. Hayakawa K, Okazaki R, Ishii K, Ueno T, Izawa N, Tanaka Y, et al. Phosphorylated neurofilament subunit NF-H as a biomarker for evaluating the severity of spinal cord injury patients, a pilot study. Spinal cord. 2012;50(7):493-6.

79. Kuhle J, Gaiottino J, Leppert D, Petzold A, Bestwick JP, Malaspina A, et al. Serum neurofilament light chain is a biomarker of human spinal cord injury severity and outcome. Journal of neurology, neurosurgery, and psychiatry. 2015;86(3):273-9.
80. Guez M, Hildingsson C, Rosengren L, Karlsson K, Toolanen G. Nervous tissue damage markers in cerebrospinal fluid after cervical spine injuries and whiplash trauma. J Neurotrauma. 2003;20(9):853-8.
81. Lee SJ, Kim CW, Lee KJ, Choe JW, Kim SE, Oh JH, et al. Elevated serum S100B levels in acute spinal fracture without head injury. Emergency medicine journal : EMJ. 2010;27(3):209-12.
82. Marquardt G, Setzer M, Seifert V. Protein S-100b as serum marker for prediction of functional outcome in metastatic spinal cord compression. Acta neurochirurgica. 2004;146(5):449-52.
83. Marquardt G, Setzer M, Seifert V. Protein S-100b for individual prediction of functional outcome in spinal epidural empyema. Spine. 2004;29(1):59-62.
84. Marquardt G, Setzer M, Szelenyi A, Seifert V, Gerlach R. Significance of serial S100b and NSE serum measurements in surgically treated patients with spondylotic cervical myelopathy. Acta neurochirurgica. 2009;151(11):1439-43.
85. Johnsson P, Blomquist S, Luhrs C, Malmkvist G, Alling C, Solem JO, et al. Neuron-specific enolase increases in plasma during and immediately after extracorporeal circulation. The Annals of thoracic surgery. 2000;69(3):750-4.
86. Marquardt G, Setzer M, Szelenyi A, Seifert V, Gerlach R. Prognostic relevance of serial S100b and NSE serum measurements in patients with spinal intradural lesions. Neurological research. 2009;31(3):265-9.
87. Yang L, Jones NR, Blumbergs PC, Van Den Heuvel C, Moore EJ, Manavis J, et al. Severity-dependent expression of pro-inflammatory cytokines in traumatic spinal cord injury in the rat. Journal of clinical neuroscience : official journal of the Neurosurgical Society of Australasia. 2005;12(3):276-84.
88. R L. Considerations for the Use of Blood Plasma and Serum for Proteomic Analysis. The Internet Journal of Genomics and Proteomics. 2003;Volume 1(Number 2).
89. Good DM TV, Novak J, Bascands JL, Schanstra JP, Coon JJ, Dominiczak A, Mishak H. Body fluid proteomics for biomarker discovery: lessons from the past hold the key to success in the future. J Proteome Res. 2007;6(12):4549-55.
90. Wang CX, Olschowka JA, Wrathall JR. Increase of interleukin-1beta mRNA and protein in the spinal cord following experimental traumatic injury in the rat. Brain research. 1997;759(2):190-6.
91. Harrington JF, Messier AA, Levine A, Szmydynger-Chodobska J, Chodobski A. Shedding of tumor necrosis factor type 1 receptor after experimental spinal cord injury. J Neurotrauma. 2005;22(8):919-28.
92. Tsai MC, Wei CP, Lee DY, Tseng YT, Tsai MD, Shih YL, et al. Inflammatory mediators of cerebrospinal fluid from patients with spinal cord injury. Surgical neurology. 2008;70 Suppl 1:S1:19-24; discussion S1:.
93. Casha S, T. R, DP. S, McGowan D, C. S, M. S, et al. CSF inflammatory changes correlate with injury severity and recovery after human spinal cord injury. Congress of Neurological Surgeons, Annual Meeting. 2009;New Orleans, LA.
94. Moghaddam A, Child C, Bruckner T, Gerner HJ, Daniel V, Biglari B. Posttraumatic inflammation as a key to neuroregeneration after traumatic spinal cord injury. International journal of molecular sciences. 2015;16(4):7900-16.
95. Stein A, Panjwani A, Sison C, Rosen L, Chugh R, Metz C, et al. Pilot study: elevated circulating levels of the proinflammatory cytokine macrophage migration inhibitory factor in patients with chronic spinal cord injury. Arch Phys Med Rehabil. 2013;94(8):1498-507.
96. Bank M, Stein A, Sison C, Glazer A, Jassal N, McCarthy D, et al. Elevated circulating levels of the pro-inflammatory cytokine macrophage migration inhibitory factor in individuals with acute spinal cord injury. Arch Phys Med Rehabil. 2015;96(4):633-44.
97. Segal JL, Gonzales E, Yousefi S, Jamshidipour L, Brunnemann SR. Circulating levels of IL-2R, ICAM-1, and IL-6 in spinal cord injuries. Arch Phys Med Rehabil. 1997;78(1):44-7.

98. Frost F, Roach MJ, Kushner I, Schreiber P. Inflammatory C-reactive protein and cytokine levels in asymptomatic people with chronic spinal cord injury. Arch Phys Med Rehab. 2005;86(2):312-7.
99. Zaaqoq AM, Namas R, Almahmoud K, Azhar N, Mi Q, Zamora R, et al. Inducible protein-10, a potential driver of neurally controlled interleukin-10 and morbidity in human blunt trauma. Critical care medicine. 2014;42(6):1487-97.
100. Liu SQ, Ma YG, Peng H, Fan L. Monocyte chemoattractant protein-1 level in serum of patients with acute spinal cord injury. Chinese journal of traumatology = Zhonghua chuang shang za zhi / Chinese Medical Association. 2005;8(4):216-9.
101. Hassanshahi G, Amin M, Shunmugavel A, Vazirinejad R, Vakilian A, Sanji M, et al. Temporal expression profile of CXC chemokines in serum of patients with spinal cord injury. Neurochemistry international. 2013;63(5):363-7.
102. Xu J, E X, Liu H, Li F, Cao Y, Tian J, et al. Tumor necrosis factor-alpha is a potential diagnostic biomarker for chronic neuropathic pain after spinal cord injury. Neuroscience letters. 2015;595:30-4.
103. Zajarias-Fainsod D, Carrillo-Ruiz J, Mestre H, Grijalva I, Madrazo I, Ibarra A. Autoreactivity against myelin basic protein in patients with chronic paraplegia. European spine journal : official publication of the European Spine Society, the European Spinal Deformity Society, and the European Section of the Cervical Spine Research Society. 2012;21(5):964-70.
104. Zhang Y, Popovich P. Roles of autoantibodies in central nervous system injury. Discovery medicine. 2011;11(60):395-402.
105. Taranova NP, Makarov A, Amelina OA, Luchakova OS, Loboda EB, Leikin IB. [The production of autoantibodies to nerve tissue glycolipid antigens in patients with traumatic spinal cord injuries]. Zhurnal voprosy neirokhirurgii imeni N N Burdenko. 1992(4-5):21-4.
106. Jeter CB, Hergenroeder GW, Hylin MJ, Redell JB, Moore AN, Dash PK. Biomarkers for the diagnosis and prognosis of mild traumatic brain injury/concussion. J Neurotrauma. 2013;30(8):657-70.
107. Diamandis EP. Mass spectrometry as a diagnostic and a cancer biomarker discovery tool: opportunities and potential limitations. Molecular & cellular proteomics : MCP. 2004;3(4):367-78.
108. Zurbig P, Jahn H. Use of proteomic methods in the analysis of human body fluids in Alzheimer research. Electrophoresis. 2012;33(24):3617-30.
109. da Silva BF, Souza GH, lo Turco EG, Del Giudice PT, Soler TB, Spaine DM, et al. Differential seminal plasma proteome according to semen retrieval in men with spinal cord injury. Fertility and sterility. 2013;100(4):959-69.
110. da Silva BF, Meng C, Helm D, Pachl F, Schiller J, Ibrahim E, et al. Towards Understanding Male Infertility After Spinal Cord Injury Using Quantitative Proteomics. Molecular & cellular proteomics : MCP. 2016;15(4):1424-34.
111. Sengupta MB, Basu M, Iswarari S, Mukhopadhyay KK, Sardar KP, Acharyya B, et al. CSF proteomics of secondary phase spinal cord injury in human subjects: perturbed molecular pathways post injury. PloS one. 2014;9(10):e110885.
112. Streijger F, Skinnider MA, Rogalski JC, Balshaw R, Shannon CP, Prudova A, et al. A Targeted Proteomics Analysis of Cerebrospinal Fluid after Acute Human Spinal Cord Injury. J Neurotrauma. 2017;34(12):2054-68.
113. Bradbury AR. The use of phage display in neurobiology. Current protocols in neuroscience / editorial board, Jacqueline N Crawley [et al]. 2010;Chapter 5:Unit 5 12.
114. Somers VA, Brandwijk RJ, Joosten B, Moerkerk PT, Arends JW, Menheere P, et al. A panel of candidate tumor antigens in colorectal cancer revealed by the serological selection of a phage displayed cDNA expression library. Journal of immunology. 2002;169(5):2772-80.
115. Cleutjens KB, Faber BC, Rousch M, van Doorn R, Hackeng TM, Vink C, et al. Noninvasive diagnosis of ruptured peripheral atherosclerotic lesions and myocardial infarction by antibody profiling. J Clin Invest. 2008;118(8):2979-85.

116. Rouwette M, Somers K, Govarts C, De Deyn PP, Hupperts R, Van Wijmeersch B, et al. Novel cerebrospinal fluid and serum autoantibody targets for clinically isolated syndrome. J Neurochem. 2012;123(4):568-77.
117. Somers V, Govarts C, Somers K, Hupperts R, Medaer R, Stinissen P. Autoantibody profiling in multiple sclerosis reveals novel antigenic candidates. Journal of immunology. 2008;180(6):3957-63.
118. Govarts C, Somers K, Hupperts R, Stinissen P, Somers V. Exploring cDNA phage display for autoantibody profiling in the serum of multiple sclerosis patients: optimization of the selection procedure. Annals of the New York Academy of Sciences. 2007;1109:372-84.
119. Somers K, Geusens P, Elewaut D, De Keyser F, Rummens JL, Coenen M, et al. Novel autoantibody markers for early and seronegative rheumatoid arthritis. Journal of autoimmunity. 2011;36(1):33-46.
120. Somers K, Stinissen P, Somers V. Optimization of High-throughput Autoantibody Profiling for the Discovery of Novel Antigenic Targets in Rheumatoid Arthritis. Annals of the New York Academy of Sciences. 2009;1173:92-102.
121. De Bock L, Fraussen J, Villar LM, Alvarez-Cermeno JC, Van Wijmeersch B, Van Pesch V, et al. Anti-SPAG16 antibodies in primary progressive multiple sclerosis are associated with an elevated progression index. Eur J Neurol. 2015;(accepted).
122. de Bock L, Somers K, Fraussen J, Hendriks JJ, van Horssen J, Rouwette M, et al. Sperm-associated antigen 16 is a novel target of the humoral autoimmune response in multiple sclerosis. Journal of immunology. 2014;193(5):2147-56.
123. Henry KA, Arbabi-Ghahroudi M, Scott JK. Beyond phage display: non-traditional applications of the filamentous bacteriophage as a vaccine carrier, therapeutic biologic, and bioconjugation scaffold. Frontiers in microbiology. 2015;6:755.
124. Criscuolo E, Spadini S, Lamanna J, Ferro M, Burioni R. Bacteriophages and Their Immunological Applications against Infectious Threats. J Immunol Res. 2017.
125. Bradbury ARM. The Use of Phage Display in Neurobiology. Current Protocols in Neuroscience: John Wiley & Sons, Inc.; 2001.
126. Bernard JM, Francis MB. Chemical strategies for the covalent modification of filamentous phage. Frontiers in microbiology. 2014;5:734.
127. Saeed AF, Wang R, Ling S, Wang S. Antibody Engineering for Pursuing a Healthier Future. Frontiers in microbiology. 2017;8:495.
128. Rouwette M, Somers K, Govarts C, De Deyn PP, Hupperts R, Van Wijmeersch B, et al. Novel cerebrospinal fluid and serum autoantibody targets for clinically isolated syndrome. J Neurochem. 2012;123(4):568-77.
129. Govarts C, Somers K, Hupperts R, Stinissen P, Somers V. Exploring cDNA phage display for autoantibody profiling in the serum of multiple sclerosis patients - Optimization of the selection procedure. Annals of the New York Academy of Sciences. 2007;1109:372-84.
130. Somers V, Govarts C, Somers K, Hupperts R, Medaer R, Stinissen P. Autoantibody profiling in multiple sclerosis reveals novel antigenic candidates. J Immunol. 2008;180(6):3957-63.
131. Vandormael P, Verschueren P, De Winter L, Somers V. cDNA phage display for the discovery of theranostic autoantibodies in rheumatoid arthritis. Immunologic research. 2017;65(1):307-25.
132. Hufton SE, Moerkerk PT, Meulemans EV, de Bruine A, Arends JW, Hoogenboom HR. Phage display of cDNA repertoires: the pVI display system and its applications for the selection of immunogenic ligands. Journal of immunological methods. 1999;231(1-2):39-51.
133. Jespers LS, Messens JH, Dekeyser A, Eeckhout D, Vandenbrande I, Gansemans YG, et al. Surface Expression and Ligand-Based Selection of Cdnas Fused to Filamentous Phage Gene Vi. Bio-Technol. 1995;13(4):378-82.
134. Somers V, Govarts C, Hellings N, Hupperts R, Stinissen P. Profiling the autoantibody repertoire by serological antigen selection. Journal of autoimmunity. 2005;25(3):223-8.

135. Clamp M, Fry B, Kamal M, Xie X, Cuff J, Lin MF, et al. Distinguishing protein-coding and noncoding genes in the human genome. Proceedings of the National Academy of Sciences of the United States of America. 2007;104(49):19428-33.
136. Ezkurdia I, Juan D, Rodriguez JM, Frankish A, Diekhans M, Harrow J, et al. Multiple evidence strands suggest that there may be as few as 19,000 human protein-coding genes. Human molecular genetics. 2014;23(22):5866-78.
137. Oyinbo CA. Secondary injury mechanisms in traumatic spinal cord injury: a nugget of this multiply cascade. Acta Neurobiol Exp (Wars). 2011;71(2):281-99.
138. Han X, Lu M, Wang SY, Lv DC, Liu HR. Targeting IKK/NF-kappa B pathway reduces infiltration of inflammatory cells and apoptosis after spinal cord injury in rats. Neuroscience letters. 2012;511(1):28-32.
139. Dekaban GA, Thawer S. Pathogenic antibodies are active participants in spinal cord injury. J Clin Invest. 2009;119(10):2881-4.
140. Ankeny DP, Popovich PG. Mechanisms and implications of adaptive immune responses after traumatic spinal cord injury. Neuroscience. 2009;158(3):1112-21.
141. Wang R, Chen J, Zhou S, Li C, Yuan G, Xu W, et al. Enzyme-linked immunoadsorbent assays for myelin basic protein and antibodies to myelin basic protein in serum and CSF of patients with diseases of the nervous system. Hua Xi Yi Ke Da Xue Xue Bao 1995;26(2):131-4.
142. Somers K, Geusens P, Elewaut D, De Keyser F, Rummens JL, Coenen M, et al. Novel autoantibody markers for early and seronegative rheumatoid arthritis. J Autoimmun. 2011;36(1):33-46.
143. de Bock L, Somers K, Fraussen J, Hendriks JJ, van Horssen J, Rouwette M, et al. Sperm-associated antigen 16 is a novel target of the humoral autoimmune response in multiple sclerosis. J Immunol. 2014;193(5):2147-56.
144. Rouwette M, Noben JP, Van Horssen J, Van Wijmeersch B, Hupperts R, Jongen PJ, et al. Identification of coronin-1a as a novel antibody target for clinically isolated syndrome and multiple sclerosis. J Neurochem. 2013;126(4):483-92.
145. De Winter LM, Hansen WL, van Steenbergen HW, Geusens P, Lenaerts J, Somers K, et al. Autoantibodies to two novel peptides in seronegative and early rheumatoid arthritis. Rheumatology (Oxford). 2016.
146. Ydens E, Palmers I, Hendrix S, Somers V. The Next Generation of Biomarker Research in Spinal Cord Injury. Molecular neurobiology. 2016.
147. Marks JD, Hoogenboom HR, Bonnert TP, McCafferty J, Griffiths AD, Winter G. By-passing immunization. Human antibodies from V-gene libraries displayed on phage. Journal of molecular biology. 1991;222(3):581-97.
148. Aceti M, Creson TK, Vaissiere T, Rojas C, Huang WC, Wang YX, et al. Syngap1 haploinsufficiency damages a postnatal critical period of pyramidal cell structural maturation linked to cortical circuit assembly. Biological psychiatry. 2015;77(9):805-15.
149. Wolf H, Krall C, Pajenda G, Leitgeb J, Bukaty AJ, Hajdu S, et al. Alterations of the biomarker S-100B and NSE in patients with acute vertebral spine fractures. The spine journal. 2014;14(12):2918-22.
150. Sorokina EG, Semenova JB, Granstrem OK, Karaseva OV, Meshcheryakov SV, Reutov VP, et al. S100B protein and autoantibodies to S100B protein in diagnostics of brain damage in craniocerebral trauma in children. Zh Nevrol Psikhiatr Im S S Korsakova. 2010;110(8):30-5.
151. Marchi N, Bazarian JJ, Puvenna V, Janigro M, Ghosh C, Zhong JH, et al. Consequences of Repeated Blood-Brain Barrier Disruption in Football Players. PloS one. 2013;8(3).
152. Cruz CD, Coelho A, Antunes-Lopes T, Cruz F. Biomarkers of spinal cord injury and ensuing bladder dysfunction. Advanced drug delivery reviews. 2015;82-83:153-9.
153. Pouw MH, Hosman AJF, van Middendorp JJ, Verbeek MM, Vos PE, van de Meent H. Biomarkers in spinal cord injury. Spinal cord. 2009;47(7):519-25.
154. Sirover MA. Structural analysis of glyceraldehyde-3-phosphate dehydrogenase functional diversity. The international journal of biochemistry & cell biology. 2014;57:20-6.

155. Tristan C, Shahani N, Sedlak TW, Sawa A. The diverse functions of GAPDH: views from different subcellular compartments. Cell Signal. 2011;23(2):317-23.
156. Nakajima H, Kubo T, Ihara H, Hikida T, Danjo T, Nakatsuji M, et al. Nuclear-translocated Glyceraldehyde-3-phosphate Dehydrogenase Promotes Poly(ADP-ribose) Polymerase-1 Activation during Oxidative/Nitrosative Stress in Stroke. jbc. 2015;290(23):14493-503.
157. Feldkamp ML, Bowles NE, Botto LD. AEBP1 gene variants in infants with gastroschisis. Birth Defects Res A Clin Mol Teratol. 2012;94(9):738-42.
158. Liu CW, Jacobson AD. Functions of the 19S complex in proteasomal degradation. Trends Biochem Sci. 2013;38(2):103-10.
159. Bartanusz V, Jezova D, Alajajian B, Digicaylioglu M. The blood-spinal cord barrier: morphology and clinical implications. Annals of neurology. 2011;70(2):194-206.
160. Wu H, Brown EV, Acharya NK, Appelt DM, Marks A, Nagele RG, et al. Age-dependent increase of blood-brain barrier permeability and neuron-binding autoantibodies in S100B knockout mice. Brain research. 2016;1637:154-67.
161. Cohen DM, Patel CB, Ahobila-Vajjula P, Sundberg LM, Chacko T, Liu SJ, et al. Blood-spinal cord barrier permeability in experimental spinal cord injury: dynamic contrast-enhanced MRI. NMR in biomedicine. 2009;22(3):332-41.
162. Skoda D, Kranda K, Bojar M, Glosova L, Baurle J, Kenney J, et al. Antibody formation against beta-tubulin class III in response to brain trauma. Brain Res Bull. 2006;68(4):213-6.
163. Chan WM, Mohammed Y, Lee I, Pearse DD. Effect of gender on recovery after spinal cord injury. Translational stroke research. 2013;4(4):447-61.
164. Farooque M, Suo Z, Arnold PM, Wulser MJ, Chou CT, Vancura RW, et al. Gender-related differences in recovery of locomotor function after spinal cord injury in mice. Spinal cord. 2006;44(3):182-7.
165. Desmetz C, Mange A, Maudelonde T, Solassol J. Autoantibody signatures: progress and perspectives for early cancer detection. J Cell Mol Med. 2011;15(10):2013-24.
166. Nesterova M, Johnson N, Cheadle C, Cho-Chung YS. Autoantibody biomarker opens a new gateway for cancer diagnosis. Bba-Mol Basis Dis. 2006;1762(4):398-403.
167. Palmers I, Ydens E, Put E, Depreitere B, Bongers-Janssen H, Pickkers P, et al. Antibody profiling identifies novel antigenic targets in spinal cord injury patients. Journal of neuroinflammation. 2016;13(1):243.
168. Gan SD, Patel KR. Enzyme Immunoassay and Enzyme-Linked Immunosorbent Assay. J Invest Dermatol. 2013;133(9):E10-E2.
169. Ghanshyam Gahlot YS, Gajanand Joshi, Rachit Saxena. Clinical Significance of Serum Biomarker S100B to Predict Outcome After Traumatic Brain Injury. Idian journal of mednodent and alled sciences. 2017;5.
170. Kabadi SV, Stoica BA, Zimmer DB, Afanador L, Duffy KB, Loane DJ, et al. S100B inhibition reduces behavioral and pathologic changes in experimental traumatic brain injury. Journal of cerebral blood flow and metabolism : official journal of the International Society of Cerebral Blood Flow and Metabolism. 2015;35(12):2010-20.
171. Rezaei O PH, Gharehgozli K, et al. S100 B: A new concept in neurocritical care. Iranian Journal of Neurology. 2017;16(2):83-9.
172. Wang Z, Fan C, Zhou HF, Lu JS, Sun MJ, Song JW, et al. S5a binds to death receptor-6 to induce THP-1 monocytes to differentiate through the activation of the NF-kappaB pathway. Journal of cell science. 2014;127(Pt 15):3257-68.
173. Ulgheri C, Paganini B, Rossi F. Antisecretory factor as a potential health-promoting molecule in man and animals. Nutr Res Rev. 2010;23(2):300-13.
174. Jennische E, Johansson E, Hansson HA, Jonson I. Immunohistochemical staining patterns using epitope-specific antibodies indicate conformation variants of antisecretory factor/S5a in the CNS. Apmis. 2006;114(7-8):529-38.
175. Davidson TS, Hickey WF. Antisecretory factor expression is regulated by inflammatory mediators and influences the severity of experimental autoimmune encephalomyelitis. Journal of leukocyte biology. 2004;76(4):835-44.
176. Kremlev SG, Gaurnier-Hausser AL, Del Valle L, Perez-Liz G, Dimitrov S, Tuszynski G. Angiocidin promotes pro-inflammatory cytokine production and antigen

presentation in multiple sclerosis. Journal of neuroimmunology. 2008;194(1-2):132-42.
177. Schaefer DM, Flanders AE, Osterholm JL, Northrup BE. Prognostic-Significance of Magnetic-Resonance-Imaging in the Acute Phase of Cervical-Spine Injury. Journal of neurosurgery. 1992;76(2):218-23.
178. Brown PJ, Marino RJ, Herbison GJ, Ditunno JF. The 72-Hour Examination as a Predictor of Recovery in Motor Complete Quadriplegia. Arch Phys Med Rehab. 1991;72(8):546-8.
179. Hakim FT, Gress RE. Immunosenescence: deficits in adaptive immunity in the elderly. Tissue antigens. 2007;70(3):179-89.
180. Ankeny DP, Popovich PG. B cells and autoantibodies: complex roles in CNS injury. Trends Immunol. 2010;31(9):332-8.
181. Poletaev AB, Morozov SG, Gnedenko BB, Zlunikin VM, Korzhenevskey DA. Serum anti-S100b, anti-GFAP and anti-NGF autoantibodies of IgG class in healthy persons and patients with mental and neurological disorders. Autoimmunity. 2000;32(1):33-8.
182. Blyth BJ, Farhavar A, Gee C, Hawthorn B, He H, Nayak A, et al. Validation of serum markers for blood-brain barrier disruption in traumatic brain injury. J Neurotrauma. 2009;26(9):1497-507.
183. Campagnolo DI, Dixon D, Schwartz J, Bartlett JA, Keller SE. Altered innate immunity following spinal cord injury. Spinal cord. 2008;46(7):477-81.
184. Cruse JM, Lewis RE, Bishop GR, Kliesch WF, Gaitan E. Neuroendocrine-Immune Interactions Associated with Loss and Restoration of Immune-System Function in Spinal-Cord Injury and Stroke Patients. Immunologic research. 1992;11(2):104-16.
185. Cruse JM, Keith JC, Bryant ML, Lewis RE. Immune system - Neuroendocrine dysregulation in spinal cord injury. Immunologic research. 1996;15(4):306-14.
186. Tanaka K. The proteasome: Overview of structure and functions. P Jpn Acad B-Phys. 2009;85(1):12-36.
187. Johansson E, Lonnroth I, Jonson I, Lange S, Jennische E. Development of monoclonal antibodies for detection of Antisecretory Factor activity in human plasma. Journal of immunological methods. 2009;342(1-2):64-70.
188. Davidson TS, Hickey WF. Distribution and immunoregulatory properties of antisecretory factor. Laboratory investigation; a journal of technical methods and pathology. 2004;84(3):307-19.
189. Hansson HA, Al-Olama M, Jennische E, Gatzinsky K, Lange S. The peptide AF-16 and the AF protein counteract intracranial hypertension. Acta neurochirurgica Supplement. 2012;114:377-82.
190. Al-Olama M, Lange S, Lonnroth I, Gatzinsky K, Jennische E. Uptake of the antisecretory factor peptide AF-16 in rat blood and cerebrospinal fluid and effects on elevated intracranial pressure. Acta neurochirurgica. 2015;157(1):129-37.
191. Tuszynski GP, Rothman VL, Papale M, Hamilton BK, Eyal J. Identification and characterization of a tumor cell receptor for CSVTCG, a thrombospondin adhesive domain. The Journal of cell biology. 1993;120(2):513-21.
192. Gaurnier-Hausser A, Rothman VL, Dimitrov S, Tuszynski GP. The novel angiogenic inhibitor, angiocidin, induces differentiation of monocytes to macrophages. Cancer research. 2008;68(14):5905-14.
193. Gaurnier-Hausser A, Tuszynski GP. The immunomodulatory role of angiocidin, a novel angiogenesis inhibitor. Current pharmaceutical design. 2009;15(17):1937-48.
194. Auwerx J. The human leukemia cell line, THP-1: a multifacetted model for the study of monocyte-macrophage differentiation. Experientia. 1991;47(1):22-31.
195. Boato F, Hendrix S, Huelsenbeck SC, Hofmann F, Grosse G, Djalali S, et al. C3 peptide enhances recovery from spinal cord injury by improved regenerative growth of descending fiber tracts. Journal of cell science. 2010;123(10):1652-62.
196. Nelissen S, Lemmens E, Geurts N, Kramer P, Maurer M, Hendriks J, et al. The role of mast cells in neuroinflammation. Acta neuropathologica. 2013;125(5):637-50.

197. Geurts N VT, Lemmens S, Nelissen S, Geboes L, Schwartz C, Voehringer D, Hendrix S. Basophils are dispensable for the recovery of gross locomotion after spinal cord hemisection injury. Journal of leukocyte biology. 2016;99(4):579-82.
198. Nelissen S VT, Geurts N, Geboes L, Lemmens E, Vidal PM, Lemmens S, Willems L, Boato F, Dooley D, Pehl D, Pejler G, Maurer M, Metz M, Hendrix S. Mast cells protect from post-traumatic spinal cord damage in mice by degrading inflammation-associated cytokines via mouse mast cell protease 4. Neurobiology of Disease 2014;62:260-72.
199. Vidal PM LE, Avila A, Vangansewinkel T, Chalaris A, Rose-John A, and Hendrix S. ADAM17 is a survival factor for microglial cells in vitro and in vivo after spinal cord injury in mice. Cell Death & Disease. 2013;4(12):e954.
200. Dooley D LE, Ponsaerts P, Hendrix S. Interleukin-25 is detrimental for recovery after spinal cord injury in mice. Journal of neuroinflammation. 2016;13(1):101.
201. Tuszynski MH SO. Concepts and methods for the study of axonal regeneration in the CNS. Neuron 2012;74(5):777-91.
202. Dooley D, Lemmens E, Vangansewinkel T, Le Blon D, Hoornaert C, Ponsaerts P, et al. Cell-Based Delivery of Interleukin-13 Directs Alternative Activation of Macrophages Resulting in Improved Functional Outcome after Spinal Cord Injury. Stem cell reports. 2016;7(6):1099-115.
203. Vangansewinkel T, Geurts N, Quanten K, Nelissen S, Lemmens S, Geboes L, et al. Mast cells promote scar remodeling and functional recovery after spinal cord injury via mouse mast cell protease 6. Faseb J. 2016;30(5):2040-57.
204. Vandesompele J, De Preter K, Pattyn F, Poppe B, Van Roy N, De Paepe A, et al. Accurate normalization of real-time quantitative RT-PCR data by geometric averaging of multiple internal control genes. Genome Biol. 2002;3(7).
205. Hellemans J, Mortier G, De Paepe A, Speleman F, Vandesompele J. qBase relative quantification framework and software for management and automated analysis of real-time quantitative PCR data. Genome Biol. 2007;8(2).
206. Johansson E, Jonson I, Bosaeus M, Jennische E. Identification of flotillin-1 as an interacting protein for antisecretory factor. Regulatory peptides. 2008;146(1-3):303-9.
207. Lange S, Jennische E, Johansson E, Lonnroth I. The antisecretory factor: synthesis and intracellular localisation in porcine tissues. Cell Tissue Res. 1999;296(3):607-17.
208. Vieira P, Rajewsky K. The Half-Lives of Serum Immunoglobulins in Adult Mice. Eur J Immunol. 1988;18(2):313-6.
209. Jain KK. The Handbook of Biomarkers Introduction. Handbook of Biomarkers. 2010:1-+.
210. Zhang M, Alicot EM, Carroll MC. Human natural IgM can induce ischemia/reperfusion injury in a murine intestinal model. Mol Immunol. 2008;45(15):4036-9.
211. Ngankam L, Kazantseva NV, Gerasimova MM. Immunological markers of severity and outcome of traumatic brain injury. Zh Nevrol Psikhiatr Im S S Korsakova. 2011;111(7):61-5.
212. Nagele EP, Han M, Acharya NK, DeMarshall C, Kosciuk MC, Nagele RG. Natural IgG Autoantibodies Are Abundant and Ubiquitous in Human Sera, and Their Number Is Influenced By Age, Gender, and Disease. PloS one. 2013;8(4).
213. Hammer C, Stepniak B, Schneider A, Papiol S, Tantra M, Begemann M, et al. Neuropsychiatric disease relevance of circulating anti-NMDA receptor autoantibodies depends on blood-brain barrier integrity. Mol Psychiatr. 2014;19(10):1143-9.
214. Castillo-Gomez E, Oliveira B, Tapken D, Bertrand S, Klein-Schmidt C, Pan H, et al. All naturally occurring autoantibodies against the NMDA receptor subunit NR1 have pathogenic potential irrespective of epitope and immunoglobulin class. Mol Psychiatry. 2016.
215. Zerche M, Weissenborn K, Ott C, Dere E, Asif AR, Worthmann H, et al. Preexisting Serum Autoantibodies Against the NMDAR Subunit NR1 Modulate Evolution of Lesion Size in Acute Ischemic Stroke. Stroke. 2015;46(5):1180-6.

216. Michetti F, Corvino V, Geloso MC, Lattanzi W, Bernardini C, Serpero L, et al. The S100B protein in biological fluids: more than a lifelong biomarker of brain distress. J Neurochem. 2012;120(5):644-59.
217. Thelin EP, Nelson DW, Bellander BM. A review of the clinical utility of serum S100B protein levels in the assessment of traumatic brain injury. Acta neurochirurgica. 2017;159(2):209-25.
218. Sharif-Alhoseini M, Khormali M, Rezaei M, Safdarian M, Hajighadery A, Khalatbari MM, et al. Animal models of spinal cord injury: a systematic review. Spinal cord. 2017;55(8):714-21.

Curriculum Vitae

Personal details

Name: Ilse Palmers

Nationality: Belgian

Date of Birth: 15/08/1989

Education

2012-present: PhD Biomedical Sciences

Hasselt University, Belgium – Promotor: Prof. dr. Veerle Somers

2010-2012: Master Clinical Molecular Sciences, Hasselt University, tUL, Belgium

2007-2010: Bachelor Biomedical Sciences, Hasselt University, tUL, Belgium

Publications

Palmers I, Ydens E, Put E, Depreitere B, Bongers-Janssen H, Pickkers P, Hendrix S, Somers V

Antibody profiling identifies novel antigenic targets in spinal cord injury patients Journal of Neuroinflammation, 2016;13(1):243. **IF(2016): 5.1**

Ydens E*, **Palmers I***, Hendrix S, Somers V

(*contributed equally to this work)

The Next Generation of Biomarker Research in Spinal Cord Injury

Molecular Neurobiology. 2017;54:1482. **IF(2016): 6.2**

Oral Presentations

2017: 13th Dresden Symposium on Autoantibodies

Dresden, Germany

2015: 12th Dresden Symposium on Autoantibodies

Dresden, Germany

Poster Presentations

2017: 56th ISCOS Annual Scientific Meeting
Dublin, Ireland
Palmers I, Ydens E, Put E, Depreitere B, Bongers-Janssen H, Pickkers P, Hendrix S, Somers V
Antibody profiling identifies novel antigenic targets in spinal cord injury patients

2017: 13th Dresden Symposium on Autoantibodies
Dresden, Germany
Palmers I, Ydens E, Put E, Depreitere B, Bongers-Janssen H, Pickkers P, Hendrix S, Somers V
Antibody profiling identifies novel antigenic targets in spinal cord injury patients

2016: International Society of Neuroimmunology
Jerusalem, Israel
Palmers I, Ydens E, Bongers-Janssen H, Depreitere B, Put E, Hendrix S, Somers V
Antibody profiling identifies novel antigenic targets in spinal cord injury patients

2016: EURON PhD days
Lille, France
Palmers I, Ydens E, Bongers-Janssen H, Depreitere B, Put E, Hendrix S, Somers V
Antibody profiling identifies novel antigenic targets in spinal cord injury patients

2016: Autoimmunity
Leipzig, Germany
Palmers I, Ydens E, Put E, Depreitere B, Bongers-Janssen H, Pickkers P, Hendrix S, Somers V
Identification of novel candidate antibody biomarkers in spinal cord injury

2015: 12th Dresden Symposium on Autoantibodies
Dresden, Germany

Palmers I, Ydens E, Depreitere B, Maas A, Timmermans K, Kox M, Put E, Hendrix S, Somers V
Identification of novel candidate antibody biomarkers in spinal cord injury

2015: Biomedica
Genk, Belgium
Palmers I, Ydens E, Depreitere B, Maas A, Timmermans K, Kox M, Put E, Hendrix S, Somers V
Identification of novel candidate antibody biomarkers in spinal cord injury

2015: The immune-brain axis: from molecules to behavior
Diepenbeek, Belgium
Palmers I, Ydens E, Depreitere B, Maas A, Timmermans K, Kox M, Put E, Hendrix S, Somers V
Identification of novel candidate antibody biomarkers in spinal cord injury

2015: Neuroinflammation
Bonn, Germany
Palmers I, Ydens E, Depreitere B, Maas A, Timmermans K, Kox M, Put E, Hendrix S, Somers V
Identification of novel candidate antibody biomarkers in spinal cord injury

Grants/Awards

2015: Poster award at 'The immune-brain axis: from molecules to behaviour' symposium

2013: PhD grant for Strategic Basic Research Flanders Innovation and Entrepreneurship

Dankwoord

Nu de thesis stilaan finaal is, wil ik de vele mensen die me ondersteund hebben nog eens extra bedanken. Ik hoop daarbij niemand te vergeten maar vergeef me, moest ik toch iemand over het hoofd zien.

Mijn eerste woord van dank gaat uit naar mijn promotor, Veerle Somers, en mijn co-promotor, Sven Hendrix. Jullie gaven mij de kans om het SCI-biomarker onderzoek vorm te geven binnen de vooropgestelde doelstellingen.
Veerle, vanaf het begin stond je me bij met raad en daad. Je was zelfs bereid om labproeven van dichtbij mee te analyseren en extra 'tips and tricks' te geven indien experimenten niet optimaal verliepen. Tijdens lange optimalisatieperiodes of bij resultaten waarvan ik zelf niet overtuigd was, wist je steeds de positieve zaken aan te halen zodat ik er weer met goede moed tegenaan kon gaan. Ook de vele verplaatsingen voor het realiseren van samenwerkingen, waren voor mij zeer leerrijk en waardevol op vlak van contacten leggen en promotie van het onderzoek.
Beste Sven, na afronding van het humane gedeelte van mijn project, gaf je me de kans om deze bevindingen te toetsen in een diermodel. Voor mij een onbekend domein, wat het een unieke, leerrijke ervaring maakte.

Aan de voorzitter en juryleden van mijn doctoraatscommissie, bedankt om mijn thesis met veel interesse te lezen en de positieve feedback die ik mocht ontvangen. Ik kijk ernaar uit om deze discussiepunten verder te bespreken tijdens de openbare verdediging.

Doordat de expertise van 2 onderzoeksgroepen werd gebundeld in mijn doctoraat, kreeg ik de kans om samen te werken met de SCI-groep onder leiding van Sven, mijn co-promotor. Stefanie, Daniela, Selien en Leen, bedankt voor het uitvoeren van de hemisectie operatie en de ondersteuning bij de analyses.
Stefanie, na onze studieperiode zijn we gelijktijdig met een doctoraat gestart en volgden we de opleiding bedrijfskunde. Op vrijdagavond en zaterdagochtend waren we paraat in de les, en ondanks de zowel late als vroege uren hebben we veel plezier gehad! Daniela, bedankt voor de vele uren die je samen met mij doorbracht in het animalium. Ze maakten dat ik stilaan mijn angst voor

knaagdieren kwijtraakte. Ook onze babbels en fijne uitjes wist ik altijd te appreciëren. Tim, bedankt voor je interesse in mijn onderzoeksproject en voor je hulp bij het interpreteren van de humane kleuringen. Derv, Evi en Myriam, bedankt voor jullie ondersteuning en bijdrage in mijn onderzoek.

Zonder stalen kon er geen biomarkeronderzoek uitgevoerd worden. Dank aan alle patiënten, artsen (Jessa Ziekenhuis, Universitair Ziekenhuis Leuven, Universitair Ziekenhuis Antwerpen, Algemeen Ziekenhuis Turnhout, Ziekenhuis Oost-Limburg, Adelante, Maastricht UMC+, Zuyderland (Heerlen)), verpleegkundigen/clinial trial medewerkers (Anne, Dominique, Ina) en Biobankmedewerkers (Veerle, Loes, Kim, Igna, Nadine en Hilke) die meegewerkt hebben aan mijn studie. Jullie reacties op update e-mails en meetings konden mijn enthousiasme steeds aanwakkeren. Verder wil ik de samenwerkingen met Nijmegen (Peter Pickkers), Spanje (Luisa Villar) en Texas (Georgene Hergenroeder) bedanken voor hun interesse en het delen van stalen die mijn cohort verder deden groeien. Bedankt aan het Fonds voor Wetenschappelijk Onderzoek en het Agentschap Innoveren & Ondernemen voor de financiële ondersteuning van mijn onderzoek.

Bij de experimenten kon ik steeds rekenen op de technische tips en tricks van de laboranten en technici (Igna, Katrien, Leen, Christel, Kim, Lotte, Joke, Yanick en Melissa). Igna, vanaf dag één kon ik bij jou terecht voor het uitwerken van experimenten, het aanleren van nieuwe technieken en zoveel meer. Bedankt om me te begeleiden en te ondersteunen! Veronique en Rani, bedankt voor de hulp bij administratieve zaken en de praktische regelingen rond de verdediging. Bedankt Regine voor de fijne babbels, het voorzien in zuiver glaswerk en het verzekeren van een proper Faaglabo.

Sarah, Katrien, Tim, Kenneth en Jolien, jullie hulp in het labo tijdens de stageperiodes, heeft eveneens een heel waardevolle bijdrage geleverd aan mijn onderzoek. Hopelijk heb ik jullie laten proeven van het wetenschappelijk onderzoek in al zijn aspecten. Jolien, veel succes met je eigen doctoraatsonderzoek.

Vervolgens wil ik de biomarker/B-cel-groep bedanken. Elke, BEDANKT voor ALLES! Ik weet niet goed waar te starten. Je wetenschappelijke triggers, je enthousiasme en doorzettingsvermogen, de gedeelde vreugdedansjes, de ontelbare tips en feedbackmomenten hielpen me te relativeren en motiveerden me steeds om terug aan de slag te gaan. Ook nu mijn doctoraat bijna is afgerond, kan ik steeds op je rekenen. Patrick, doorheen de afgelopen jaren stond je altijd paraat voor een wetenschappelijke discussie omtrent de experimentele set-ups, de resultaten en de opbouw/afwerking van mijn thesis. Je input en enthousiasme voor het onderzoek wist ik telkens te appreciëren. Liesbeth, na mijn stage onder jouw supervisie zag ik een vervolg in onderzoek wel zitten. Ik kon bij jou terecht voor advies omtrent het onderzoek, de thesis, maar zeker ook voor een gezellige babbel. Ook in onze nieuwe werksituatie zullen we deze samenwerking verderzetten. Steven, Wendy, Judith, Leen, Laura en Myrthe, ook jullie trachtten mij te helpen waar mogelijk. Bedankt voor jullie ondersteuning en bijdrage in mijn onderzoek. Vervolgens wil ik mijn bureaugenoten bedanken. Nele, jij verwelkomde me in Biomed en nu opnieuw bij mijn nieuwe uitdaging. Bedankt voor de steun en de leuke desk activities. Gwendoline, de vele babbels over (niet) wetenschappelijk zaken, je steun en openheid maakte mijn tijd op de bureau onvergetelijk. Dana, ik denk regelmatig even terug aan je vrolijke JIPPIES wanneer ik iets verwezenlijkt heb. Verder zullen de gedeelde kerstmis gezelligheid en de leuke babbels me zeker bijblijven. Rut, during my last PhD year you joined us at the desk. Besides the time at biomed, we also had many good times outside the lab. Thanks for the talks and support. Together with the new people (Nadine and Jolien), I want to wish you all best luck for your research!
Naast de Biomarker/B-cel bureaugenoten zorgden ook Annelies, Raf, Stelios en Elien G voor een leuke sfeer op de bureau. Steeds kon ik met mijn vragen bij jullie terecht. Bedankt voor de hulp bij het opstarten/afronden van mijn doctoraat, de steun, de fijne gesprekken en de bureau-activiteiten!

Graag wil ik ook collega's uit andere onderzoeksgroepen bedanken voor de leuke werksfeer. Met een speciaal bedankje voor Dorien, vanaf het begin was je mijn steun en toeverlaat. Met alles kon ik bij jou terecht, bedankt! Silke, na ons tripje naar het IWT was onze band gesmeed. Regelmatig wisten we elkaar te vinden voor een babbel over zowel wetenschappelijke als minder wetenschappelijke

thema's. Dames, bedankt voor jullie steun en ik kijk al uit naar het volgende uitje taart eten ☺! Elien W, bedankt voor je hulp bij de weekendcontrole in het animalium, maar ook de gezellige babbels en de leuke uitjes! Marjan, samen gaan sporten was niet enkel ontspanning, maar ook een moment om bij te babbelen. Ze waren kort, maar krachtig. Jens en Maxim, bedankt voor de leuke cooking nights en andere uitjes. Liesbet, bedankt voor je hulp bij de statistische analyses.

Ik wil ook familie en vrienden bedanken ('De Kliek', Britt, Birgitte, David, Mandy, Marjan, Leen, Jolien, Sabina, Yanick, Karen, Stephanie, Stefanie, Sylvia, Jo, Kenneth, Frank, Robin, Kristof). Jullie zorgden ervoor dat er naast inspanning ook voldoende aan ontspanning werd gedaan. De sportjes, de etentjes, de drankjes en andere activiteiten wist ik altijd te appreciëren. Een speciaal bedankje gaat uit naar Guus. Tijdens mijn doctoraat mocht ik jouw meter worden, één van de mooiste gebeurtenissen tijdens mijn doctoraat. Ook jij zorgde op je eigen manier voor relativering!

Mama en papa, bedankt voor alles! Jullie hebben mij de mogelijkheid gegeven om me te ontwikkelen tot wie ik vandaag ben. Jullie hebben me steeds gesteund en stonden altijd voor me klaar. Jullie waren dan ook slechts een telefoontje verwijderd en ik kon altijd bij jullie terecht. Stijn, bedankt voor je relativeringsvermogen en aanmoedigingen. Op moeilijke momenten kon je me altijd laten inzien dat een doctoraat met de nodige 'ups en downs' verloopt, een traject waar de meeste doctoraatsstudenten zich zullen in herkennen, los van het onderwerp.

Bedankt!

Ilse
April 2018